JYU DISSERTATIONS 70

Evgeny Bulatov

Synthetic and Structural Studies of Covalent and Non-covalent Interactions of Ligands and Metal Center in Platinum(II) Complexes Containing 2,2′-Dipyridylamine or Oxime Ligands

UNIVERSITY OF JYVÄSKYLÄ
FACULTY OF MATHEMATICS
AND SCIENCE

JYU DISSERTATIONS 70

Evgeny Bulatov

Synthetic and Structural Studies of Covalent and Non-covalent Interactions of Ligands and Metal Center in Platinum(II) Complexes Containing 2,2′-Dipyridylamine or Oxime Ligands

Esitetään Jyväskylän yliopiston matemaattis-luonnontieteellisen tiedekunnan suostumuksella
julkisesti tarkastettavaksi yliopiston Ylistönrinteen salissa YlistöKem4
huhtikuun 18. päivänä 2019 kello 12.

Academic dissertation to be publicly discussed, by permission of
the Faculty of Mathematics and Science of the University of Jyväskylä,
in Ylistönrinne, auditorium YlistöKem4, on April 18, 2019 at 12 o'clock noon.

JYVÄSKYLÄN YLIOPISTO
UNIVERSITY OF JYVÄSKYLÄ

JYVÄSKYLÄ 2019

Editors
Matti Haukka
Department of Chemistry, University of Jyväskylä
Ville Korkiakangas
Open Science Centre, University of Jyväskylä

Permanent link to this publication: http://urn.fi/URN:ISBN:978-951-39-7707-8

ISBN 978-951-39-7707-8 (PDF)
URN:ISBN:978-951-39-7707-8
ISSN 2489-9003

ABSTRACT

Bulatov, Evgeny
Synthetic and structural studies of covalent and non-covalent interactions of ligands and metal center in platinum(II) complexes containing 2,2′-dipyridylamine or oxime ligands
Jyväskylä: University of Jyväskylä, 2019, 58 p.
(JYU Dissertations
ISSN 2489-9003; 70)
ISBN 978-951-39-7707-8 (PDF)

Coordination compounds of platinum(II) have played an important role in the development of coordination chemistry, and even nowadays new aspects of their structural diversity and reactivity continue to emerge. Applications of platinum(II) complexes span across various fields of modern technology and medicine. For this reason, the chemistry of platinum(II) complexes remains an important area of modern research. This dissertation aims to advance the knowledge of chemistry of this class of coordination compounds by classifying their chemical interactions in two domains: strength and location.

The first chapter provides a short introduction into concepts of covalent and non-covalent interactions and coordination compounds. Next, platinum(II) complexes are introduced, and their key structural and electronic features are discussed utilizing very simple models.

In the second chapter, the classification of various interactions of platinum(II) complexes into covalent and non-covalent by strength, and into those affecting ligands and the metal center by location is introduced. The resulting four types of interactions are discussed in more detail.

The third chapter presents new contributions to each of the four fields. Benzylation of 2,2′-dipyridylamine (dpa) coordinated to platinum(II) involves covalent interactions of the ligands. Formation of hydrogen bonded supramolecular ensembles from oxime platinum(II) complexes and crown ether 18-crown-6 involves non-covalent interactions of the ligands. Oxidative chlorination of oxime platinum(II) complexes using *N,N*-dichlorotosylamide (dichloramine T) represents an example of covalent interactions of the metal center. Finally, unusual intramolecular Pt···I interactions in a platinum(II) complex with 2-iodobenzyldi(2-pyridyl)amine ligands involve non-covalent interactions of the metal center.

The last chapter summarizes the key findings and conclusions of this work. Overall, the reported results demonstrate that the proposed classification of chemical interactions of platinum(II) complexes can be useful in development of novel reactivity and applications of these compounds.

Keywords: coordination chemistry, platinum, non-covalent interactions, 2,2′-dipyridylamine, crown ether, *N,N*-dichlorotosylamide, dichloramine T

Author's address

Evgeny Bulatov
Department of Chemistry
P.O. Box 35
FI-40014 University of Jyväskylä
Jyväskylä, Finland
evgeny.e.bulatov@jyu.fi

Supervisor

Professor Matti Haukka
Department of Chemistry
University of Jyväskylä
Jyväskylä, Finland

Reviewers

Professor Timo Repo
Department of Chemistry
University of Helsinki
Helsinki, Finland

Docent Ari Lehtonen
Department of Chemistry
University of Turku
Turku, Finland

Opponent

Dr. Ebbe Nordlander
Natural Science Faculty
Lund University
Lund, Sweden

PREFACE

The research reported in this dissertation was carried out during my BSc, MSc, and PhD studies at the Institute of Chemistry, Saint Petersburg State University, Russia (2009–2012), and the Department of Chemistry, University of Jyväskylä, Finland (2012–2019). Research funding during my PhD studies was provided by the Department of Chemistry, University of Jyväskylä. Prof. Timo Repo and Dr. Ari Lehtonen are warmly acknowledged for their insightful revision of this dissertation.

This dissertation summarizes four quite independent projects, in which I was involved during these years, reduced to a common denominator for sake of integrity. This implies that some other parts (even ones particularly memorable for me) had to be omitted, which was not an easy decision to make. Yet, I believe that this book represents a major milestone in my growth as a scientist. Writing it required me to step back and look at the bigger picture of the field in which I've been working, of chemistry in general, and even of science and the scientific community as a whole. I found myself being proud and happy to belong to this community, which is my most significant personal achievement in my PhD studies.

This could hardly be possible without all of the freedom, trust, and encouragement from my supervisor Prof. Matti Haukka. I thank you for finding financial support for my studies, for the inspiration that you gave me, and for the coffee breaks and meetings we've had during these years.

Working under supervision of Dr. Tatiana Chulkova at the earlier stages of my studies was fundamental for all of my following endeavors. Thank you for taking care of a young chemist trying to get his hands on organic synthesis for the first time, for sharing your wisdom in academic life, and for all the tea and cookies during my first hungry years at the University.

As the famous proverb says, "Tell me who your friends are and I will tell you who you are." I am very proud to have so many educated and interesting friends whom I've met during my studies. Thank you all for the nice moments we shared, for being who you are, and for keeping in touch sometimes even despite the distance.

I'm grateful to my beloved wife Margarita for all her support during the ups and downs of my studies. Thank you for believing in me at all times, and thank you for our little Evelina—writing this dissertation could have appeared much more difficult without the charm of her first smiles. Finally, I'd like to thank my parents for appreciating my way of life and always being there for support and advice.

Jyväskylä 7.3.2019
Evgeny Bulatov

LIST OF ORIGINAL PUBLICATIONS

I E. Bulatov and M. Haukka, Non-conventional Synthesis and Photophysical Studies of Platinum(II) Complexes with Methylene Bridged 2,2′-Dipyridylamine Derivatives, *Dalton Trans.*, **2019**, *48*, 3369–3379.

II E. Yu. Bulatov, T. G. Chulkova, M. Haukka and V. Yu. Kukushkin, A 2D Network in Co-Crystal (1:1) Based on *trans*-[$PtBr_2$(Acetoxime)$_2$] and 18-Crown-6, *J. Chem. Crystallogr.*, **2012**, *42*, 352–355.

III E. Yu. Bulatov, T. G. Chulkova, I. A. Boyarskaya, V. V. Kondratiev, M. Haukka and V. Yu. Kukushkin, Triple Associates Based on (Oxime)Pt(II) Species, 18-Crown-6, and Water: Synthesis, Structural Characterization, and DFT Study, *J. Mol. Struct.*, **2014**, *1068*, 176–181.

IV A. M. Afanasenko, E. Yu. Bulatov, T. G. Chulkova, M. Haukka and F. M. Dolgushin, An Efficient Method for Selective Oxidation of (Oxime)Pt(II) to (Oxime)Pt(IV) Species Using *N,N*-Dichlorotosylamide, *Transition Met. Chem.*, **2016**, *41*, 387–392.

V E. Bulatov, T. Eskelinen, A. Ivanov, P. Tolsoy, P. Hirva and M. Haukka, Unusual Intramolecular Pt···I Non-covalent Interactions in Bis(2-iodobenzyldi(2-pyridyl)amine)platinum(II) Complex, *manuscript in preparation*.

Author's contribution

The author of the present dissertation performed all syntheses, characterizations, X-ray structural analyses, and photophysical studies presented in publications **I** and **V**, crystallization experiments presented in publications **II** and **III**, and contributed to synthesis and characterization presented in publication **IV**. The author took part in writing all of the aforementioned publications, and wrote the first drafts of publications **I** and **V**.

Other related publications by the author

vi E. Bulatov, A. Afanasenko, T. Chulkova and M. Haukka, Bis(hydroxyammonium) Hexachloridoplatinate(IV) – 18-Crown-6 (1/2), *Acta Cryst. E*, **2014**, 70, m7–8.

vii E. Bulatov and M. Haukka, Revisited Dual Luminescence of 2,2′-Dipyridylamine Hydrochloride in Solution and Physical Processes behind It, *ChemistrySelect*, **2018**, 3, 11535–11540.

viii D. V. Boyarskaya, E. Bulatov, I. A. Boyarskaya, T. G. Chulkova, V. A. Rassadin, E. G. Tolstopjatova, I. E. Kolesnikov, M. S. Avdontceva, T. L. Panikorovskii, V. V. Suslonov and M. Haukka, Syntheses, Structures and Photophysical Properties of a Series of Acyclic Diaminocarbene Palladium(II) Complexes Derived from 3,4-Diaryl-1*H*-pyrrol-2,5-diimines and Bisisocyanide Palladium(II) Complexes, *Organometallics,* **2019**, 38, 300–309.

ix K. Kolari, R. Tatikonda, K. Bertula, E. Bulatov, Nonappa and M. Haukka, Metallogelation of Perfluorinated Terpyridine Complexes Induced by Formation of Pt···Pt and F···F Interactions, *manuscript in preparation*.

CONTENTS

ABBREVIATIONS

BCP	Bond critical point
bipy	Bipyridine
C-PCM	Conductor-like polarizable continuum model
CSD	Cambridge Structural Database
DFT	Density functional theory
diars	*o*-Phenylenebis(dimethylarsine)
dpa	2,2′-Dipyridylamine
dpme	1,2-Bis(dimethylphosphino)ethane
en	1,2-Ethylenediamine
HOMO	Highest occupied molecular orbital
ICSD	Inorganic Crystal Structure Database
IMMS	Ion mobility mass spectrometry
IUPAC	International Union of Pure and Applied Chemistry
LUMO	Lowest unoccupied molecular orbital
MOF	Metal-organic frameworks
mt	Methimazolyl
OEP	Octaethylporphyrin
POLED	Phosphorescent organic light emitting device
QTAIM	Quantum theory of atoms in molecules

1 INTRODUCTION

Before diving into the diverse chemistry of coordination compounds, key definitions and models need to be established. In this chapter, main concepts used in this dissertation are defined at very basic levels. More in-depth discussions focused on coordination chemistry of platinum(II) are presented in chapter 2.

1.1 Chemical bond, covalent and non-covalent interactions

According to the International Union of Pure and Applied Chemistry (IUPAC),[1] a chemical bond is an attractive interaction between two or more atoms. Formation of a *covalent* chemical bond is usually understood as sharing of an electron pair between two or more atoms. True covalent interaction implies sharing the electrons equally between the atoms, whereas in reality, the electron density is usually shifted more to one of the bonded atoms, and the extent of that shift defines how much covalent and ionic characters the given bond possesses.

On the other hand, atoms and molecules also interact with each other without sharing their electrons. Such *non-covalent* interactions include electrostatic interactions between charged and/or polarized entities and dispersive interactions. Ion-ion, dipole-dipole, and ion-dipole interactions are examples of electrostatic non-covalent interactions, which are due to Coulomb interactions of charged particles. Dispersion is, in principle, a kind of polarization, and dispersive interactions are in fact also due to Coulomb interactions of polarizable moieties.[2]

Non-covalent interactions are sometimes considered to involve both non-covalent (electrostatic and dispersive) and electron sharing (charge transfer or covalent) components to different extents. However, the amount of electron sharing in weak interactions is not only practically impossible to observe experimentally but is also principally indistinguishable from the polarization of electron density.[3] Therefore, experimentally observed energetic and geometry crite-

ria are better suited to describe and compare various non-covalent and covalent interactions.

Covalent bonds are typically of a short range (less than 2 Å) and high energy (over 200 kJ/mol), whereas non-covalent interactions act within longer distances (typically 2–5 Å) and are less energetic (typically under a few tens of kJ/mol).[4] Naturally, there is no sharp line between the two types of interactions, and borderline cases (for example, very strong hydrogen bonds)[5] can be considered as either strong non-covalent or weak covalent interactions, as depicted in Fig. 1.

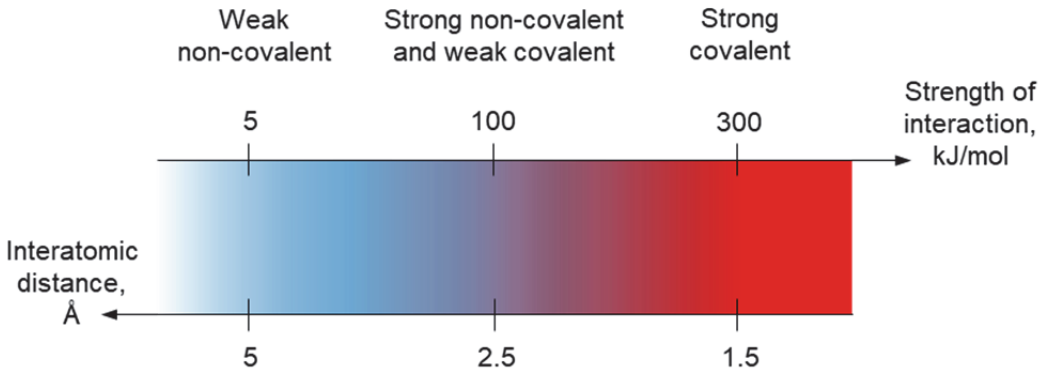

FIGURE 1 Differentiation of non-covalent and covalent interactions by strength and length.

Interaction energies can be estimated computationally or obtained experimentally, using methods of physical chemistry and thermodynamics. Interatomic distances are observed with help of X-ray diffraction methods in crystalline materials; various spectroscopy methods can also be used. The values presented in Fig. 1 are only illustrative; interaction strengths and lengths depend on types of atoms involved.

In addition to drawing a line between covalent and non-covalent interactions (middle region of the scale in Fig. 1), the problem also exists in determining the very existence of extremely weak chemical interactions between given entities (leftmost region of the scale). It makes practical sense to associate existence of a chemical interaction with an observation of its impact on some macroscopic properties of materials.[6] One of the most common primary criteria of an interaction between two atoms is a structural one: two atoms may interact with each other when distance between them is less than sum of their Van der Waals radii.[7,8] Due to the fact that atoms are generally not spherical, and that Van der Waals radii are in turn determined by averaging observed non-bonding distances, this criterion, despite its practicality, is insufficient. Therefore, in order to verify presence or absence of weak non-covalent interactions, further spectroscopic or computational studies should be employed.

1.2 Coordination compounds

1.2.1 Definition and structure

According to the Red Book of IUPAC,[9] a coordination compound is any compound that contains a coordination entity. A coordination entity, or complex, is an ion or neutral molecule that is composed of a central atom (metal), to which other atoms or groups of atoms (ligands) are attached. A coordination entity is schematically presented in Fig. 2, where M is the central atom and $L^{a\text{-}d}$ are ligands.

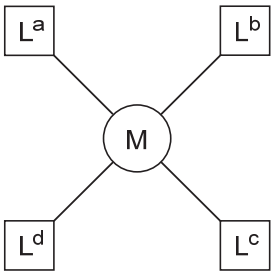

FIGURE 2 Schematic representation of a coordination entity (complex).

Diversity of coordination chemistry comes, first of all, from a great variety of metal atoms and practically an infinite number of possible ligands. Moreover, Fig. 2 represents only one type of complexes (ML_4). The number of both central atoms and ligands can be in principle any (more or equal to one), and multiple metal centers and ligands may or may not be the same. A ligand may have single (monodentate) or multiple (polydentate) metal binding sites, and may be bound to one (terminal in case of one bond and chelating in case of multiple bonds) or more (bridging) central atoms. Moreover, multiple metal centers may form bonds with each other. This thesis focuses on mononuclear coordination compounds containing platinum as a single central atom.

Bonding between ligands and the metal center, represented by solid lines in Fig. 2, is typically referred to as *dative* covalent bonding, meaning that ligands serve as donors and the central atom as the acceptor of electron pairs.[1] In other words, ligands and the metal center typically act as Lewis bases and acid accordingly. In some instances, however, the roles can be interchanged, and some ligands (referred to as Z-type ligands, for example, compounds of boron)[10] can act as Lewis acids. Even though this concept is normally used to classify covalent bonding between the central atom and ligands in coordination compounds, the Lewis acid-base approach can also be used to describe their weaker non-covalent interactions, as discussed later in chapter 2.

Various modes of reactivity of coordination compounds further contribute to diversity of coordination chemistry. Just like any other entities, coordination compounds can participate in covalent and non-covalent interactions. Additionally, division by location can be made: chemical interactions may take place

on either ligand or central atom sites, or both. Reactions located on ligands may involve destruction and/or formation of chemical bonds within the ligand structure. Reactions located on the central atom may involve destruction and/or formation of chemical bonds with ligands (reactions of coordination, decoordination, and ligand exchange), change of coordination geometry around central atom, and change in oxidation state. In most of real chemical processes, the mentioned reactions are elementary stages of more complex reaction mechanisms, such as metal-catalyzed or metal-promoted reactions. Moreover, changes in structure of ligands can affect coordination geometry and electron density on metal center and *vice versa*. Therefore, such separation of chemical interactions by location is not absolute, and not every reaction can be classified into either of the two categories. This dissertation focuses on reactions affecting selectively ligands or the metal center.

1.2.2 Coordination compounds of platinum

The history of platinum begins from as far as ancient Egypt; however, it has been recognized as an individual element only since the middle of the XVIII century after careful separation from other platinum group metals.[11] Platinum is known as a noble metal due to its rarity and high resistance towards corrosion. Nevertheless, its chemistry is very broad and diverse, and its exploration has led to milestone discoveries, such as Zeise's salt as one of the first known organometallic compounds,[12] Magnus' green salt and metal wires derived from it,[13,14] *cis*- and *trans*-effects of ligands in metal complexes.[15] More recently, development of platinum chemistry made significant contribution to the field of cross-coupling reactions,[16] anticancer treatment,[17] and to the technology of phosphorescent organic light emitting devices (POLEDs).[18]

The most common oxidation states for platinum mononuclear coordination compounds are +2 and +4, whereas odd oxidation states +1 and +3 are usually stable in polynuclear complexes only.[19] The great variety of platinum(0) mono and polynuclear complexes has been discovered in the last half century,[20] and experimental evidence on negative oxidation states in platinides has only been acquired relatively recently.[21] This dissertation mostly focuses on coordination compounds of platinum in oxidation state +2 (in part also including +4); thus, the key features of these compounds are considered below from the electronic point of view. A simple model of the electronic structure of the metal center includes its *electronic configuration* and its interaction with surrounding ligands, the latter treated using *crystal field theory*.

1.2.2.1 Electronic configuration of central atom

Electronic configuration includes number of electrons formally residing on a metal center, taking into account its oxidation state, and their distribution on atomic orbitals. Normally, for d-block metals only electrons of the outmost electron shell and d-electrons from the previous shell are considered, whereas the rest of electrons are deemed as the electronic core with configuration of preceding noble gas atom. For platinum, the number of electrons on the outmost shell

is 8 and 6, and electronic configurations of the metal are $5d^8$ and $5d^6$ in coordination compounds of platinum(II) and platinum(IV), accordingly.[22]

1.2.2.2 Crystal field theory

Unlike a free atom in vacuum, in which all five d-orbitals, presented in Fig. 3a, are degenerate in energy, the metal center in a coordination compound is surrounded by ligands, and differently oriented d-orbitals interact with ligands to different extents, leading to the removal of degeneracy. The model obtained from crystal field theory[23] allows analysis of this energy separation by treating ligands as negative point charges located around a positively charged metal center, thus assuming ionic ligand-metal interactions. Splitting of d-orbital energies ultimately depends on location of the ligands around the metal center. The two geometries most relevant for this thesis are octahedral (coordination number 6, with ligands located on the three axes) and square-planar (coordination number 4, with ligands located on axes Ox and Oy), typical for platinum in oxidation states +4 and +2 accordingly. The splitting presented in Fig. 3b is obtained by considering repulsive interaction between electrons on d-orbitals and the negatively charged ligands, resulting in destabilization of the orbitals, and the extent of destabilization depends on orbital orientation. The orbitals are then filled with electrons according to electron count on the metal starting from lowest in energy, thus leaving empty d_{z^2} and $d_{x^2-z^2}$ orbitals in octahedral d^6 complexes and single empty $d_{x^2-z^2}$ orbitals in square-planar d^8 complexes.

It must be noted that the diagrams presented in Fig. 3b assume identical ligands and ligand-metal distances, which is not often encountered in practice. Even then, these diagrams are strictly derived for d^1 or d^6 configurations, whereas for d^6 and d^8, these are only an approximation, as they do not account for repulsion between d-electrons.[24]

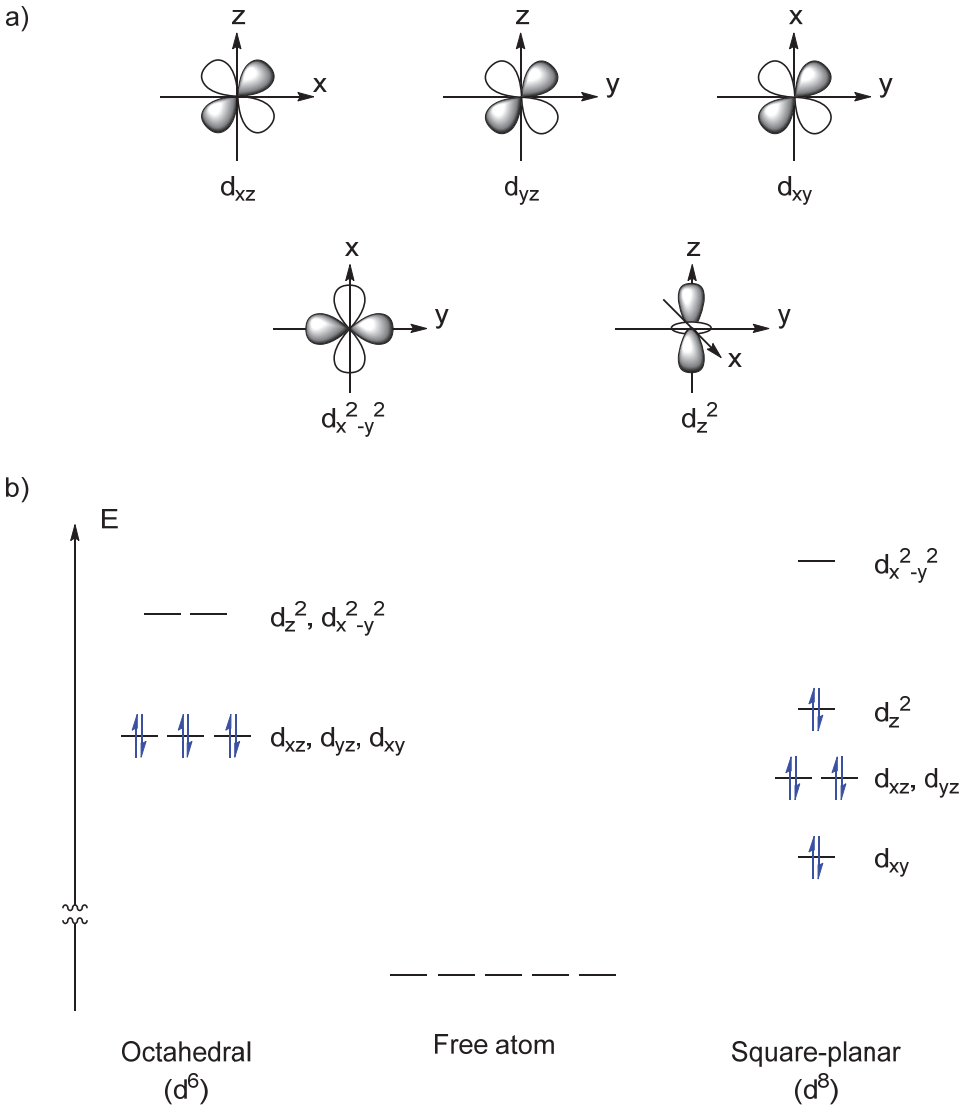

FIGURE 3 Spatial orientation of d-orbitals (a) and their splitting in energy in octahedral and square-planar environments according to crystal field theory (b).

In addition, relative positions of all orbitals (except $d_{x^2-z^2}$) in square planar environment can be different, and the d_{z^2} orbital can appear the second or third highest or even the lowest among them, depending on the properties of metal-ligand bonding.[25–27] In order to describe bonding between ligands and the metal center in more detail, ligand field theory[28] may be used, which combines crystal field and molecular orbital theories. However, the presented basic model of crystal field orbital splitting is sufficient for this dissertation. It can be just mentioned that the relative energy of d_{z^2} orbital depends on the σ- and π-bonding properties of ligands: it is relatively destabilized with ligands acting as strong σ-donors and π-acceptors, and is stabilized in cases of weak σ-donor but π-donating ligands.[27]

The location above and below the coordination plane makes d_{z^2} orbital sterically available and thus very important for covalent and non-covalent interactions located on the metal center, such as oxidative addition reactions,[29]

axial bonding with Lewis acids and bases,[30] hydrogen[31] and halogen[32] bonding, and metallophilic interactions.[33]

1.2.2.3 Key features of platinum(II) complexes

Pronounced ability of coordination compounds of platinum(II) to participate in various interactions involving the metal center (described later in chapter 2) is largely due to their square-planar geometry, which allows access to the central atom without significant steric hindrance. In addition, platinum compounds are known to possess high kinetic stability towards ligand exchange,[34] attributed to high electron density on the platinum center and consequent destabilization of 5-coordinate transition state. This kinetic inertness allowed discoveries of *cis-trans* isomerism[35] and *cis-* and *trans*-effects of ligands[15] on platinum(II) coordination compounds in the past and their use as anti-tumor drugs in the present.[36] The rigid and well-defined structure of these compounds allows their use in design of supramolecular synthons.[37] On the other hand, such kinetic inertness limits catalytic applicability of platinum complexes compared, for example, with their palladium congeners,[38,39] even though platinum based catalysts have been developed as well.[16]

Two particular complexes of platinum(II), presented in Fig. 4, have played central roles in two major discoveries of the last century: transition metal based anticancer drugs and transition metal doped POLEDs. Since the discovery of the anticancer activity of *cis*-$[PtCl_2(NH_3)_2]$ **1**, also known as cisplatin, numerous platinum(II) based drugs have been developed, and currently about 50% of all cancer treatments are based on platinum(II) drugs.[17] The first successful preparation of POLED has been achieved by introduction of [Pt(OEP)] (OEP = octaethylporphyrin) **2** as a doping material into conventional dye based electroluminescent device, and has consequently led to the development of other transition metal based POLEDs.[18] These two examples demonstrate that studies on synthesis and properties of platinum(II) complexes remain an important area of coordination chemistry, medicine, and materials science.

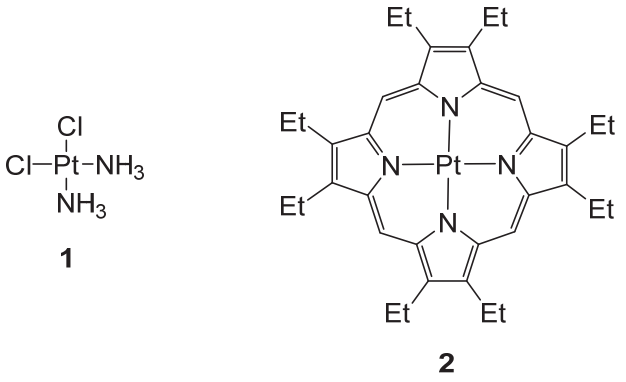

FIGURE 4 Structures of cisplatin **1** and platinum(II) octaethylporphyrin **2**.

2 CHEMISTRY OF COORDINATION COMPOUNDS OF PLATINUM(II)

One possible way to classify the diverse chemistry of square-planar coordination compounds of platinum(II) is by considering their reactivity in two dimensions: location and strength of chemical interactions. Location-wise, coordination compounds may participate in chemical interactions *via* the central atom or ligands. Possible interactions on those sites, in turn, can range from weak non-covalent to strong covalent. Accordingly, chemistry of coordination compounds can be virtually broken down to four separate fields, as presented in Fig. 5.

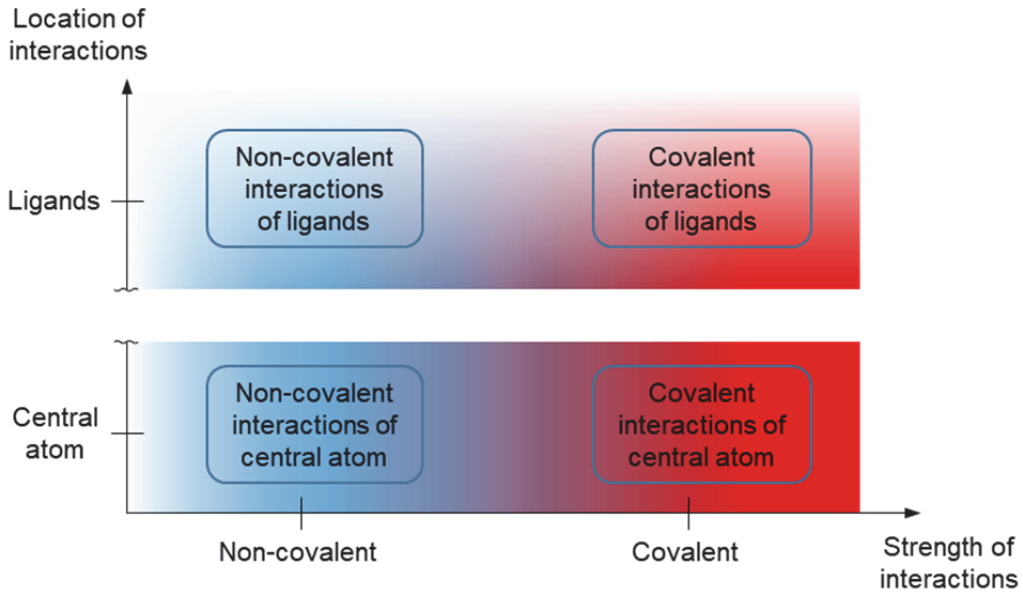

FIGURE 5 Classification of interactions of platinum(II) coordination compounds used in this work.

The color gradients in Fig. 5 further illustrate the classification approach used in this dissertation: a smooth transition from non-covalent to covalent interactions in the strength dimension, but an abrupt change from the central atom to ligands in the location dimension. The continuous scale of strength was

introduced in the previous chapter, and the ambiguous borderline examples are presented later in this chapter. However, the discrete separation of interactions by location does not correspond well to the majority of coordination chemistry, which relies on interplay between ligands and central atoms. Nevertheless, it is used in this dissertation for the purpose of clarity in discussion of reactivity of coordination compounds. Accordingly, the selection of presented in this chapter examples of reactivity of coordination compounds is limited to those where only ligands or only the central atom is affected. While the majority of the chemistry of square-planar platinum(II) complexes involves participation of both ligands and the metal, and thus can not be assigned to either of the two groups, these processes can often be considered as sequences of elementary stages, involving either the central atom or ligands.

The following sections in this chapter focus on relevant literature regarding each of the four fields of chemistry of square-planar platinum(II) complexes from Fig. 5. Other metals are considered only when relevant information related to platinum is scarce or unavailable. Each section includes discussions of general principles of corresponding reactivity and its existing or potential applications. Due to the vast amount of literature available on non-covalent interactions of coordinated ligands in platinum(II) complexes (including hydrogen and halogen bonding, π-stacking and hydrophobic interactions), section 2.2 is limited to discussion of hydrogen bonding interactions, which are relevant for the experimental part of the work. The field of non-covalent interactions on the metal center receives particular attention and is discussed more comprehensively in section 2.4, since it possesses very recent discoveries in some aspects.

2.1 Covalent interactions on ligands

In coordination chemistry, central atoms of coordination compounds are often directly involved in chemical transformations, and properties of the metal center and its interactions with other reaction partners have a major impact on reaction outcomes. However, chemistry of coordinated ligands can be significantly altered even without participation of the metal center in chemical interactions. In other words, the central atom can have an impact on chemical interactions of ligands in remote sites, not directly connected with the metal. In some cases, coordination of an organic molecule to metal may allow reactions, which would be very difficult or impossible to perform by means of pure organic chemistry.

For example, the templating effect of metal atoms allows spatial preorientation of organic molecules by coordination on a metal center, and consequent reactions of the ligands can be used, for example, in synthesis of macrocyclic natural products.[40] Synthesis of interlocked structures, such as rotaxanes, catenanes, and molecular knots, initiated by J.P. Sauvage and coworkers,[41] also relies heavily on the templating effect.[42]

Another example of reactions on coordinated ligands is post synthetic modification of metal-organic frameworks (MOFs). Harsh conditions, often

employed in their solvothermal synthesis, may not be compatible with various organic functional groups, which thus need to be introduced after formation of MOFs by chemical modification of coordinated and immobilized organic ligands.[43]

Yet, examples of modification of coordinated ligands in synthesis of coordination compounds are quite limited, and small complexes are usually obtained by organic synthesis of ligands followed by their coordination on the metal center as the last step. Particularly, reactions on remote from the metal centers sites of ligands are much less exploited, even though benefits of such an approach have been demonstrated for complexes of osmium(II) and ruthenium(II), probably due to their applicability as photoactive materials. Such reactions have been termed as "organic chemistry of coordination compounds,"[44] "metal-directed synthesis,"[45] or "chemistry-on-the-complex."[46] The same approach has been utilized for modification of N-heterocyclic carbene complexes of some other metals.[47,48]

Surprisingly, this approach is almost unexplored in synthesis of platinum(II) compounds. Two of the rare examples of organic chemistry on ligands of platinum(II) complexes are presented in Fig. 6. Reaction of bis(imidoylamidinate)platinum(II) complex **3** with methyl trifluoromethanesulfonate furnishes the methylated derivative **4**.[49] Chlorination of bis(salicylaldoximato)platinum(II) complex **5** with molecular chlorine results in oxidation of the metal center and chlorination of the aromatic rings, thus affording platinum(IV) product **6**.[50]

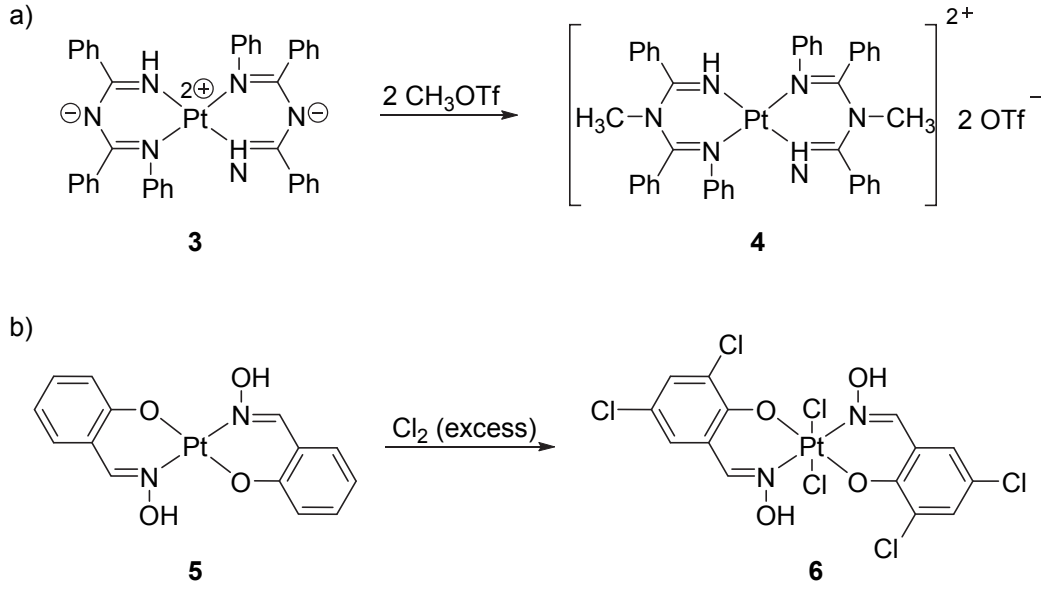

FIGURE 6 Examples of modification of ligands coordinated to platinum(II): a) methylation of bis(imidoylamidinate)platinum(II) **3**;[49] b) chlorination of bis(salicylaldoximato)platinum(II) **5**.[50]

The latter example involves reactions of both ligands and the metal center, but its importance is to demonstrate the potential to perform organic reactions

on molecules coordinated to platinum(II). Chlorination of salicylaldoxime in free form proceeds with partial deoximation, whereas coordination to platinum(II) results in protection of the oxime moiety, and the chlorination proceeds selectively in the phenyl ring in good yield.[50,51]

Since modification of ligands after coordination appeared useful in synthesis of ruthenium(II) complexes,[46] the same approach could be borrowed and developed for efficient synthesis of coordination compounds of platinum(II). The latter could be advantageous, for instance, in preparation of luminescent materials, catalysts, or antitumor drugs.

2.2 Hydrogen bonding interactions on ligands

With the development of coordination chemistry into branches of coordination polymers, MOFs, and finite supramolecular coordination complexes, it has become apparent that including transition metal atoms in supramolecular structures can provide novel materials with a wide range of properties and applications.[52] Metal containing supramolecular structures, formed by non-covalent interactions, are also of great potential, as such systems can possess well-defined and yet flexible structures.[53] Among the non-covalent interactions, hydrogen bonding is usually the strongest one, and its use has been well established in the field of supramolecular organic chemistry.[37] Upon coordination to the metal center, hydrogen bonding properties of ligands may be altered to different extents, depending on the metal center and how remote the coordinating and hydrogen bonding moieties are.[54] In particular, hydrogen bond donor and acceptor abilities (acidity and basicity) of ligands are affected by electronic interactions with metal, whereas their spatial orientation is determined by coordination geometry of the central atom.

Rigidity and stability of platinum(II) complexes favors their use in construction of hydrogen-bonded supramolecular structures. Examples include isomeric linear chains $[H_2bipy][PtCl_4]$ (bipy = 2,2′-, 3,3′-, or 4,4′-bipyridine, **7-9** accordingly), in which chloride atoms of $[PtCl_4]^{2-}$ form hydrogen bonds with the organic cations, as presented in Fig. 7a.[55,56] Further studies on the combination of the tetrachloroplatinate anion with other organic cations illustrated applicability of $[PtCl_4]^{2-}$ as a tecton for synthesis of hydrogen bonded supramolecular networks.[57]

Directional hydrogen bonding between the ligands and rigid coordination geometry are responsible for formation of he square net structure of $Pt(4\text{-py-COO})_2(4\text{-py-COOH})_2{\cdot}2H_2O$ **10**, presented in Fig. 7b. Therefore, **10** represents an example of platinum(II) based hydrogen bonded supramolecular structure with voids, capable of accommodation of guest molecules.[58]

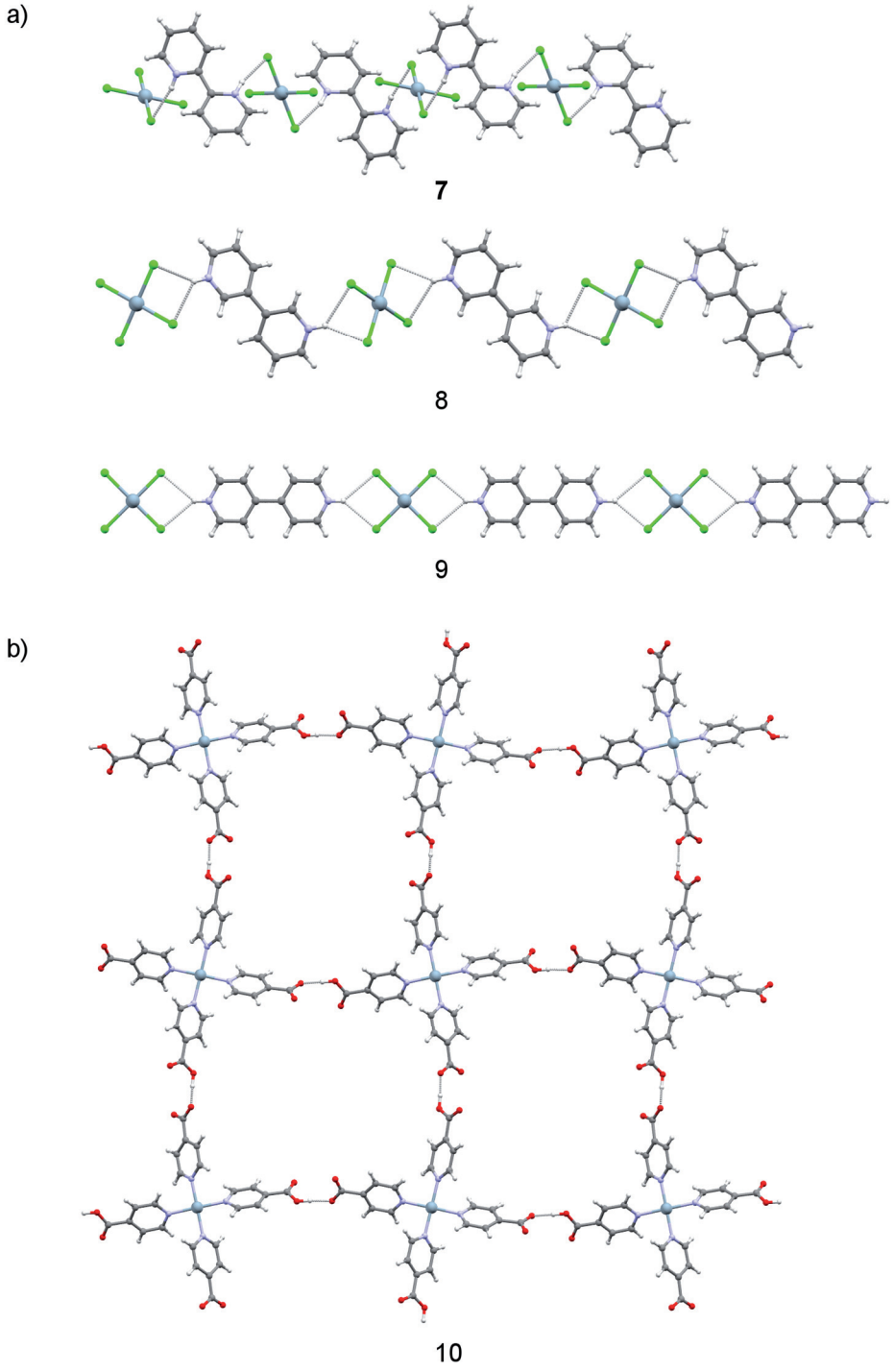

FIGURE 7 Crystal structures of hydrogen bonded associates of platinum(II) complexes: a) linear chains of $[H_2bipy][PtCl_4]$ **7-9** (CSD ref. codes: MADGEE, MADGAA, JITYEQ);[55,56] b) square net of $Pt(4\text{-py-COO})_2(4\text{-py-COOH})_2{\cdot}2H_2O$ **10** (water molecules are omitted for clarity, CSD ref. code: GOKMOI).[58]

Inclusion of additional neutral components can further push the boundaries of potential applications of metal-containing supramolecular structures, but it may also be challenging.[59] Crown ethers are among the molecules, which are likely to form multi-component supramolecular systems. Synthesized by C.

Pedersen in 1967, crown ethers have become famous for their property to form stable complexes with alkali and rare-earth metal cations.[60,61] Despite Pedersen's observation of crown ethers forming complexes with neutral molecules,[62] their potential to bind neutral hydrogen bond donors has been realized significantly later.[63,64]

Some co-crystals of neutral platinum(II) complexes with 18-crown-6 have been reported, including discrete associates 2[*trans*-$PtCl_2(PMe_3)(NH_3)$]·(18-crown-6) **11** presented on Fig. 8. In these associates, the components are held together in crystal structure by hydrogen bonds between ammonia ligands and oxygen atoms of 18-crown-6.[65]

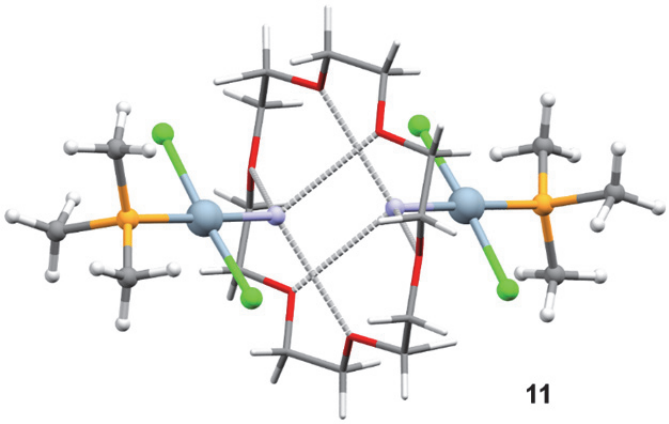

FIGURE 8 Crystal structure of hydrogen bonded discrete associates 2[*trans*-$PtCl_2(PMe_3)(NH_3)$]·(18-crown-6) **11** (CSD ref. code: BAHWEM). Positions of the amino hydrogen atoms are not specified in the crystal structure.[65]

Relatively recently, new supramolecular 1D chain associates *trans*-[$PtCl_n${HN=C(OMe)Et}$_2$]·(18-crown-6) **12** (n = 2) and **13** (n = 4), presented in Fig. 9, were obtained, in which the components are held together in crystal structure by N-H···O and additional C-H···O hydrogen bonds.[66]

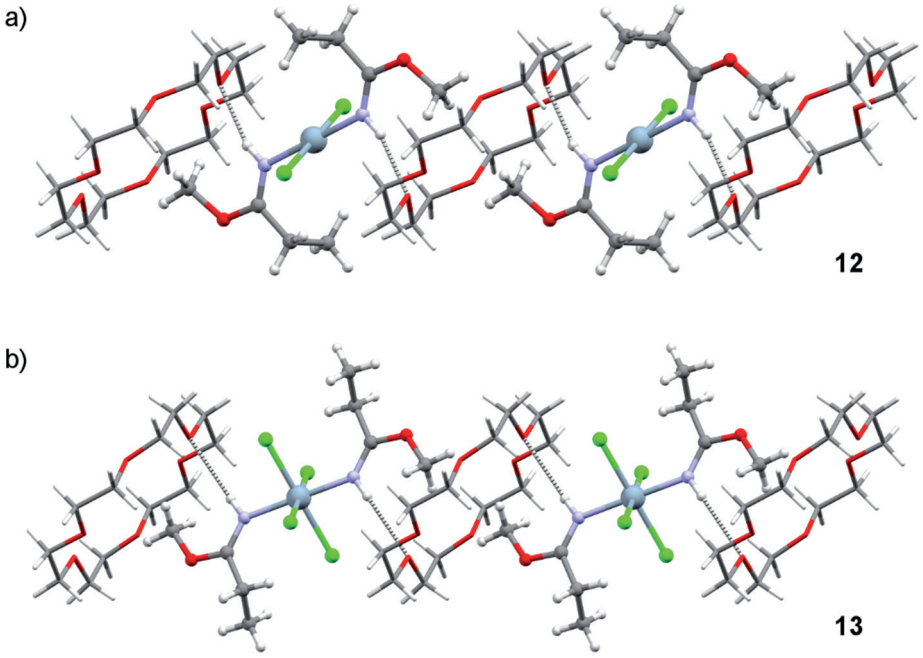

FIGURE 9 Crystal structures of hydrogen bonded chains *trans*-$[PtCl_n\{HN{=}C(OMe)Et\}_2]\cdot$(18-crown-6): a) n = 2, **12**, b) n = 4, **13**. C-H···O hydrogen bonds are not drawn for clarity (CSD ref. codes: YUXZOH, YUXZUN).[66]

2.3 Covalent interactions on metal center

A significant part of coordination chemistry focuses on the central atoms of coordination compounds. As mentioned in chapter 1, reactions on the central atoms may involve destruction and/or formation of chemical bonds with ligands, change of coordination geometry around the central atoms, and change in oxidation states. Among these reactions, only the latter may in principle proceed without substantial changes in ligand environment, for example, in hexaammine ruthenium(II/III)[67] or cobalt (II/III)[68] complexes. However, change in oxidation state is usually accompanied by change in preferred coordination number and/or geometry, and clear isolation of interactions on metal from interactions from ligands is not easy. Platinum in oxidation states +2 and +4 strongly favors 4-coordinate square-planar and 6-coordinate octahedral geometries accordingly, and oxidation of platinum(II) to platinum(IV) is usually accompanied by the addition of two new ligands, hence the name of the reactions—oxidative addition. Reactions of oxidative addition to platinum(II) complexes, in which ligands of the starting complexes remain intact in the products, are considered in this section.

In fact, such reactions are becoming very important in production of anticancer drugs. Since the discovery of the antitumor activity of cisplatin **1**, the

search for alternative antitumor drugs has been heavily focused on platinum(II) coordination compounds.[17] However, more recently, attention has been shifting towards platinum(IV) based prodrugs, typically synthesized by oxidation of the corresponding platinum(II) precursors using simple oxidants, such as molecular halogens or hydrogen peroxide.[69,70]

The mechanism of oxidative addition may be different depending on the reagents, and its elucidation requires thorough studies. Thus, oxidation with peroxide is likely to proceed *via* a concerted three-centered transition state (Fig. 10a), as supported by the observation that oxidation of [(6,6'-diamino-bipy)$PtMe_2$] **14** with hydrogen peroxide affords corresponding *cis*-dihydroxo platinum(IV) product **15** due to the interligand hydrogen bond, in absence of which the product would quickly isomerize into corresponding *trans*-isomer.[71] On the other hand, reaction with halogens is usually considered as an S_N2-type reaction, involving end-on coordination of halogen molecules in the transition state (Fig. 10b). Such a mechanism is supported by the reaction of [PtI(NCN)] (NCN = $C_6H_3\{CH_2NMe_2\}_2$-2,6) **16** with iodine leading to the five-coordinate product [PtI(NCN)(η^1-I_2)] **17** with an axial η^1-coorinated iodine molecule.[72]

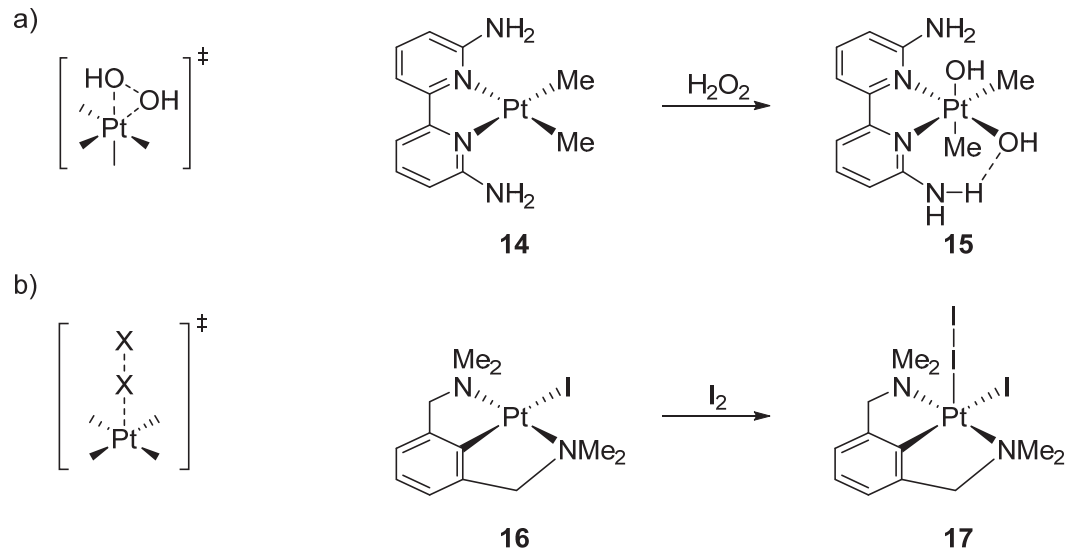

FIGURE 10 Two possible transition states in oxidative addition to platinum(II) complexes and reactions supporting the mechanisms: a) three-centered transition state in reaction with H_2O_2;[71] b) end-on coordinated transition state in reaction with halogens.[72]

Chlorine and hydrogen peroxide are effective, but harmful oxidizing agents. Moreover, oxidation using these reagents is not always selective and may affect not only the metal center but also ligands. For example, in the previously mentioned chlorination of bis(salicylaldoximato)platinum(II) **5,** the reaction proceeds on both metal center and ligands, resulting in the oxidized product **6** with chlorine substituted aromatic rings (Fig. 6).[50] New methods of oxidation of platinum(II) complexes under milder conditions and using more con-

venient oxidizing agents are, therefore, desired particularly in production of antitumor platinum(IV) based prodrugs.[73]

2.4 Non-covalent interactions on metal center

The central atom in a coordination compound can participate not only in strong interactions, such as coordinate bonding, but also in weaker non-covalent ones. These include metallophilic interactions, as well as other σ-hole type non-covalent interactions, such as hydrogen and halogen bonding, and π-hole type interactions with aromatic systems, observed also in organic compounds.

Coordination compounds of platinum(II) are known to participate in various weak interactions *via* the metal atom, majorly due to the geometrically exposed filled d_z^2 orbital, as mentioned in chapter 1. One of the most famous and historically important examples of non-covalent interactions, involving platinum(II), is stacking of planar cations and anions in the crystal structure of Magnus' green salt (**18**, Fig. 11a).[74,75] This and the following discoveries of stacking of anionic (for example, $[Pt(CN)_4]^{2-}$)[76] and cationic (for example, $[Pt(tpy)Cl]^{+}$)[77] species, accompanied with substantial changes in photophysical properties of the materials, ignited great interest in metallophilic interactions of platinum(II).[33]

Another aspect of non-covalent interactions in platinum(II) compounds, namely, hydrogen bonding, in which platinum(II) acts as hydrogen bond acceptor. Such interaction has been structurally evidenced by means of neutron diffraction crystallography almost 30 years ago[78] but became a popular topic of research and discussions mainly after the demonstration of "inverse hydration" of neutral platinum(II) complex **19** in 2010 (Fig. 11b).[79]

Even more recently, halogen bonding capabilities of platinum(II) have been realized from crystal structures of co-crystals of $[PtCl_2(Me_2NCN)_2]$ **20** and analogous platinum(II) complexes with iodoform (Fig. 11c).[80,81] Perhaps, the first example of halogen bonded platinum(II) was the aforementioned five-coordinate compound **17** with an axial η^1-coorinated iodine molecule, but in that case Pt-I bond length of 2.89 Å suggests a rather strong interaction.[72]

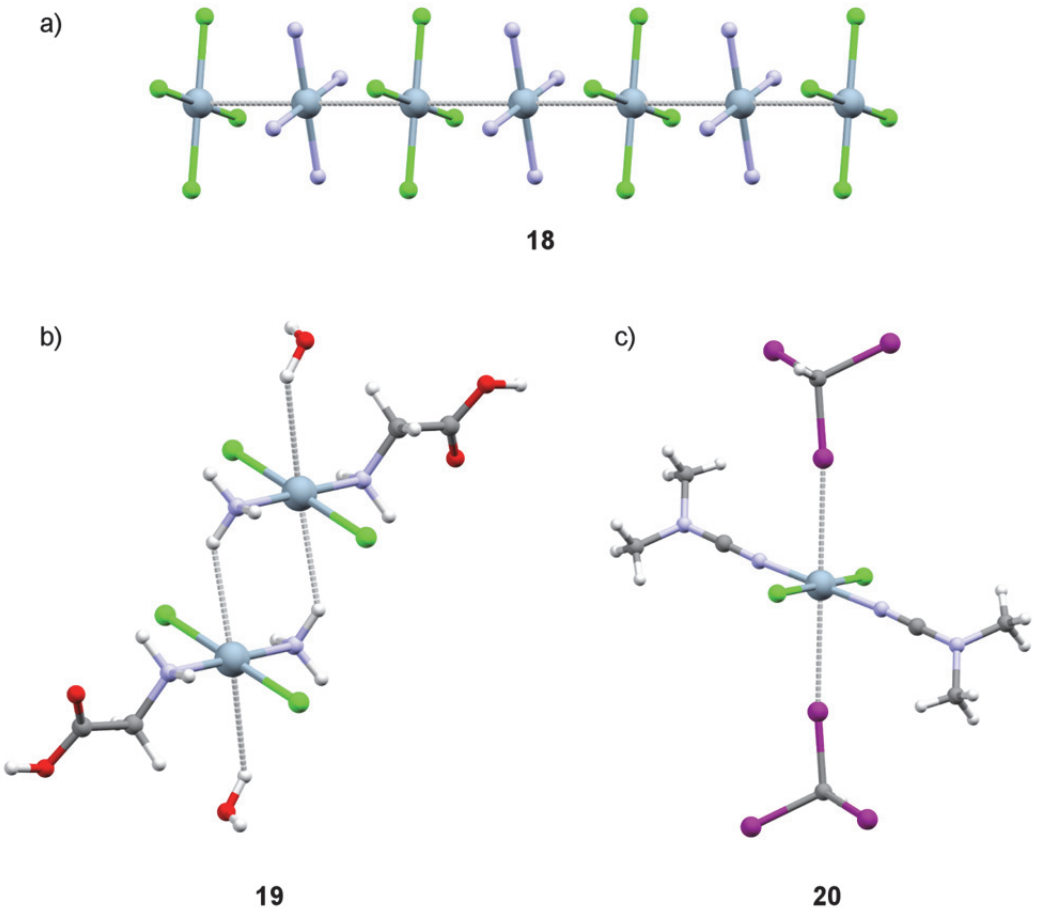

FIGURE 11 Crystal structures of platinum(II) compounds possessing metal-centered non-covalent interactions: a) metallophilic interactions in Magnus' green salt **18** (ICSD coll. code: 26615);[75] b) hydrogen bonding in **19**·H_2O (CSD ref. code: CCAPGC11);[79] c) halogen bonding in **20**·2CHI_3 (CSD ref. code: UKEKIG).[80]

The common feature of all three of these interactions is that they are always located above and below the square plane of the platinum(II) complex. Such orientation suggests involvement of the d_z^2 orbital of the metal center in all of these interactions, whereas electronic structures of the partners vary. In order to rationally classify these and other non-covalent interactions on platinum(II), the model of Lewis bases and acids can be used. In fact, the ability of platinum(II) complexes to act as Lewis bases and acids (which has been attributed to the filled $5d_z^2$ and co-axial vacant $6p_z$ orbitals accordingly), has been realized with substantial data accumulated. Moreover, the cooperative effect of the two interactions has been noticed: interaction with a Lewis acid from one side of the square plane enhances ability of platinum(II) complexes to interact with a base from the other side of the plane, and *vice versa*.[30]

In terms of the Lewis acid and base formalism, platinum(II) can be considered as a Lewis base in both hydrogen and halogen bonding interactions, donating electron pair from the $5d_z^2$ orbital to a proton or a halogen atom, acting, in turn, as Lewis acids. While such interactions of a single platinum(II) complex with two Lewis acids are well established by now, examples of interactions

with two Lewis bases are virtually limited to $[Pt(diars)_2]I_2$ (diars = *o*-phenylenebis(dimethylarsine)) **21**, in crystal structure of which two iodides occupy apical positions above and below the square plane with Pt-I distances of 3.50 Å (Fig. 12).[82]

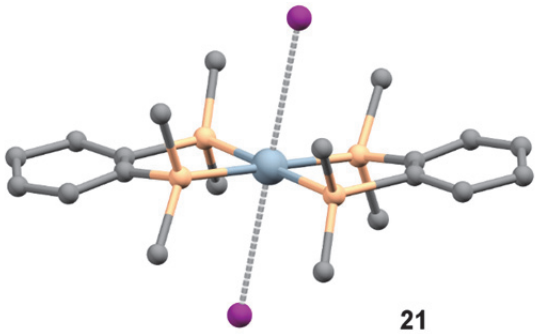

FIGURE 12 Crystal structure of $[Pt(diars)_2]I_2$ **21** (CSD ref. code: IPASPT).

Examples of strong cooperative Lewis acid and base interactions on platinum(II) include octahedral compounds $[PtI(dpme)(\eta^1\text{-}I_2)]I_3$ **[22]I$_3$** (dpme = 1,2-bis(dimethylphosphino)ethane) [83] and $[PtI_2B(mt)_3]$ **23** (mt = methimazolyl).[84] In both of these complexes, the base ligand is iodide anion, and the acid ligands are iodine molecule in **[22]$^+$** and boron atom in **23** (Fig. 13). In the case of compound **23**, the oxidation state of the metal center is a matter of debate, since the donation of an electron pair from platinum to boron in high extent must naturally lead to oxidation of the metal.[85,86] This illustrates well that oxidation state is only a formality, not necessarily reflecting the electron density on the metal center,[29] and that there is no abrupt change from weak non-covalent to strong covalent interactions, as discussed in chapter 1.

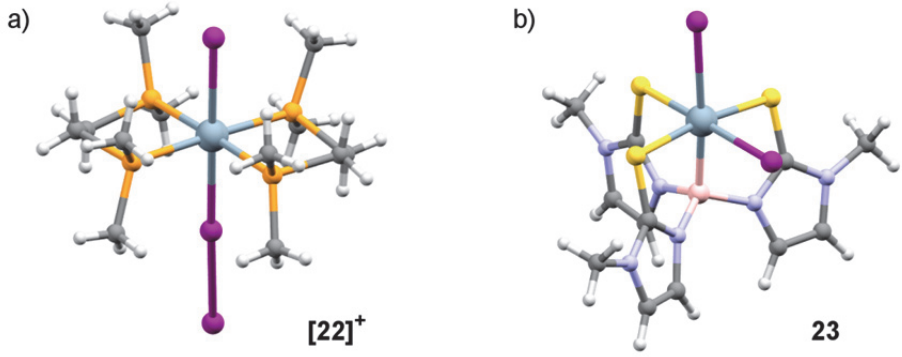

FIGURE 13 Crystal structures of platinum(II) complexes interacting with a Lewis acid from one side and a Lewis base from the other side of square plane: a) cation of $[PtI(dpme)(\eta^1\text{-}I_2)]I_3$ **[22]I$_3$** (CSD ref. code: QUMFIN),[83] b) $[PtI_2B(mt)_3]$ **23** (CSD ref. code: GIXMOQ).[84]

Metallophilic interactions of platinum(II) are not easy to perceive from the point of view of Lewis acid-base interactions because, in this case, platinum atoms simultaneously donate their own d_z^2 electrons and accept d_z^2 electrons from neighboring metal atoms. Such interactions can be thought of as a superposition of resonance structures, as presented in Fig. 14. Since a single platinum is a very weak Lewis acid, both resonance structures in a dimer (Fig. 14a) are unfavorable, but the resonance stabilization can still account for a weak attractive interaction. In a polymeric chain (Fig. 14b), the ability of each platinum to interact with a Lewis base on one side is enhanced by interaction with a Lewis acid on the other side; thus, both resonance structures become more favorable, in agreement with the tendency of metallophilic interactions to facilitate formation of chain structures. Moreover, comparison of these two structures with a double iodide adduct (model for **21**, Fig. 14c) disfavors the latter due to its lack of resonance stabilization, in agreement with the rarity of such interactions.

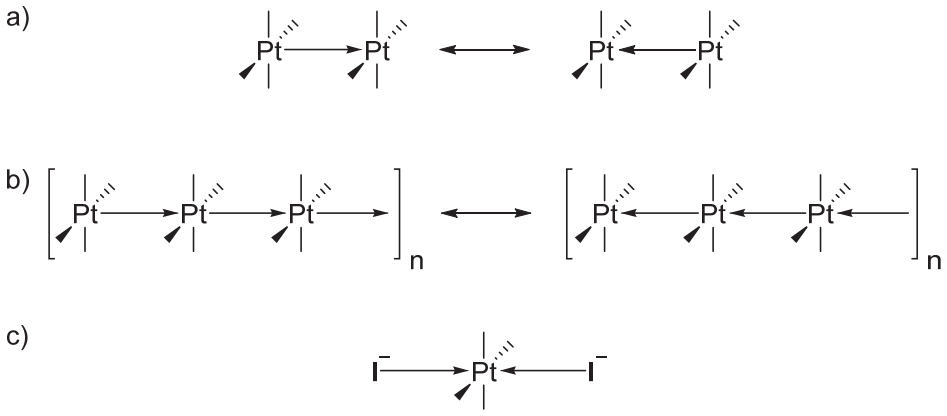

FIGURE 14 Interpretation of metallophilic interactions of platinum(II) complexes within the concept of Lewis acid-base interactions by resonance structures: a) dimer with metallophilic interaction, b) chain of metallophilic interactions, and c) double iodide adduct as a model of **21**.

Thus, application of the simple Lewis acid-base concept allows consideration of all types of covalent and non-covalent interactions of platinum(II), mentioned in this section, within a single framework, without referring to their physical origin. The nature of metallophilic and other non-covalent interactions involving platinum is better described in terms of electrostatic interactions, polarization, and dispersion,[3] whereas models of molecular orbitals[33] and atoms in molecules[87] are commonly used in practice to identify and consistently analyze those interactions.

The importance of non-covalent interactions on the metal center in platinum complexes is in their impact on macroscopic properties of materials rather than their nature or classification. Such interactions can be used as tools in design of supramolecular assemblies.[88] Metallophilic interactions in crystals have been long recognized to induce anisotropic conducting properties, especially upon partial oxidation.[14] In solution, such interactions can promote aggregation and formation of metallogels as well as determine their photophysical proper-

ties.[89] Quenching of fluorescence of dinuclear platinum(II) complexes in solution has been attributed to hydrogen bonding between solvent molecules and metal centers.[90] Other properties attributed to non-covalent interactions on the metal centers will probably be discovered in the near future.

2.5 Aim of the study

The aim of this dissertation was to classify the diverse chemistry of square-planar coordination compounds of platinum(II) by location and strength of chemical interactions, as discussed above, and to make new contributions in the four fields within this framework using platinum(II) complexes with substituted 2,2′-dipyridylamine (dpa) and oxime ligands. The latter were chosen as representatives of N-donor ligands capable of covalent and non-covalent chemical interactions. Accordingly, the following four goals were established to study the four types of chemical interactions:

1) To investigate the reactions of benzylation of dpa coordinated to platinum(II) center, as an example of covalent interactions of ligands, sometimes also referred to as "chemistry on the complex". The applicability of such approach in synthesis of benzyldi(2-pyridyl)amine platinum(II) complexes was then evaluated by comparison with the conventional organic synthesis of the ligands, *i. e.* benzylation of uncoordinated dpa.[I]

2) To obtain and study the structures of hydrogen bonded supramolecular associates of platinum(II) complexes with oxime ligands and crown ether 18-crown-6 in solid state, as an example of non-covalent interactions of ligands. Further, the possibility of using such platinum(II) complexes as supramolecular tectons in hydrogen bonded assemblies was evaluated.[II,III]

3) To develop a method for oxidative chlorination of platinum(II) complexes with oxime ligands using oxidizing agent *N,N*-dichlorotosylamide (dichloramine T) as an example of covalent interactions of the metal center. Selectivity of the new method was then compared to that of the conventional chlorination using molecular chlorine.[IV]

4) One of the complexes with benzylated dpa ligands possessed short intramolecular Pt···I contact in its crystal structure, which was studied as an example of non-covalent interactions of the metal center. The impact of this interaction on conformational equilibria and photophysical properties of the complexes was investigated.[V]

3 RESULTS AND DISCUSSION

This chapter presents findings from separate research projects dealing with coordination chemistry of platinum(II) and described in papers **I–V**, in a logical sequence, corresponding to the classification of chemical interactions of platinum(II) complexes and the goals of the study, established in chapter 2.

Benzylation of coordinated dpa, described in paper **I**, represents an example of the formation of a covalent bond on a ligand site. Hydrogen bonding interactions of coordinated oximes, described in papers **II** and **III**, demonstrate non-covalent interactions of coordinated ligands. Paper **IV** describes application of *N,N*-dichlorotosylamide for chlorination of platinum(II) complexes as an example of strong covalent bonding on the metal center. Finally, paper **V** describes structural, photophysical, and computational studies on weak intramolecular platinum···iodine interaction, which appears to be an unusual example of non-covalent interactions on the platinum(II) center.

3.1 Synthesis of starting platinum(II) complexes[I-IV]

Chemical structures of oxime containing platinum(II) complexes used in this work are presented in Fig. 15a. Complexes *trans*-[$PtCl_2$(acetaldoxime)$_2$] **24**,[91] *cis*-[$PtCl_2$(acetoxime)$_2$] **25**,[92] *cis*-[$PtBr_2$(acetoxime)$_2$] **26**,[93] *trans*-[$PtCl_2$(cyclopentanone oxime)$_2$] **27**,[93] and *trans*-[Pt(*o*-$OC_6H_4CH{=}NOH)_2$] **28**[94] were obtained directly from the reaction of K_2PtCl_4 with corresponding oximes in water (in case of **26**, excess KBr was also added to the reaction mixture). Compounds *trans*-[$PtCl_2$(acetoxime)$_2$] **29**[92] and *trans*-[$PtBr_2$(acetoxime)$_2$] **30**[93] were obtained by thermal isomerization of corresponding *cis*-complexes **25** and **26** in solid state at 140 °C. All of the synthetic procedures have been published previously.

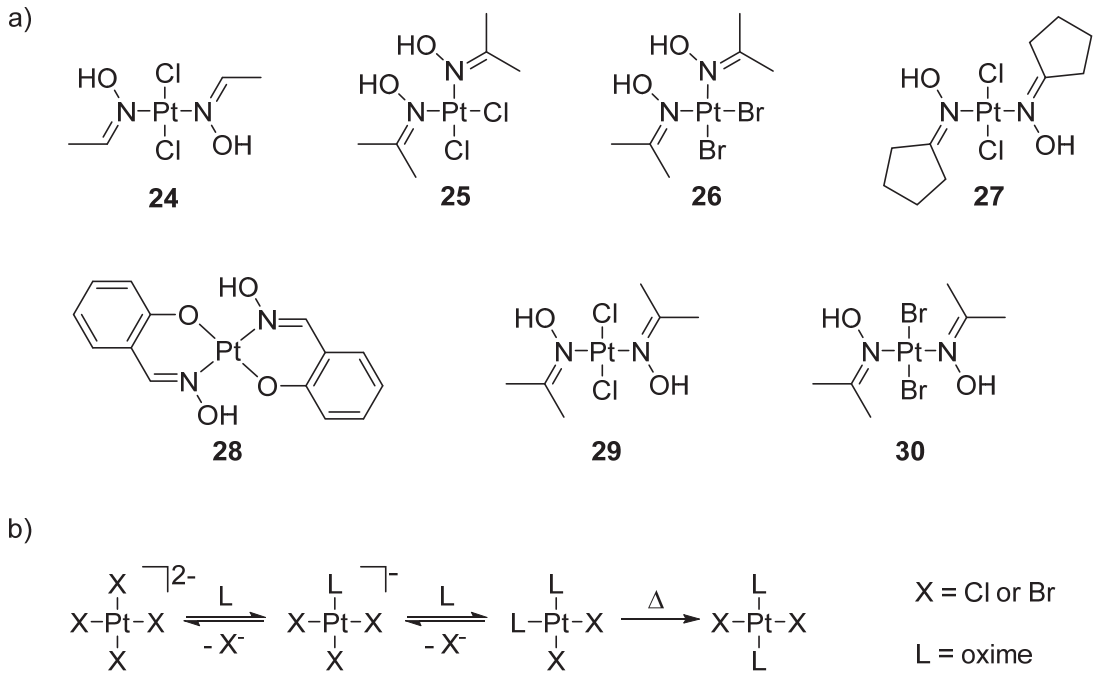

FIGURE 15 Chemical structures of oxime containing platinum(II) complexes **24-30** (a) and general principle of their synthesis (apart from **28**) through reactions of ligand exchange and *cis*/*trans*-isomerization (b).

The ligand exchange on tetrahaloplatinate anion $[PtX_4]^{2-}$, in which two halogenide ligands X^- are replaced with oximes L (Fig. 15b), results initially in kinetic *cis*-products, which can then undergo thermal isomerization into more thermodynamically stable *trans*-products in accordance with the *trans*-effects of the ligands.[35] While some of the *cis*-complexes can be isolated selectively (by controlling reaction time and temperature), in other cases, the isomerization takes place to a significant extent already during the ligand exchange reaction. In particular, *cis*-$[PtCl_2(acetaldoxime)_2]$ could not be isolated, as a mixture of *cis*- and *trans*-isomers results from the ligand exchange reaction at room temperature.[91]

Coordination of two equivalents of dpa **31** to platinum by reacting it with K_2PtCl_4 in two steps, followed by deprotonation of the amino groups, afforded the bis(2,2′-dipyridylamide)platinum(II) complex **32**. The three-step synthetic procedure, published previously,[95] is presented in Fig. 16.

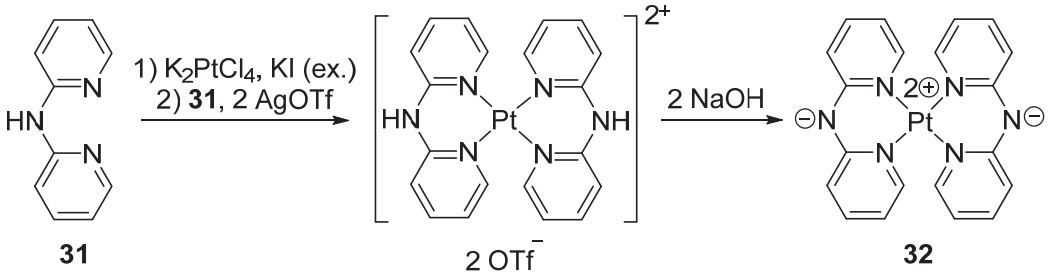

FIGURE 16 Synthesis of bis(2,2′-dipyridylamide)platinum(II) complex **32**.[95]

3.2 Synthesis of methylene bridged 2,2′-dipyridylamine derivatives[I]

In continuation of study on luminescent properties of dpa salts,[96] methylene bridged dpa derivatives with benzyl substituents at the amino nitrogen atom of dpa were investigated, due to the substituent's bulkiness and flexibility. Derivatives with hydrogen, iodine, nitro, and cyano group in the *ortho*-position of the phenyl ring (compounds **33-36**, Fig. 17) were chosen as simple representatives with various steric and electronic properties. However, organic synthesis of derivatives **33-36** using known procedure[97] from dpa and corresponding benzyl bromides appeared to be problematic, especially for derivatives with electron withdrawing substituents.

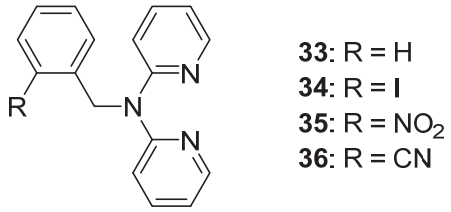

FIGURE 17 Chemical structures of methylene bridged dpa derivatives **33-36** studied in this work.

3.2.1 Organic synthesis

Compounds **33** and **34** were obtained with 26 and 44% yields accordingly using published procedure by reacting dpa with corresponding benzyl bromides in DMSO in the presence of potassium hydroxide (Fig. 18a).[97] However, this method proved unsuitable for synthesis of **35**, and identification of side products in this case allowed to conclude what side processes reduce the yield of the target derivatives. Benzyl bromide, apart from the target reaction with dpa on the amino nitrogen atom, can also react with pyridine nitrogen atoms of dpa, affording bis-pyridine-substituted derivative **37**, and with the base, affording corresponding stilbene **38** (Fig. 18b,c). The latter reaction is particularly significant, when the substituent in phenyl ring possesses strong electron withdrawing properties, leading to enhanced acidity of the methylene moiety.

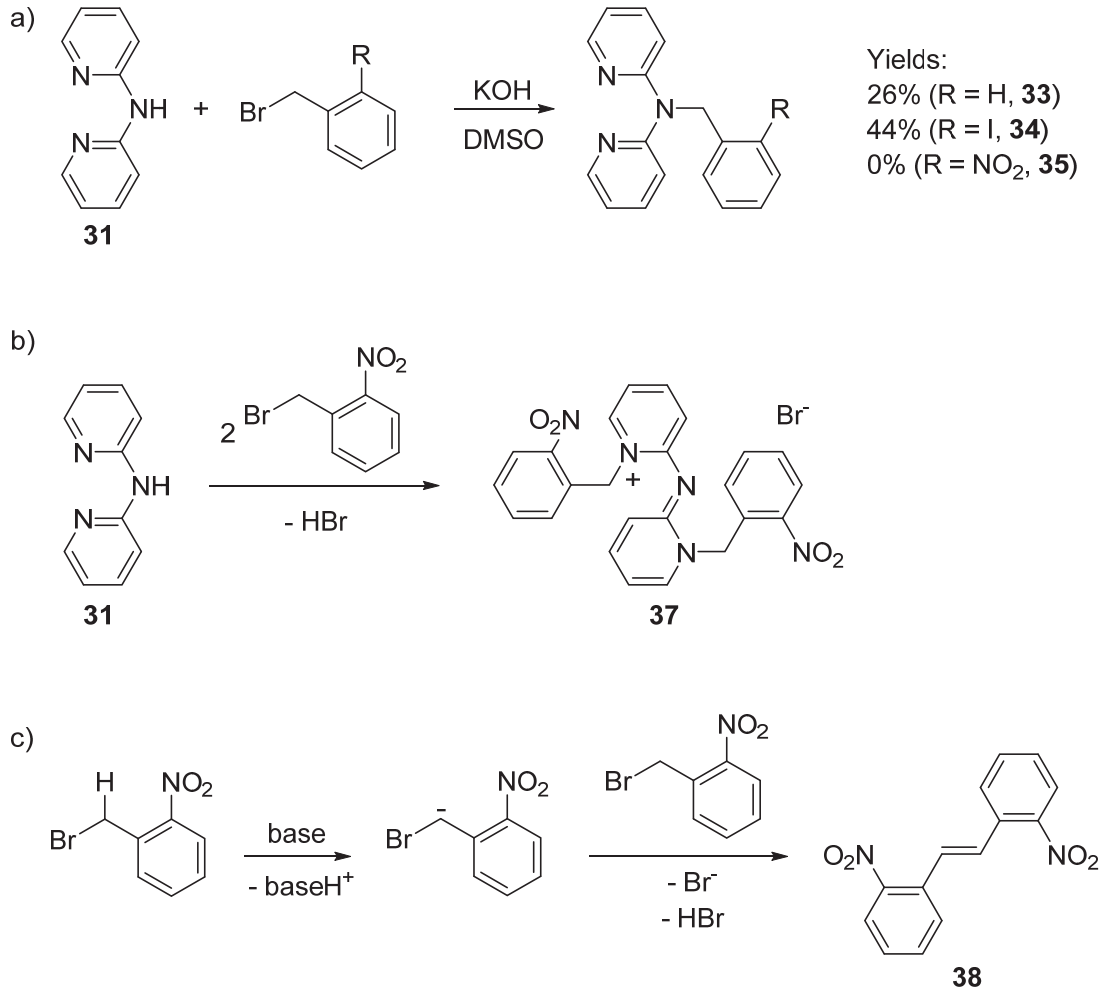

FIGURE 18 Target reaction (a) and undesired side processes (b, c) in synthesis of **33-36** using organic synthetic approach.

3.2.2 "Chemistry on the complex"

In light of these observations, no attempts to synthesize the cyano-substituted derivative **36** using the organic approach were made, and an alternative synthesis of the derivatives based on implication of the "chemistry on the complex" approach[46] was undertaken. In this case, platinum(II) was used as a metal center, since preparation of the corresponding starting complex **32** has been reported previously.[95] In addition, analysis of literature on platinum(II) complexes with methylene bridged dpa derivatives revealed that some of those works could take advantage of such a synthetic approach.[98,99]

Complex **32** was successfully subjected to benzylation reactions using two equivalents of corresponding benzyl bromides, as presented in Fig. 19. The target complexes **[39-42]Br$_2$** were obtained in 64–97% yields by evaporating the reaction mixtures and recrystallizing the obtained precipitates.

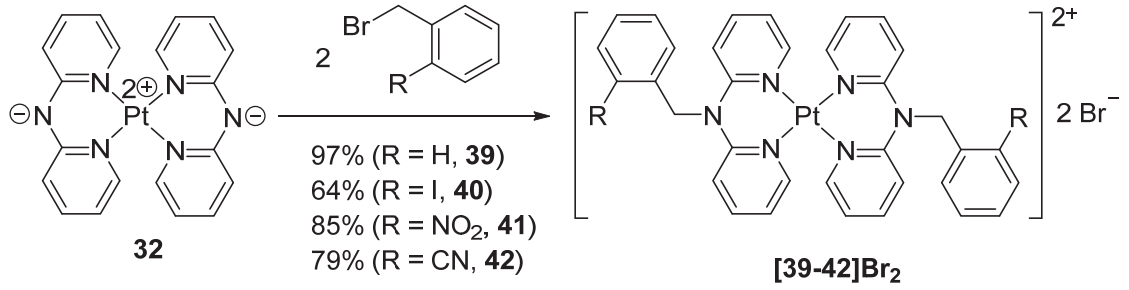

FIGURE 19 Synthesis of methylene bridged dpa derivatives using "chemistry on the complex" approach by benzylation of **32**.

3.2.3 Comparison of the two approaches

Coordination of dpa **31** on platinum(II) protects the pyridine nitrogen atoms from benzylation, thus preventing formation of pyridine-substituted side products like **37**. Synthesis of stable **32** with deprotonated dpa ligands allows to avoid contact between benzyl bromides and a base, thus preventing formation of stilbenes like **38**. As a result, coordination on platinum(II) greatly improves yield of the benzylation reaction (Table 1), even though the reaction site on dpa is not directly connected with the metal center.

TABLE 1 Yields of reactions of benzylation of dpa in free and coordinated forms

R	Yields of benzylation in two approaches, %	
	Organic	On the complex
H	26	97
I	44	64
NO_2	0	85
CN	–	79

If synthesis of a series of platinum(II) complexes with methylene bridged dpa derivatives is considered as the primary objective, modification of the organic ligand after coordination on metal center represents a much more efficient synthetic strategy, compared to the conventional "organic synthesis → coordination chemistry" sequence. Indeed, a strategy involving derivatization at the last stage of synthesis decreases the number of steps compared to a strategy employing derivatization in the first step, and the efficiency difference is proportional to the number of intermediate steps and complexes in the series (Fig. 20).

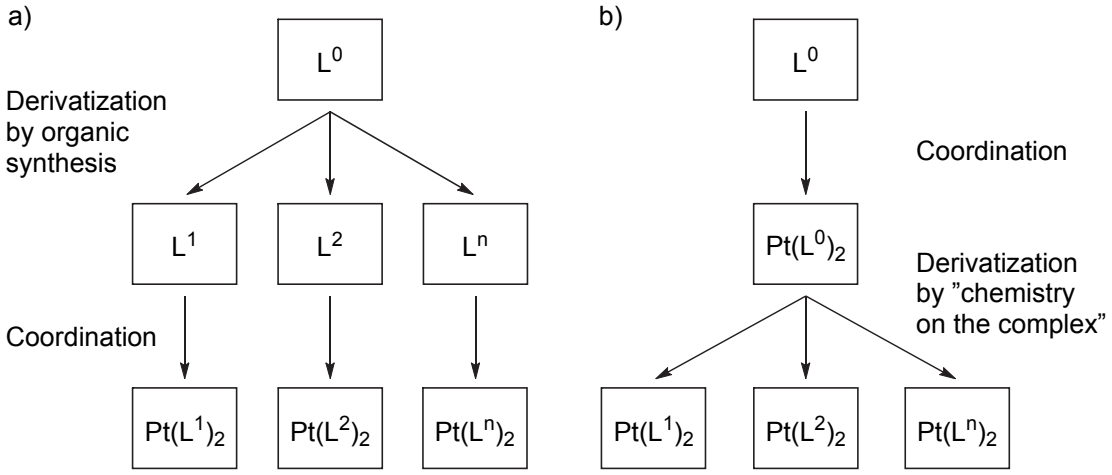

FIGURE 20 Comparison of two synthetic strategies for multiple derivatives: conventional "organic synthesis → coordination chemistry" sequence (a) and non-conventional "chemistry on the complex" approach (b). In this work, L^0 = dpa **31**, and L^1, L^2, …L^n = methylene bridged dpa derivatives **33-36**.

To conclude, benzylation of dpa after coordination to a platinum(II) center results in improved reaction yields and functional group tolerance, and allows a more efficient strategy for synthesis of platinum(II) complexes with methylene bridged dpa ligands. While the proposed alternative synthetic approach is not truly innovative, since the reactions of this type and even the term "chemistry on the complex" are known, it is often overlooked in routine coordination chemistry synthesis.

3.3 Hydrogen bonded supramolecular ensembles based on oxime platinum(II) complexes and 18-crown-6[II,III]

The reported supramolecular associates of platinum(II) complexes and crown ether 18-crown-6 presented in chapter 2 (Fig. 8 and 9)[65,66] evoke our interest in potential use of coordinated on platinum(II) oximes, which have been the subject of long-going studies,[100] as hydrogen bond donors for supramolecular ensembles. Indeed, it has been shown that acidity of oxime OH groups increases dramatically upon coordination to the platinum(II) center,[101] and accordingly platinum(II) acetoxime complexes have been found to form various hydrogen bonded structures.[102] On the other hand, rigidness and *cis-trans* isomerism of square-planar platinum(II) complexes may allow their use as supramolecular tectons similarly to organic ones. Thus, crown ether 18-crown-6, a well-established hydrogen bond acceptor to bind neutral molecules,[63,64] and oxime containing platinum(II) complexes were used for construction of hydrogen bonded supramolecular ensembles.

3.3.1 Crystallizations and crystal structures

Complexes **24-26** and **30** were co-crystallized with crown ether 18-crown-6 by slow evaporation of their solutions in 2:1 or 1:1 molar ratio in acetone/chloroform or acetone/p-xylene solvent mixtures under ambient conditions. Crystallization of **24** with 18-crown-6 afforded triple 1D associate **24**·(18-crown-6)·2H_2O, presented in Fig. 21. In this associate, water molecules play role of hydrogen bonding linkers between the complex and crown ether molecules.

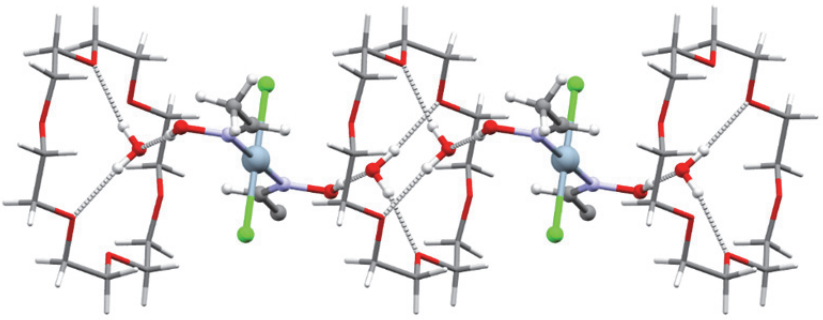

FIGURE 21 Infinite 1D chain in crystal structure of **24**·(18-crown-6)·2H_2O (CSD ref. code: SOHSEP).

When complexes **25** and **26** in *cis*-configuration were used, isostructural discrete triple associates 2(**25**)·(18-crown-6)·2H_2O and 2(**26**)·(18-crown-6)·2H_2O were formed, which also include water molecules as linkers (Fig. 22).

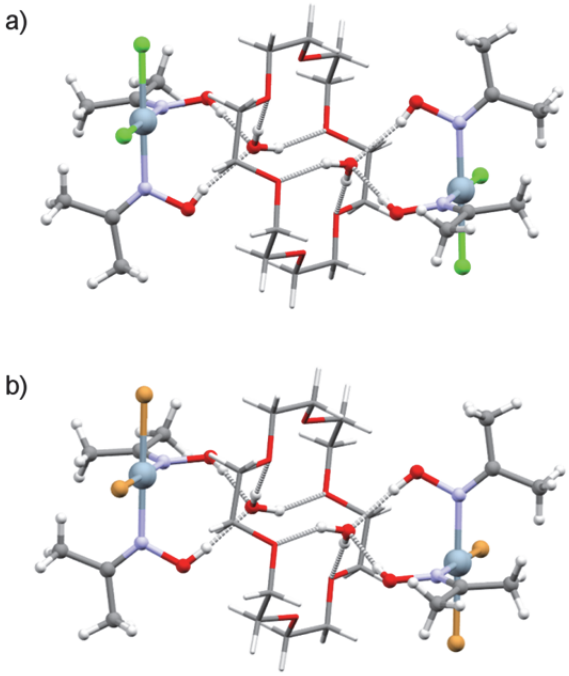

FIGURE 22 Discrete associates in crystal structures of 2(**25**)·(18-crown-6)·2H_2O (a) and 2(**26**)·(18-crown-6)·2H_2O (b) (CSD ref. codes: SOHSAL, SOHRUE).

Surprisingly, in the case of **30** in *trans*-configuration, a 2D network of 1:1 associate **30**·(18-crown-6) was obtained, in which molecules of platinum(II) complex and crown ether are directly hydrogen bound through not only OH, but also CH_3 groups of the ligands (Fig. 23).

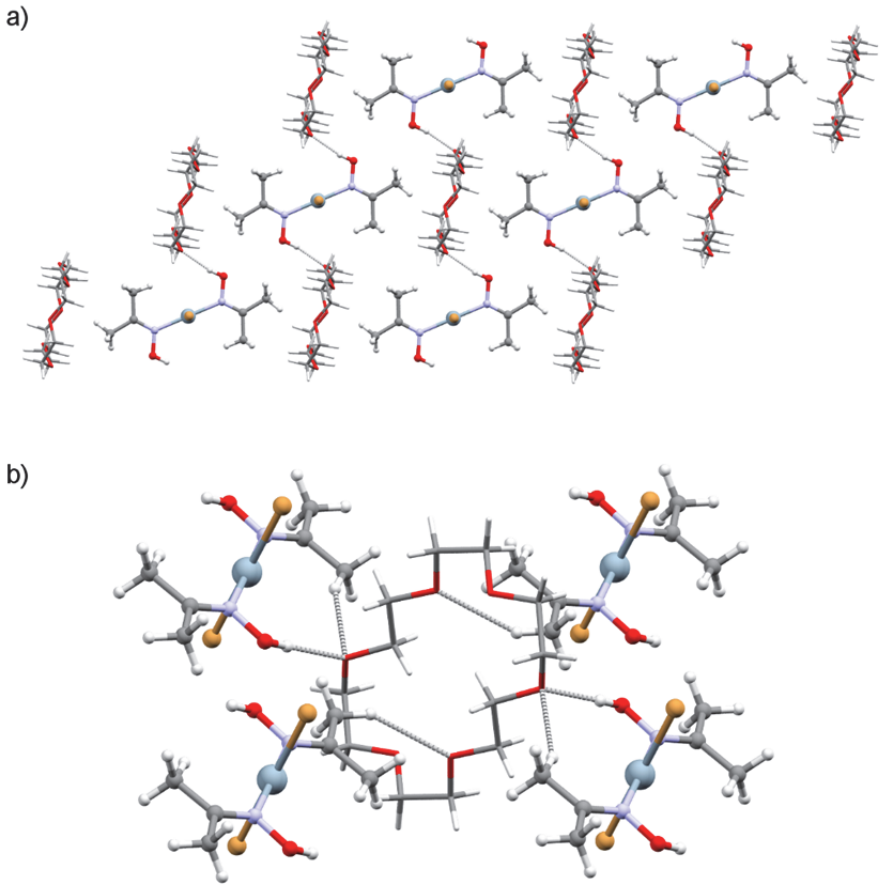

FIGURE 23 Crystal structure of **30**·(18-crown-6): a) infinite 2D sheet (C-H···O contacts are not drawn for clarity); b) single molecule of 18-crown-6 and four molecules of **30** connected *via* O-H···O and C-H···O contacts (CSD ref. code: DAVGOY).

3.3.2 General observations

The inclusion of water molecules in the first three structures is attributed to the use of undried solvents for crystallizations. The average energy of hydrogen bonds in these associates was estimated by means of DFT calculations to be in the range 31–35 kJ/mol. Such relatively strong hydrogen bonding interactions can explain inclusion of water molecules within these structures. However, the structure of **30**·(18-crown-6) does not contain water molecules, even though the same solvents were used in that case, and more hydrophobic CH_3···O interactions are present instead.

Platinum(II) complexes with two hydrogen bond donor groups in *cis*- and *trans*-positions can be expected to form hydrogen bonded discrete and infinite chain structures, accordingly. This is indeed observed in the first three struc-

tures, obtained in this work, as well as in **12** and **13** (Fig. 9).[66] In addition, the change of chloride ligands in **25** to bromides in **26** results in isostructural associates. These observations indicate the possibility to use these complexes to design hydrogen bonded supramolecular structures. However, the example of **30**·(18-crown-6) demonstrates how difficult it may be to predict the resulting architectures based on structures of the components, due to the large variety of possible weak interactions within the structures. *Trans*-orientation of the hydrogen bond donors would otherwise warrant formation of 1D chains in **30**·(18-crown-6), but additional weak $CH_3\cdots O$ hydrogen bonding interaction appeared sufficient for creating additional dimensionality in the co-crystal.

Another striking difference of associate **30**·(18-crown-6) is the conformation of the crown ether molecules. In all of the other associates of 18-crown-6, mentioned in this dissertation, namely **11** (Fig. 8),[65] **12** and **13** (Fig. 9),[66] **24**·(18-crown-6)·$2H_2O$ (Fig. 21), 2(**25**)·(18-crown-6)·$2H_2O$ and 2(**26**)·(18-crown-6)·$2H_2O$ (Fig. 22), the crown ether possesses "classical" crown shape, in which all the methylene groups are oriented outwards from the ring. In **30**·(18-crown-6), the crown ether molecules are "stretched" in one direction by inward orientation of two of the methylene groups, similarly to conformation of pure 18-crown-6 in crystalline state.[103]

To conclude, the use of crown ether 18-crown-6 provides great possibilities for construction of hydrogen bonded self-assembled supramolecular structures, containing neutral platinum(II) complexes with hydrogen bond donor groups. In the oxime complexes **24-26** and **30**, the presence of the metal center increases hydrogen bond donor abilities of the ligands and controls their spatial orientation. Nevertheless, flexibility of 18-crown-6 and possibilities of additional weak interactions make design of supramolecular motifs using these components a challenging task. Possibly, more research is this area will allow development of new platinum(II) containing supramolecular tectons.

3.4 Selective chlorination of oxime platinum(II) complexes using *N,N*-dichlorotosylamide[IV]

As mentioned in chapter 2, development of convenient methods for conversion of platinum(II) species into platinum(IV) analogues is important, in particular, in search for efficient platinum(IV) based anticancer prodrugs.[69] While use of conventional reagents—chlorine and hydrogen peroxide—provides great atom efficiency, it may also be associated with difficulties due to hazardous properties and low selectivity of the oxidants. In the aforementioned work, describing synthesis of supramolecular chains of imino ester platinum complexes and 18-crown-6, *N,N*-dichlorobenzenesulfonamide **43** (also known as dichloramine B) was used to oxidize platinum(II) complex **44** to its platinum(IV) analog **45** (Fig. 24).[66] Since *N,N*-dichlorosulfonamides are easily available and are well-known reagents, used in a variety of organic reactions,[104] it was of interest to test them

further as chlorinating agents for platinum(II) complexes. In this work, *N,N*-dichlorotosylamide **46**, also known as dichloramine T, was chosen as the reagent for chlorination of platinum(II) complexes bearing oxime ligands.

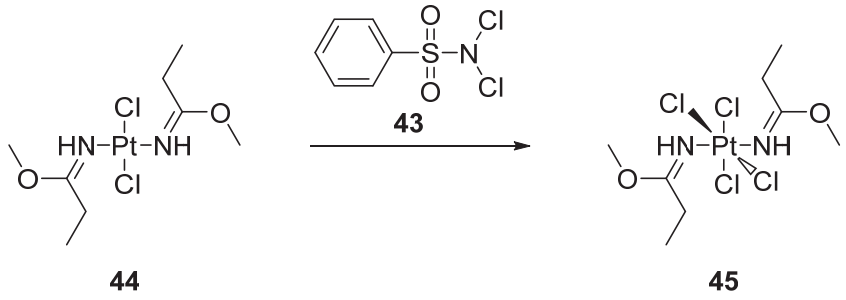

FIGURE 24 Chlorination of imino ester platinum(II) complex **44** using *N,N*-dichlorobenzenesulfonamide **43**.[66]

Dichloramine T is a commercially available solid reagent for synthesis, also used as an antiseptic, which is relatively easy to store and handle. This may allow its use as a stoichiometric equivalent of chlorine for oxidation of platinum(II) compounds. Reactivity of **46** towards oxime containing platinum(II) complexes represents particular interest, since it has been found to effectively convert free oximes into corresponding carbonyl compounds.[105]

3.4.1 Chlorination of oxime platinum(II) complexes

Starting platinum(II) complexes *trans*-[$PtCl_2$(oxime)$_2$] **24**, **27**, and **29** were refluxed with **46** in 1:1 molar ratio in chloroform for 2 hours (Fig. 25). Resulting platinum(IV) complexes *trans*-[$PtCl_4$(oxime)$_2$] **47-49** were isolated from the reaction mixture in good yields (71–83%) using column chromatography.

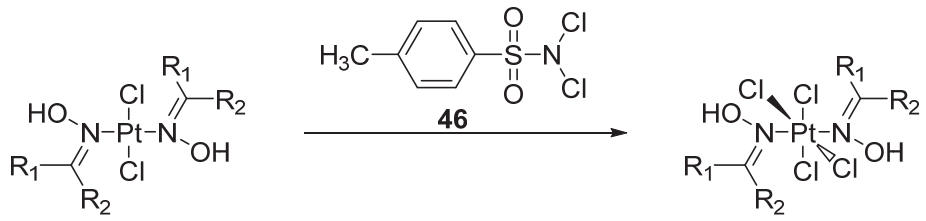

FIGURE 25 Chlorination of oxime platinum(II) complexes using *N,N*-dichlorotosylamide **46**.

In order to test selectivity of the chlorinating agent, chlorination of bis(salicylaldoximato)platinum(II) complex **28** was performed. Refluxing of **28** with **46** in chloroform afforded mixture of products, which, according to mass-spectrometry analysis, contained platinum(IV) complexes with chlorinated ligands. However, when the reaction was performed at ambient temperature

overnight, the desired selective chlorination of platinum center was achieved, and compound **50** was isolated in 60% yield (Fig. 26).

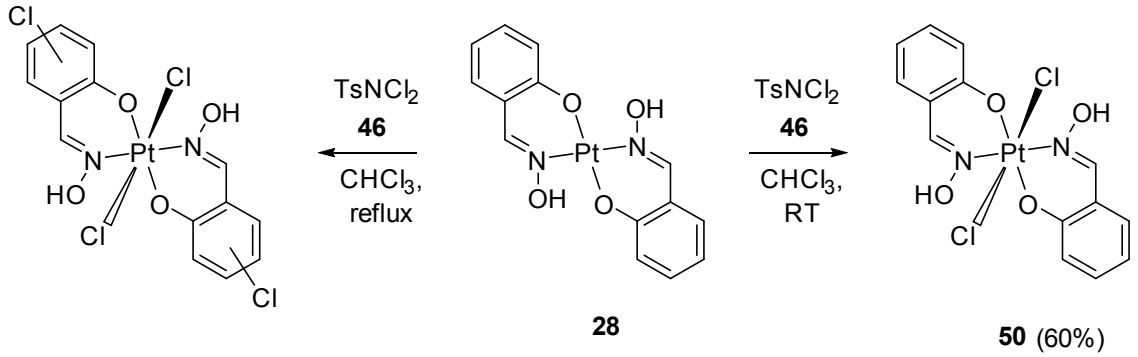

FIGURE 26 Influence of reaction temperature on selectivity of chlorination of **28** using **46**.

3.4.2 Structures of the products and perspectives

Configurations of obtained complexes **47** and **48** were verified by examining their crystal structures, presented in Fig. 27. However, crystals of sufficient quality could not be obtained for **49** and **50**. *Trans*-configuration of **49** was verified by comparison of melting point of the obtained product (189–191 °C) with the reported values (*trans*: 187–190 °C, *cis*: 148–153 °C).[92] In case of **50**, *trans*-orientation of the chloride ligands was verified by inspecting the IR spectrum in the 400 – 300 cm^{-1} region, which revealed a single peak at 346 cm^{-1}, attributed to asymmetric stretching vibrations of the linear Cl-Pt-Cl group (in the case of *cis*-configuration, doublet corresponding to symmetric and antisymmetric stretching vibrations of angular *cis*-$PtCl_2$ moiety would be expected).[106]

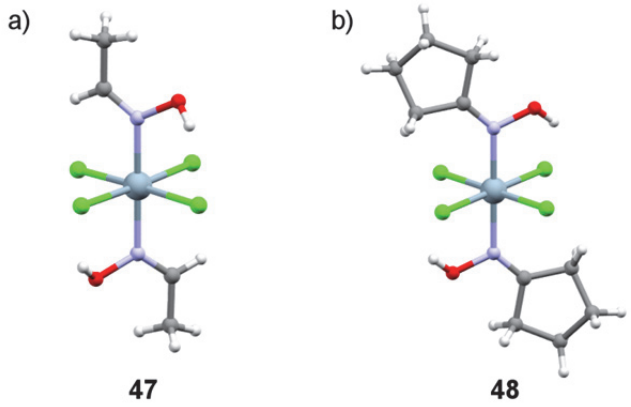

FIGURE 27 Crystal structures of products of chlorination **47** (a) and **48** (b) (CSD ref. codes: EHISOF, EHISIZ).

Therefore, dichloramine T **46** was shown to be a suitable chlorinating agent for oxidizing oxime platinum(II) complexes. Preservation of the oxime ligands, including the easily subjected to electrophilic substitution salicylaldox-

ime, in the course of the reaction demonstrates high selectivity of the reagent. Analyses of the reaction mixtures revealed formation of tosylamide as the side product, which, however, was not isolated. For further potential usability of **46** on large scales, following the principles of atom economy, the resulting tosylamide can be recovered and converted back into dichloramine T **46** using existing methods.[104] Additional studies on oxidation of oxime containing platinum(II) complexes in *cis*-configuration are required in order to verify its applicability in development of platinum(IV) based anticancer prodrugs.

3.5 Unusual non-covalent Pt···I interactions in platinum(II) complex[V]

Complex **[40]Br$_2$**, obtained in the previous work,[I] displayed an interesting feature in the solid state, as it could be crystallized in two different conformations, depending on crystallization conditions. The two conformations, referred to as "in" and "out", are presented in Fig. 28. Crystals of **[***in*-**40]Br$_2$**·3.5H$_2$O are the most common outcome of crystallizations by slow evaporation of solutions of **[40]Br$_2$** in various solvents under ambient conditions. Crystals of **[***out*-**40]Br$_2$**·4CH$_3$CN were obtained once from acetonitrile solution with an equimolar amount of pyrazine added. However, consequent recrystallizations always resulted in the "in"-conformation, and crystallization of **[***out*-**40]Br$_2$**·4CH$_3$CN could not be reproduced. Nevertheless, the obtained structure was of sufficient quality for further investigations.

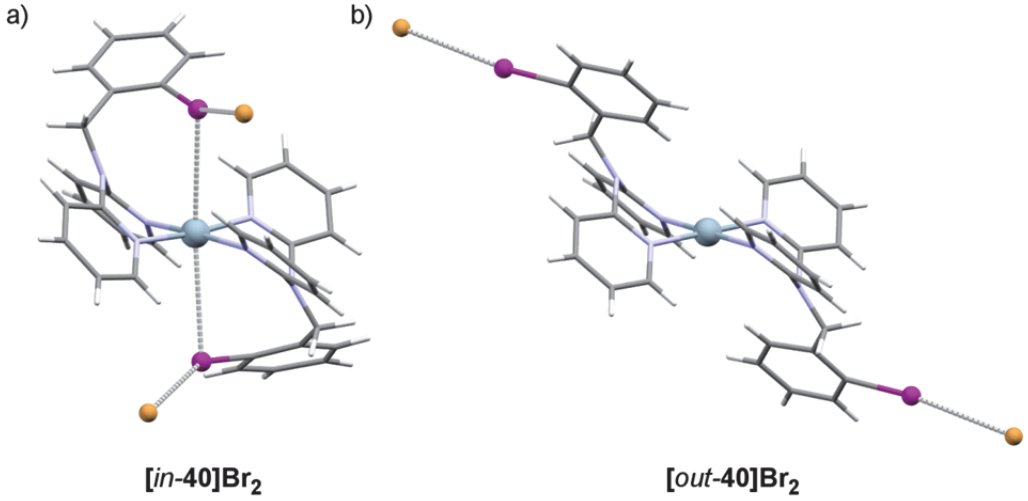

FIGURE 28 Two conformations of **[40]**$^{2+}$: a) "in" in crystal structure of **[***in*-**40]Br$_2$**·3.5H$_2$O, b) "out" in crystal structure of **[***out*-**40]Br$_2$**·4CH$_3$CN. Solvent molecules are omitted for clarity.

In the structure of **[***in*-**40]Br$_2$**·3.5H$_2$O, short Pt···I distances (3.65 and 3.66 Å) are observed, which are slightly shorter than the sum of Bondi's Van-der-Waals

radii of the atoms (3.73 Å).[7,8] This observation suggested that there may be a weak attractive interaction between platinum and iodine atoms. On the other hand, in the crystal structure of **[***out*-**40]Br$_2$**·4CH$_3$CN the Pt···I contacts are absent. In addition, crystal structures of **[40]I$_2$** and **[40](NO$_3$)$_2$** in both conformations were obtained, but the "in"-form was again more common outcome of crystallizations. Finally, crystallization of **[40](CF$_3$SO$_3$)$_2$** afforded a disordered structure, with the "out"-conformation being dominant. These observations indicate that the weak, if any, attractive Pt···I interaction is comparable in strength with other packing effects. In order to confirm the attractive Pt···I interaction, careful analysis of the crystal structures was conducted in cooperation with computational and spectroscopic studies of **[40]**$^{2+}$.

3.5.1 Structural considerations on the Pt···I contact

In order to make conclusions about the Pt···I contact from the geometry point of view, crystal structures of the two conformations, presented in Fig. 28, were carefully compared. Noticeably, both structures possess close Br···I contacts, indicating halogen bonding between iodine atoms and bromide anions, whereas only "in" conformation possesses close Pt···I contact. Essential structural parameters of the complex were examined in order to find any significant changes associated with the close Pt···I contact.

Among such essential parameters are Pt-N$_{(py)}$ bond lengths and angles, reflecting a square-planar coordination mode of the dpa ligands; bond lengths and angles within C$_{(py)}$-N$_{(amino)}$-C$_{(py)}$ fragment, reflecting the degree of conjugation between the pyridine rings; and bond lengths and angles within Br···I-C fragment, reflecting the strength of the halogen bond. Values of these parameters, extracted from the crystal structures, are presented in Table 2, columns 1 and 2.

TABLE 2 Selected bond lengths and angles extracted from the experimental and computationally optimized structures of *in/out*-**40**.

parameter	**[***in*-**40]Br$_2$**·3.5H$_2$O (X-ray)	**[***out*-**40]Br$_2$**·4CH$_3$CN (X-ray)	[*in*-**40**]$^{2+}$ (PBE0-D3)	[*out*-**40**]$^{2+}$ (PBE0-D3)
bond lengths, Å				
Pt-N$_{(py)}$	2.006(4)–2.034(4)	2.008(2), 2.016(2)	2.014, 2.027	2.019, 2.020
C$_{(py)}$-N$_{(am)}$	1.392(7)–1.402(7)	1.406(3)	1.395, 1.398	1.393, 1.399
I···Br	3.5117(8), 3.6065(10)	3.4313(5)	xxx	xxx
I···Pt	3.6523(5), 3.6615(5)	xxx	3.753	xxx
I-C	2.109(6), 2.112(6)	2.120(3)	2.097	2.095
bond angles, °				
N$_{(py)}$-Pt-N$_{(py)}$	85.59(17)–95.91(17)	85.97(9), 94.03(9)	85.9–94.7	86.1, 93.9
C$_{(py)}$-N$_{(am)}$-C$_{(py)}$	118.5(4), 120.3(4)	118.5(2)	118.7	119.2
I···Pt-N$_{(py)}$	85.02(12)–97.35(13)	xxx	84.7, 95.1	xxx
C-I···Pt	90.46(16), 96.90(15)	xxx	95.8	xxx
Br···I-C	155.08(16), 160.91(16)	173.25(8)	xxx	xxx

From the presented values, it can be concluded that close Pt···I contact in *in*-**40** is not associated with any significant structural changes in the complex other than orientation of the phenyl ring. The only other noticeable difference is slight weakening of the Br···I halogen bond, as observed from longer Br···I and shorter I-C distances and more bent Br-I-C angle in **[***in*-**40]Br$_2$**·3.5H_2O. This change can be, in principle, directly associated with electronic effects of the Pt···I interaction, but at the same time, it may be a result of increased steric hindrance of the iodine atoms, or involvement of the bromide anions in hydrogen bonding network with water molecules. This indicates the necessity of computational analysis of the observed halogen bond.

Regarding structural analysis of the Pt···I contact, the observed C-I···Pt and I···Pt-$N_{(py)}$ angle values close to 90° indicate that the iodine atoms are located above and below the square plane, approximately where the electrons of filled d_{z^2} orbital of the platinum center reside. Unlike in metal-involving halogen bonding interactions (in which case the C-I···Pt angle would be close to 180°),[32,72,80,81] the iodine atoms in this case seem to be oriented with their electron rich areas ("electron belts")[107] towards the platinum center. Therefore, the observed interaction (if present) can be classified as an interaction of platinum(II) with two Lewis bases, similarly to **21** (Fig. 12 and 14c). On the whole, the geometric considerations indicate rather weak non-covalent Pt···I interaction, which was, therefore, subjected to computational studies.

3.5.2 Computational studies

All structural optimizations and single point calculations were conducted within the density functional theory (DFT) approach using PBE0-D3 functional[108] with dispersion correction[109] and def2-TZVPPD[110] (Pt, I) and 6-31G(d) (other atoms) basis sets. Topological analysis of the calculated electron density was performed using quantum theory of atoms in molecules (QTAIM) approach.

First, single point calculations were performed on the non-optimized crystal structures of **[***in*-**40]Br$_2$**·3.5H_2O and **[***out*-**40]Br$_2$**·4CH_3CN with and without inclusion of bromide anions (solvent molecules were always omitted). Consequent QTAIM analysis revealed the presence of bond critical points (BCPs) between bromine and iodine atoms in both structures, as well as between platinum and iodine atoms in **[***in*-**40]** with and without bromide anions. It must be noted that existence of BCPs does not necessarily mean attractive chemical interaction;[111] the important point at this stage was to observe any changes in electron density distribution, particularly at the BCP (Pt···I), associated with inclusion of Br···I short contact. The results displayed negligible differences; therefore, the bromide anions were omitted in the following calculations.

Next, full optimizations of **[***in*-**40]**$^{2+}$ and **[***out*-**40]**$^{2+}$ were performed in the ground (S_0) and the lowest triplet (T_1) electronic states using the corresponding crystal structures as starting points. Structural parameters of the optimized structures in S0 state, presented in columns 3 and 4 of Table 2, are close to the experimental values. According to calculations, **[***in*-**40]**$^{2+}$ in vacuum is energetically 33.5 kJ/mol more favorable than **[***out*-**40]**$^{2+}$. Therefore, the calculated ener-

gy difference supported relative stability of the "in"-conformation, observed in the crystallization experiments.

Topological analysis of the calculated electron density distribution revealed numerous BCPs, including those on Pt···I, I···$N_{(amino)}$, and I···H bond paths. The optimized structures and located BCPs are presented in Fig. 29.

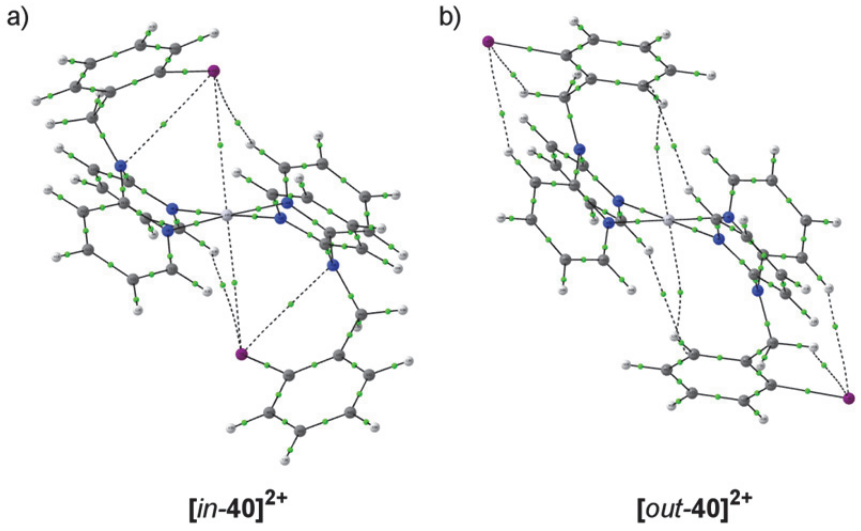

FIGURE 29 Optimized structures with located BCPs (green dots) and bond paths (solid and dotted lines) of a) **[***in*-**40]**$^{2+}$, b) **[***out*-**40]**$^{2+}$.

As mentioned above, BCPs and bond paths do not always correspond to chemically meaningful interactions. Common sense of chemistry can be used to select BCPs of particular interest, and analysis of properties of electron density in these points can provide some information about corresponding interactions. In this case, Pt···I contacts and the corresponding BCPs were considered. Both the interatomic distance and the observed values of selected parameters, presented in Table 3, row 1 (positive Laplacian, positive total energy, very small interaction energy and delocalization index), indicate that Pt···I interactions are of closed-shell nature.

TABLE 3 Lengths of Pt···I contacts and selected properties of electron density at the corresponding BCPs in optimized **[***in*-**40]**$^{2+}$ in S_0 and T_1 states.

State	d(Pt···I), Å	ρ, e/Å^3	$\nabla^2\rho$, e/Å^5	|V/G|	H, a.u.	E, kJ/mol	δ
S_0	3.75	0.078	0.593	0.98	0.0001	-7.7	0.13
T_1	2.91	0.311	1.793	1.3	-0.0081	-45.7	0.57

ρ = local electron density; V/G = ratio of potential energy density and kinetic energy density; H = V + G = total energy; E = V/2 =interaction energy;[112] δ = delocalization index.

Non-covalent character and low energy of the Pt···I interactions are in agreement with the interpretation of platinum(II) interacting with two Lewis bases. Moreover, presented in Table 3, row 2 properties of electron density at

BCPs (Pt···I) in the T_1 electronic state indicate strengthening of the Pt···I interaction and appearance of partial covalent character upon promotion to the higher electron configuration (structurally, significant contraction of Pt···I contacts from 3.75 to 2.91 Å was also observed). Such strengthening in the excited electronic state is known for metallophilic interactions.[113] In order to gain better understanding of the Pt···I interaction and its strengthening upon excitation, the generated from DFT calculations Kohn-Sham molecular orbitals of **[*in*-40]**$^{2+}$ in S_0 state were analyzed. In particular, molecular orbitals HOMO-13 and HOMO were found to be essentially bonding and antibonding orbitals of the I···Pt···I fragment accordingly, formed primarily from p_z atomic orbitals of the iodine atoms and d_{z^2} atomic orbital of the platinum atom (Fig. 30)

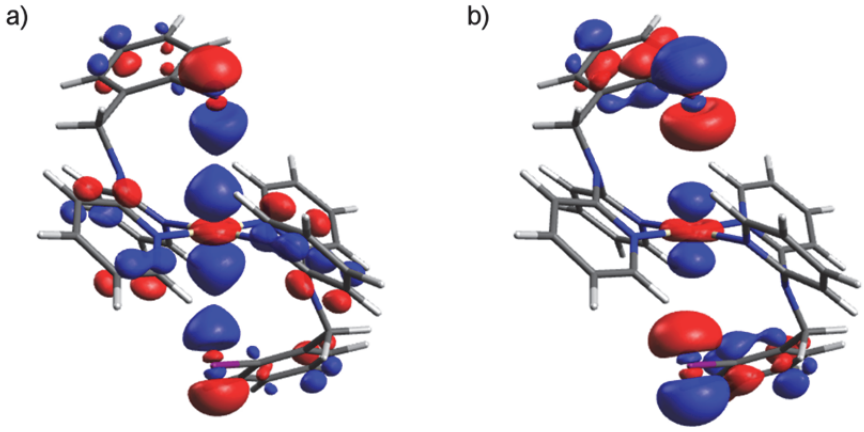

FIGURE 30 Isosurface plots of Kohn-Sham molecular orbitals of optimized **[*in*-40]**$^{2+}$: a) HOMO-13, b) HOMO.

A similar picture is observed in metallophilic interactions, where filled d_{z^2} atomic orbitals of closely located platinum(II) atoms overlap to form filled bonding and antibonding MOs. The attractive nature of such metallophilic interaction, which otherwise would be non-bonding, is usually explained in terms of strong dispersion interactions, or mixing of the higher lying empty p_z orbitals, leading to stabilization of both filled orbitals.[33] While iodine does not possess empty orbitals sufficiently close in energy to stabilize the orbital interaction, it is known to participate in dispersive interactions.[114,115]

The large significance of dispersion in the Pt···I interactions was demonstrated by optimization of **[*in*-40]**$^{2+}$ using PBE0 functional without dispersion correction, or using PBE0-D3 with inclusion of methanol solvent using the conductor-like polarizable continuum solvent model (C-PCM).[116] Both optimizations resulted in elongation of Pt···I contact from 3.75 to 3.90 Å and decrease in energy difference between the two conformations from 33.5 to 13 and 18.6 kJ/mol respectively. The latter result agrees with the generally observed attenuation of dispersion interactions in polarizable solvents.[117]

Qualitative analysis of the MOs presented on Fig. 30 also provides explanation for the predicted strengthening of Pt···I interactions upon photoexcita-

tion. Indeed, if an electron were removed from the HOMO, the antibonding orbital I···Pt···I interaction would be weakened, whereas the bonding one would be preserved. In order to support the obtained results experimentally, optical studies were conducted.

3.5.3 Optical spectroscopy studies

Absorption spectrum of **[40]Br$_2$** in methanol is presented in Fig. 31a. Absorption spectra, calculated for **[***in*-**40]**$^{2+}$ and **[***out*-**40]**$^{2+}$ in methanol using time-dependent DFT calculations and C-PCM solvent model,[116] appear to be very similar to the experimental one and between each other. Therefore, according to calculations, absorption spectroscopy cannot be used to distinguish the two conformations in solution. The lowest energy absorptions at $\lambda_{abs} \approx$ 300–330 nm can be attributed to metal to ligand charge transfer and π→π* transitions within dpa moieties in "in" and "out" conformations accordingly.

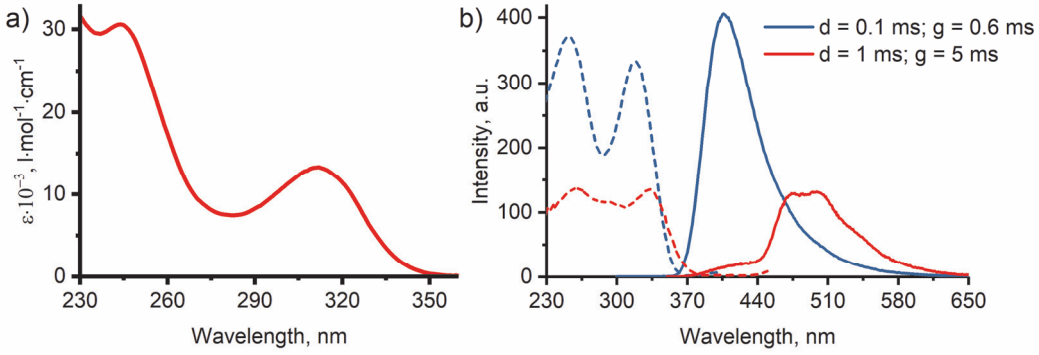

FIGURE 31 Optical spectra of **[40]Br$_2$** in solution: a) absorption in methanol at room temperature, b) phosphorescence excitation (dashed lines) and emission (solid lines) spectra in methanol/ethanol mixture (1:4, v/v) at 77 K at different timing parameters (d = delay, g = gate).

Solution of **[40]Br$_2$** in methanol is not emissive at room temperature, which is an often encountered feature for platinum(II) complexes.[118] In order to observe photoluminescence, a solution of **[40]Br$_2$** in 1:4 (v/v) mixture of methanol and ethanol was cooled to 77 K to form semi-rigid transparent glass. No emission was observed in fluorescence mode, but emission peak at λ_{em} = 417 nm and a shoulder at $\lambda_{em} \approx$ 475 nm were observed in phosphorescence mode. The spectrum appeared to be time-dependent, and the two peaks were resolved by varying delay and gate timing parameters (Fig. 31b). Close similarity of the excitation spectra, measured for the two peaks, with the absorption spectrum of **[40]Br$_2$** suggests dual emission of the complex. Additional time resolved measurements revealed lifetimes of the two peaks being τ_1 = 37 μs (λ_{em} = 417 nm) and τ_2 = 3.5 ms (λ_{em} = 500 nm) at 80 K (λ_{ex} = 320 nm), supporting assignment of the observed emission to phosphorescence.

The dual emission of **[40]Br$_2$** can be associated with the different conformations in the excited state. In semi-rigid environment of frozen metha-

nol/ethanol mixture, **[40]**$^{2+}$ can be considered to exists as a mixture of "in"- and "out"-forms (more details on the conformational equilibrium in solution are discussed in NMR studies section below), which can form the excited states of different nature. Optimization of T_1 state for both "in"- and "out"-forms of **[40]**$^{2+}$ yielded essentially metal centered excited states, which are known to be dark (non-emissive) due to proximity of the crossing point with the ground state.[118] Therefore, **[40]**$^{2+}$ is suggested to possess non-Kasha emissive behavior, when phosphorescence takes place from an energetically higher lying excited state owing to relatively high activation barrier towards the non-emissive metal centered T_1 state. Such suggestion is in line with the observation that **[40]Br$_2$** is not emissive in fluid methanol solution at room temperature, since thermal energy allows to overcome the barrier and populate the non-emissive T1 state, thus quenching phosphorescence. The proposed relations between the ground and excited electronic states are illustrated in Fig. 32.

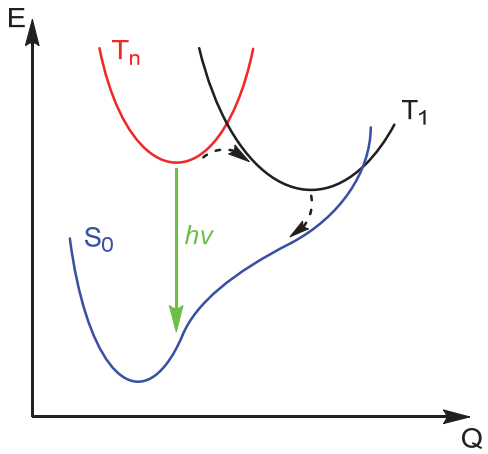

FIGURE 32 Schematic potential energy diagram illustrating the non-Kasha emissive behavior of **[40]**$^{2+}$: E = potential energy, Q = combined geometry coordinate, T_n = the emissive excited triplet state. Green arrow denotes phosphorescence emission and dashed black arrows denote thermally activated radiativeless transitions.

As an approximation of the emissive excited state, the HOMO and LUMO of **[40]**$^{2+}$ in the ground state can be considered, which indicate ligand centered π→π* state for **[***out*-**40]**$^{2+}$ and metal to ligand charge transfer σ*(I-Pt-I)→π* state for **[***in*-**40]**$^{2+}$. Thus, the two experimentally observed emission bands were tentatively attributed to emissions of **[***out*-**40]**$^{2+}$ (λ_{em} = 417 nm) and **[***in*-**40]**$^{2+}$ (λ_{em} = 470/500 nm).

For comparison, phosphorescence emission properties of complexes **[39,41,42]Br$_2$** were studied, and their overlaid emission spectra are presented in Fig. 33. Generally, all of the complexes possess the blue emission band with λ_{em} = 407–425 nm and τ = 37–200 μs. In the case of **[42]Br$_2$**, broader band was observed with additional peaks at λ_{em} = 448 and 480 nm, but their lifetime value was very close to that of the first peak.

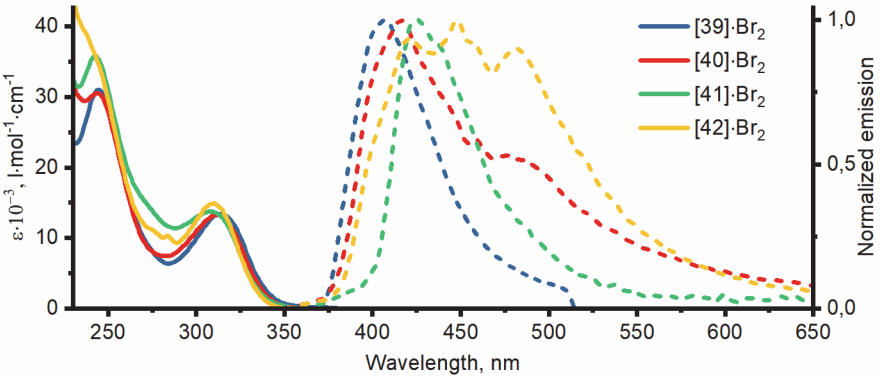

FIGURE 33 Absorption (room temperature, solid lines) and emission (80 K, dashed lines) spectra of **[39-42]·Br₂** in methanol/ethanol solution (C = 20 μM). Emission spectra were measured under excitation at λ_{ex} = 320 nm, delay 20 ns, gate 10 μs (30 μs for **[40]·Br₂**).

Excitation state lifetimes of microsecond order are typical for complexes of platinum(II),[118] whereas the long lifetime of the green emission of **[40]Br₂** (3.5 ms) is quite unusual. Together with the uniqueness of this emission among the series **[39-42]Br₂**, these observations further support its origin as being associated with the Pt···I interaction.

3.5.4 Other studies and perspectives

In order to observe influence of the intramolecular Pt···I interactions in complex **[40]Br₂** on its conformational behavior in solution, variable temperature ^{1}H and ^{195}Pt NMR measurements were performed. The obtained spectra displayed temperature dependence; however, very similar behavior was also observed for the non-substituted complex **[39]Br₂**. Therefore, the observed temperature dependences were attributed to the equilibrium between "symmetric" and "asymmetric" conformations of the complexes, associated with flipping of one of the benzyl groups, as presented in Fig. 34.

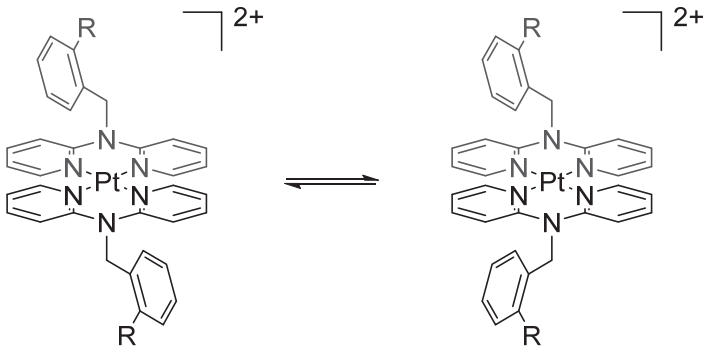

FIGURE 34 Equilibrium between the "symmetric" and "asymmetric" conformations of **[39]**$^{2+}$ (R = H) and **[40]**$^{2+}$ (R = I), presumably observed in variable temperature ^{1}H and ^{195}Pt NMR experiments.

According to computational results, the energetic barrier for transition between "symmetric" and "asymmetric" conformations is 30 and 20 kJ/mol in **[***in*-**40]**$^{2+}$ and **[***out*-**40]**$^{2+}$ respectively. On the other hand, rotational barriers of the benzyl groups are calculated to be negligibly low. Therefore, **[40]**$^{2+}$ is assumed to exist in solution in four conformations with approximately equal populations, namely, "symmetric" and "asymmetric" "in"- and "out"-conformations. Due to fast transformations, the "in"-and "out"-forms are predicted to be averaged in the NMR timescale at any accessible temperature. Combination of NMR spectroscopy with pulsed UV irradiation could be of potential interest to observe conformation changes in solution upon excitation.[119]

Ion mobility mass spectrometry (IMMS) measurements were performed in an attempt to observe different forms of **[40]**$^{2+}$ in gas phase. Once again, the experiment was not able to resolve conformations, and a single peak in the mobility dimension of IMMS spectrum was observed. Combination of IMMS with pulsed UV irradiation could also be worth trying, as the greater stability of "in"-conformations in the excited electronic state may be observed through changes in ion mobilities.[120]

To conclude, all the obtained experimental and computational results indicate that there are weak intramolecular attractive Pt···I interactions in complex **[40]Br$_2$**, which are observed in crystal structures, but too weak to be observed in solution or gas phase. Upon photoexcitation, these interactions strengthen substantially, resulting in dual time-dependent phosphorescence emission of **[40]Br$_2$** in frozen solution. Therefore, **[40]Br$_2$** seems to be the first experimentally and computationally verified example of weak non-covalent interaction of platinum(II) with two Lewis bases.

4 SUMMARY AND CONCLUSIONS

This dissertation describes four research projects centered on the chemistry of square-planar platinum(II) complexes containing dpa or oxime ligands. Each project focuses on one of the four types of chemical interactions, classified by strength and location in the coordination compound.

The first project,[I] focusing on covalent interactions of ligands, demonstrates great potential of the "chemistry on the complex" approach applied to coordination compounds of platinum(II). Benzylation of dpa coordinated to platinum(II) proceeds with higher yields and tolerance to functional groups, compared to the purely organic approach. In synthesis of platinum(II) complexes with various dpa-based ligands, such an approach allows significantly more efficient synthetic strategies compared to the conventional procedure of organic synthesis of ligands, followed by their coordination on the metal center.

The second project,[II,III] focusing on non-covalent interactions of ligands, demonstrates applicability of platinum(II) complexes with oxime ligands as neutral hydrogen bond donors in supramolecular chemistry. Enhanced ability of the ligands to form hydrogen bonds together with their pre-defined spatial orientation allow design and synthesis of supramolecular ensembles with crown ether 18-crown-6. The resulting structural motifs, defined by hydrogen bonding interactions, may, however, be interfered by additional weak interactions, making reliable predictions of the resulting structures difficult.

The third project,[IV] focusing on covalent interactions of the metal center, describes new method of oxidative chlorination of platinum(II) complexes with oxime ligands into their platinum(IV) analogues using *N,N*-dichlorotosylamide (dichloramine T). The oxidation reaction proceeds selectively on the metal center, leaving ligands intact. Further studies may prove the employed oxidizing agent useful in the production of anticancer prodrugs based on platinum(IV).

Finally, the last project,[V] focusing on non-covalent interactions of the metal center, discusses weak non-covalent intramolecular Pt···I interactions in one of the platinum(II) dpa complexes, obtained in the first project. In terms of the Lewis acid-base classification of non-covalent interactions of platinum(II), this is the first verified example of platinum(II) interacting with two Lewis bases.

The interactions are observed in crystal structure and confirmed computationally, but are too weak to be observed in solution or in gas phase. Upon photoexcitation, the Pt···I interactions strengthen substantially, affecting phosphorescence properties of the complex in solution.

4.1 The "big picture"

The chemistry of square-planar coordination compounds of platinum(II) is very diverse and complex, and their practical applications span across various fields of modern technology and medicine. On the other hand, relatively high structural rigidity and kinetic inertness of the platinum(II) compounds not only promote their applicability in functional materials and drugs, but also allow thorough studies of their structures and reactivity. Historically, many important discoveries have been made by studying square-planar platinum(II) complexes, and nowadays new aspects of their structural diversity and reactivity continue to emerge.

The main objective of this dissertation was to survey and classify known to date chemical interactions involving square-planar platinum(II) coordination compounds, based on their strength and location in the complexes, and to contribute to the knowledge of platinum(II) chemistry in various fields within this framework. Location-wise, the interactions were divided into those involving only ligands or only the metal center. In terms of strength, weak non-covalent and strong covalent interactions were separated. Corresponding examples of each type of interaction, known from literature, were described in chapter 2, and new contributions to each of those fields, constituting the work behind this dissertation, were presented in chapter 3.

Clearly, the proposed classification by location and strength has its limitations, and, while being well-suited for distinguishing some interactions, it can be less appropriate for borderline cases. Particularly, the discrete separation of interactions by location in the complexes denies the true wealth of coordination chemistry, which relies on interplay between chemical interactions of ligands and central atoms. In other words, the majority of chemistry of square-planar platinum(II) complexes involves participation of both ligands and the metal, and thus cannot be assigned to either of the two groups. Nevertheless, the proposed separation remains useful, for example, in elucidation of reaction mechanisms, or in designing synthons for supramolecular chemistry.

Classifying the interactions by strength, on the other hand, is presented in a more continuous fashion, particularly for the interactions involving metal centers. Transition from strong covalent bonding to weak non-covalent interactions naturally implies an intermediate state of weak covalent or strong non-covalent bonding. Attempts to draw a sharp borderline between the two categories may result in ambiguities in assignment of electron configurations or oxidation states, which, in the light of emerging new metal-involving chemical interactions, become a matter of continuous needless debates. On the other hand, the

borderline between weak non-covalent bonding and absence of bonding in chemical sense is not easy to define either. Perhaps, the best criterion for existence of any bonding is an observation of its impact on some macroscopic properties of materials.

Overall, this dissertation contributed to the field of coordination chemistry of square-planar platinum(II) coordination compounds in its various aspects. The presented results demonstrate how separate approaches to chemistry of ligands and central atoms within coordination compounds, implying strong or weak interactions, can provide novel reactivity and structures. Hopefully, the rest of platinum chemistry, combining these aspects to various extents, can take advantage of the knowledge presented herein.

REFERENCES

1 V. I. Minkin, *Pure Appl. Chem.*, 1999, 71, 1919–1981.
2 T. Clark, *Faraday Discuss.*, 2017, **203**, 9–27.
3 T. Clark, *J. Mol. Model.*, 2017, **23**, 297.
4 K. Müller-Dethlefs and P. Hobza, *Chem. Rev.*, 2000, **100**, 143–168.
5 J. Emsley, *Chem. Soc. Rev.*, 1980, **9**, 91–124.
6 S. Grimme, C. Mück-Lichtenfeld, G. Erker, G. Kehr, H. Wang, H. Beckers and H. Willner, *Angew. Chem. Int. Ed.*, 2009, **48**, 2592–2595.
7 A. Bondi, *J. Phys. Chem.*, 1964, **68**, 441–451.
8 R. S. Rowland and R. Taylor, *J. Phys. Chem.*, 1996, **100**, 7384–7391.
9 *Nomenclature of Inorganic Chemistry - IUPAC recommendations 2005*, eds. N. G. Connelly, T. Damhus, R. M. Hartshorn, A. T. Hutton, The Royal Society of Chemistry, 2005.
10 M. L. H. Green, *J. Organomet. Chem.*, 1995, **500**, 127–148.
11 D. MacDonald and L. B. Hunt, *A history of platinum and its allied metals*, Johnson Matthey, London, 1982.
12 K. Meyer and H. Braunschweig, *Organometallics*, 2018, **37**, 625–627.
13 J. Bremi, D. Brovelli, W. Caseri, G. Hähner, P. Smith and T. Tervoort, *Chem. Mater.*, 1999, **11**, 977–994.
14 C. H. Hendon, A. Walsh, N. Akiyama, Y. Konno, T. Kajiwara, T. Ito, H. Kitagawa and K. Sakai, *Nat. Commun.*, 2016, **7**, 11950.
15 F. R. Hartley, *Chem. Soc. Rev.*, 1973, **2**, 163–179.
16 A. R. Chianese, S. J. Lee and M. R. Gagné, *Angew. Chem. Int. Ed.*, 2007, **46**, 4042–4059.
17 T. C. Johnstone, K. Suntharalingam and S. J. Lippard, *Philos. Trans. R. Soc., A* , 2015, **373**, 20140185.
18 B. Minaev, G. Baryshnikov and H. Agren, *Phys. Chem. Chem. Phys.*, 2014, **16**, 1719–1758.
19 A. L. Balch, *Comments Inorg. Chem.*, 1984, **3**, 51–67.
20 F. Gordon and A. Stone, *Inorg. Chim. Acta*, 1981, **50**, 33–42.
21 A. Karpov, M. Konuma and M. Jansen, *Chem. Commun.*, 2006, 838–840.
22 S.-G. Wang and W. H. E. Schwarz, *Angew. Chem. Int. Ed.*, 2009, **48**, 3404–3415.
23 H. Bethe, *Ann. Phys.*, 1929, **395**, 133–208.
24 J. J. Zuckerman, *J. Chem. Educ.*, 1965, **42**, 315–317.
25 H. Basch and H. B. Gray, *Inorg. Chem.*, 1967, **6**, 365–369.
26 R. J. Deeth, *Faraday Discuss.*, 2003, **124**, 379–391.
27 J. Börgel, M. G. Campbell and T. Ritter, *J. Chem. Educ.*, 2016, **93**, 118–121.
28 J. S. Griffith and L. E. Orgel, *Q. Rev., Chem. Soc.*, 1957, **11**, 381–393.
29 L. M. Rendina and R. J. Puddephatt, *Chem. Rev.*, 1997, **97**, 1735–1754.
30 G. Aullón and S. Alvarez, *Inorg. Chem.*, 1996, **35**, 3137–3144.
31 R. Sánchez-de-Armas and M. S. G. Ahlquist, *Phys. Chem. Chem. Phys.*, 2015, **17**, 812–816.

32 B. Lu, X. Zhang, L. Meng and Y. Zeng, *ChemistrySelect*, 2016, **1**, 5698–5705.
33 L. H. Doerrer, *Dalton Trans.*, 2010, **39**, 3543–3553.
34 F. Basolo, H. B. Gray and R. G. Pearson, *J. Am. Chem. Soc.*, 1960, **82**, 4200–4203.
35 Yu. N. Kukushkin, *Platinum Metals Rev.*, 1991, **35**, 28–31.
36 B. Lippert and P. J. Sanz Miguel, *Inorg. Chim. Acta*, 2018, **472**, 207–213.
37 G. R. Desiraju, *Angew. Chem. Int. Ed.*, 1995, **34**, 2311–2327.
38 C. C. C. Johansson Seechurn, M. O. Kitching, T. J. Colacot and V. Snieckus, *Angew. Chem. Int. Ed.*, 2012, **51**, 5062–5085.
39 Á. Molnár, *Chem. Rev.*, 2011, **111**, 2251–2320.
40 T. Lifa, W. Tieu, R. K. Hocking and R. Codd, *Inorg. Chem.*, 2015, **54**, 3573–3583.
41 J. P. Sauvage, *Acc. Chem. Res.*, 1990, **23**, 319–327.
42 S.-L. Huang, T. S. A. Hor and G.-X. Jin, *Coord. Chem. Rev.*, 2017, **333**, 1–26.
43 S. M. Cohen, *Chem. Rev.*, 2012, **112**, 970–1000.
44 Y. Tor, *Synlett*, 2002, **2002**, 1043–1054.
45 E. C. Constable, P. Harverson, C. E. Housecroft, E. Nordlander and J. Olsson, *Polyhedron*, 2006, **25**, 437–458.
46 T. Mede, M. Jäger and U. S. Schubert, *Chem. Soc. Rev.*, 2018, **47**, 7577–7627.
47 D. A. Valyaev, M. A. Uvarova, A. A. Grineva, V. César, S. N. Nefedov and N. Lugan, *Dalton Trans.*, 2016, **45**, 11953–11957.
48 F. Aznarez, W.-X. Gao, Y.-J. Lin, F. E. Hahn and G.-X. Jin, *Dalton Trans.*, 2018, **47**, 9442–9452.
49 G. H. Sarova, N. A. Bokach, A. A. Fedorov, M. N. Berberan-Santos, V. Yu. Kukushkin, M. Haukka, J. J. R. Frausto da Silva and A. J. L. Pombeiro, *Dalton Trans.*, 2006, 3798–3805.
50 S. F. Kaplan, V. Yu. Kukushkin, S. Shova, K. Suwinska, G. Wagner and A. J. L. Pombeiro, *Eur. J. Inorg. Chem.*, 2001, **2001**, 1031–1038.
51 Yu. N. Kukushkin, V. K. Krylov, S. F. Kaplan, M. Calligaris, E. Zangrando, A. J. L. Pombeiro and V. Yu. Kukushkin, *Inorg. Chim. Acta*, 1999, **285**, 116–121.
52 T. R. Cook, Y.-R. Zheng and P. J. Stang, *Chem. Rev.*, 2013, **113**, 734–777.
53 L. Brammer, *Chem. Soc. Rev.*, 2004, **33**, 476–489.
54 L. Brammer, *Dalton Trans.*, 2003, 3145–3157.
55 G. R. Lewis and A. G. Orpen, *Chem. Commun.*, 1998, 1873–1874.
56 A. Angeloni, P. C. Crawford, A. G. Orpen, T. J. Podesta and B. J. Shore, *Chem. Eur. J.*, 2004, **10**, 3783–3791.
57 C. J. Adams, A. Angeloni, A. G. Orpen, T. J. Podesta and B. Shore, *Cryst. Growth Des.*, 2006, **6**, 411–422.
58 C. B. Aakeröy, A. M. Beatty and D. S. Leinen, *Angew. Chem. Int. Ed.*, 1999, **38**, 1815–1819.
59 M. D. Ward and P. R. Raithby, *Chem. Soc. Rev.*, 2013, **42**, 1619–1636.
60 C. J. Pedersen, *J. Am. Chem. Soc.*, 1967, **89**, 2495–2496.
61 C. J. Pedersen, *J. Am. Chem. Soc.*, 1967, **89**, 7017–7036.
62 C. J. Pedersen, *J. Org. Chem.*, 1971, **36**, 1690–1693.

63 A. Elbasyouny, H. J. Bruegge, K. Von Deuten, M. Dickel, A. Knochel, K. U. Koch, J. Kopf, D. Melzer and G. Rudolph, *J. Am. Chem. Soc.*, 1983, **105**, 6568–6577.

64 J. N. Spencer, A. I. Zafar, T. F. Ganunis, C. H. Yoder, L. J. Fenton, J. L. Ealy, S. Gupta, C. M. Salata and I. M. Paul, *J. Phys. Chem.*, 1992, **96**, 3475–3477.

65 H. M. Colquhoun, J. F. Stoddart and D. J. Williams, *J. Chem. Soc., Chem. Commun.*, 1981, 847–849.

66 T. G. Chulkova, P. V Gushchin, M. Haukka and V. Yu. Kukushkin, *Inorg. Chem. Commun.*, 2010, **13**, 580–583.

67 H. C. Stynes and J. A. Ibers, *Inorg. Chem.*, 1971, **10**, 2304–2308.

68 M. T. Barnet, B. M. Craven, H. C. Freeman, N. E. Kime and J. A. Ibers, *Chem. Commun.*, 1966, 307–308.

69 R. G. Kenny, S. W. Chuah, A. Crawford and C. J. Marmion, *Eur. J. Inorg. Chem.*, 2016, **2017**, 1596–1612.

70 M. Crespo, *J. Organomet. Chem.*, 2019, **879**, 15–26.

71 R. A. Taylor, D. J. Law, G. J. Sunley, A. J. P. White and G. J. P. Britovsek, *Chem. Commun.*, 2008, 2800–2802.

72 R. A. Gossage, A. D. Ryabov, A. L. Spek, D. J. Stufkens, J. A. M. van Beek, R. van Eldik and G. van Koten, *J. Am. Chem. Soc.*, 1999, **121**, 2488–2497.

73 Z. Xu, C. Li, Z. Tong, L. Ma, M.-K. Tse and G. Zhu, *Eur. J. Inorg. Chem.*, 2017, 1706–1712.

74 G. B. Kauffman, *Platinum Metals Rev.*, 1976, **20**, 21–24.

75 M. Atoji, J. W. Richardson and R. E. Rundle, *J. Am. Chem. Soc.*, 1957, **79**, 3017–3020.

76 G. Gliemann and H. Yersin, in *Clusters. Structure and Bonding*, Springer, Berlin, Heidelberg, 1985, pp. 87–153.

77 J. A. Bailey, M. G. Hill, R. E. Marsh, V. M. Miskowski, W. P. Schaefer and H. B. Gray, *Inorg. Chem.*, 1995, **34**, 4591–4599.

78 L. Brammer, J. M. Charnock, P. L. Goggin, R. J. Goodfellow, A. G. Orpen and T. F. Koetzle, *J. Chem. Soc., Dalton Trans.*, 1991, 1789–1798.

79 S. Rizzato, J. Bergès, S. A. Mason, A. Albinati and J. Kozelka, *Angew. Chem. Int. Ed.*, 2010, **49**, 7440–7443.

80 D. M. Ivanov, A. S. Novikov, I. V. Ananyev, Y. V. Kirina and V. Yu. Kukushkin, *Chem. Commun.*, 2016, **52**, 5565–5568.

81 S. V Baykov, U. Dabranskaya, D. M. Ivanov, A. S. Novikov and V. P. Boyarskiy, *Cryst. Growth Des.*, 2018, **18**, 5973–5980.

82 N. C. Stephenson, *J. Inorg. Nucl. Chem.*, 1962, **24**, 791–795.

83 R. Makiura, I. Nagasawa, N. Kimura, S. Ishimaru, H. Kitagawa and R. Ikeda, *Chem. Commun.*, 2001, 1642–1643.

84 I. R. Crossley, A. F. Hill and A. C. Willis, *Organometallics*, 2008, **27**, 312–315.

85 G. Parkin, *Organometallics*, 2006, **25**, 4744–4747.

86 A. F. Hill, *Organometallics*, 2006, **25**, 4741–4743.

87 A. S. Novikov, *Inorg. Chim. Acta*, 2018, **483**, 21–25.

88 E. R. T. Tiekink, *Coord. Chem. Rev.*, 2017, **345**, 209–228.

89 N. K. Allampally, C. A. Strassert and L. De Cola, *Dalton Trans.*, 2012, **41**, 13132–13137.
90 R. M. van der Veen, A. Cannizzo, F. van Mourik, A. Vlček and M. Chergui, *J. Am. Chem. Soc.*, 2011, **133**, 305–315.
91 Y. Y. Scaffidi-Domianello, A. A. Legin, M. A. Jakupec, A. Roller, V. Yu. Kukushkin, M. Galanski and B. K. Keppler, *Inorg. Chem.*, 2012, **51**, 7153–7163.
92 V. Yu. Kukushkin, V. K. Bel'skii, E. A. Aleksandrova, V. E. Konovalov and G. A. Kirakosyan, *Inorg. Chem.*, 1992, **31**, 3836–3840.
93 V. Yu. Kukushkin, D. Tudela, Y. A. Izotova, V. K. Belsky and A. I. Stash, *Polyhedron*, 1998, **17**, 2455–2461.
94 E. G. Cox, F. W. Pinkard, W. Wardlaw and K. C. Webster, *J. Chem. Soc.*, 1935, 459–462.
95 Q. Wang, P. V Gushchin, N. A. Bokach, M. Haukka and V. Yu. Kukushkin, *Russ. Chem. Bull.*, 2012, **61**, 828–835.
96 A. N. Chernyshev, D. Morozov, J. Mutanen, V. Yu. Kukushkin, G. Groenhof and M. Haukka, *J. Mater. Chem. C*, 2014, **2**, 8285–8294.
97 B. Antonioli, D. J. Bray, J. K. Clegg, K. Gloe, K. Gloe, O. Kataeva, L. F. Lindoy, J. C. McMurtrie, P. J. Steel, C. J. Sumby and M. Wenzel, *Dalton Trans.*, 2006, 4783–4794.
98 M. J. Rauterkus, S. Fakih, C. Mock, I. Puscasu and B. Krebs, *Inorg. Chim. Acta*, 2003, **350**, 355–365.
99 W. A. Panyako and D. Jaganyi, *Int. J. Chem. Kinet.*, 2017, **49**, 545–561.
100 V. Yu. Kukushkin and A. J. L. Pombeiro, *Coord. Chem. Rev.*, 1999, **181**, 147–175.
101 V. Yu. Kukushkin, D. Tudela and A. J. L. Pombeiro, *Coord. Chem. Rev.*, 1996, **156**, 333–362.
102 V. Yu. Kukushkin, T. Nishioka, D. Tudela, K. Isobe and I. Kinoshita, *Inorg. Chem.*, 1997, **36**, 6157–6165.
103 J. D. Dunitz and P. Seiler, *Acta Cryst. B*, 1974, **30**, 2739–2741.
104 P. V. Kattamuri and G. Li, in *Encyclopedia of Reagents for Organic Synthesis*, 2013.
105 P. K. Gupta, L. Manral and K. Ganesan, *Synthesis*, 2007, 1930–1932.
106 A. D. Allen and T. Theophanides, *Can. J. Chem.*, 1964, **42**, 1551–1554.
107 Z. M. Bikbaeva, D. M. Ivanov, A. S. Novikov, I. V. Ananyev, N. A. Bokach and V. Yu. Kukushkin, *Inorg. Chem.*, 2017, **56**, 13562–13578.
108 C. Adamo and V. Barone, *J. Chem. Phys.*, 1999, **110**, 6158–6170.
109 S. Grimme, J. Antony, S. Ehrlich and H. Krieg, *J. Chem. Phys.*, 2010, **132**, 154104.
110 D. Rappoport and F. Furche, *J. Chem. Phys.*, 2010, **133**, 134105.
111 R. F. W. Bader, *J. Phys. Chem. A*, 2009, **113**, 10391–10396.
112 E. Espinosa, E. Molins and C. Lecomte, *Chem. Phys. Lett.*, 1998, **285**, 170–173.
113 J. Romanova, M. R. Ranga Prabhath and P. D. Jarowski, *J. Phys. Chem. C*, 2016, **120**, 2002–2012.

114 A. Bauzá and A. Frontera, *ChemPhysChem*, 2015, **16**, 3108–3113.
115 S. Tsuzuki, T. Uchimaru, A. Wakisaka and T. Ono, *J. Phys. Chem. A*, 2016, **120**, 7020–7029.
116 M. Cossi, N. Rega, G. Scalmani and V. Barone, *J. Comput. Chem.*, 2003, **24**, 669–681.
117 L. Yang, C. Adam, G. S. Nichol and S. L. Cockroft, *Nat. Chem.*, 2013, **5**, 1006.
118 J. A. G. Williams, in *Photochemistry and Photophysics of Coordination Compounds II. Topics in Current Chemistry*, eds. V. Balzani and S. Campagna, Springer, Berlin, Heidelberg, 2007, pp. 205–268.
119 M. Pietrzak, J. Dobkowski, A. Gorski, S. Gawinkowski, M. Kijak, R. Luboradzki, P. E. Hansen and J. Waluk, *Phys. Chem. Chem. Phys.*, 2014, **16**, 9128–9137.
120 J. N. Bull, M. S. Scholz, E. Carrascosa and E. J. Bieske, *Phys. Chem. Chem. Phys.*, 2018, **20**, 509–513.

ORIGINAL PAPERS

I

Non-conventional Synthesis and Photophysical Studies of Platinum(II) Complexes with Methylene Bridged 2,2′-Dipyridylamine Derivatives

by

Evgeny Bulatov & Matti Haukka

Dalton Trans., **2019**, *48*, 3369-3379

Dalton Transactions

PAPER

Cite this: *Dalton Trans.*, 2019, **48**, 3369

Non-conventional synthesis and photophysical studies of platinum(II) complexes with methylene bridged 2,2′-dipyridylamine derivatives†

Evgeny Bulatov and Matti Haukka *

Received 28th September 2018,
Accepted 12th February 2019

DOI: 10.1039/c8dt03912g

rsc.li/dalton

Methylene bridged 2,2′-dipyridylamine (dpa) derivatives and their metal complexes possess outstanding properties due to their inherent structural flexibility. Synthesis of such complexes typically involves derivatization of dpa followed by coordination on metals, and may not always be very efficient. In this work, an alternative synthetic approach, involving the derivatization step after – rather than prior to – coordination of dpa on metal center, is proposed and applied to synthesis of a number of platinum(II) complexes with substituted benzyldi(2-pyridyl)amines. Comparison with the more conventional synthetic route reveals greater efficiency and versatility of the proposed approach. The obtained complexes are not luminescent in solution at room temperature, but display blue phosphorescence emission (*ca.* 415 nm) with the lifetimes of μs order in glassy matrix at 77 K, with additional green (*ca.* 485 nm) and relatively long living (τ = 3.7 ms) emission in the case of iodine substituted derivative.

Introduction

Profound flexibility and chelating capabilities of 2,2′-dipyridylamine (di(2-pyridyl)amine, dpa) have stimulated excessive studies of its coordination chemistry,[1] as well as incorporation of this moiety as a metal binding center into more complex organic materials.[2] The latter is usually achieved by connecting dpa with an organic fragment *via* the amino nitrogen atom, and the resulting derivatives can be conjugated or non-conjugated (Scheme 1). Such organic molecules can be applicable in organic light emitting devices,[3–6] while their ability to bind various transition metals through the dpa moiety allows their use as various luminescent sensors.[7,8] Since dpa complexes of platinum(II) and palladium(II) have been found to possess cytotoxic activities comparable to or higher than cisplatin,[9–11] complexes with dpa derivatives have been considered as potential antitumor agents.[12–15]

Variety of conjugated derivatives and their metal complexes, in which the amino nitrogen atom of dpa is directly connected with an aromatic system, have been synthesized and studied by the group of S. Wang[6,16–18] and more recently by K.-J. Wei *et al.*[19–21] Despite their attractive luminescent properties, real life application of such materials can be hindered by the complicated synthesis, which often involves transition metal catalyzed cross-coupling reactions (Scheme 1, left).

Non-conjugated derivatives, in which dpa moiety is connected with an aliphatic carbon atom, represent another family of dpa based materials. The number of studies on alkyl-substituted di(2-pyridyl)amines is rather limited,[12,13] whereas methylene bridged aromatic derivatives receive more attention recently (Scheme 1, right). Inherent flexibility provided by the methylene linker not only expands the range of possibilities for various supramolecular motifs in solid state, as studied by L. Lindoy *et al.*,[22–24] but also allows for non-trivial reactivity[25] and luminescent properties[26,27] of these compounds and their metal complexes. Compared to their conjugated counterparts, methylene bridged dpa derivatives are much easier to synthesize from dpa and corresponding halides *via* nucleophilic substitution reaction in presence of a base. Corresponding

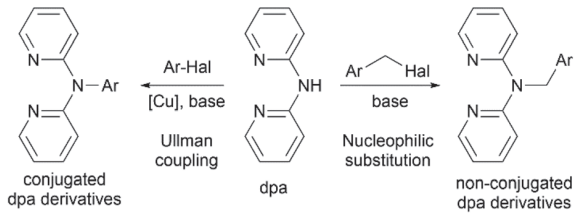

Scheme 1 Conjugated and non-conjugated dpa derivatives and their syntheses.

Department of Chemistry, University of Jyväskylä, P.O. Box 35, FI-40014 Jyväskylä, Finland. E-mail: matti.o.haukka@jyu.fi

†Electronic supplementary information (ESI) available: Additional details and discussion on syntheses and side products, photocyclization of **1**, phosphorescence excitation and variable temperature time resolved emission spectra of **[7–10]·Br$_2$**, ^{1}H NMR spectra of all compounds, and crystallographic data. CCDC 1868987–1868999. For ESI and crystallographic data in CIF or other electronic format see DOI: 10.1039/c8dt03912g

metal complexes can be then obtained by coordinating the dpa fragment on metals using conventional methods of coordination chemistry.

In this work we demonstrated, that the aforementioned conventional synthesis of methylene bridged dpa derivatives from dpa and corresponding halides does not always provide sufficient yields, and proposed an alternative synthetic approach, which involves the derivatization step after – rather than prior to – coordination of dpa on metal center. This approach makes the nucleophilic substitution reaction easier and more tolerant to various substituents in the halides, and allows more efficient synthesis of series of dpa based metal complexes with various organic backbones. Efficiency and versatility of the proposed synthetic approach were demonstrated on synthesis of series of substituted benzyldi(2-pyridyl)amines and their platinum(II) complexes. In addition, the products were structurally characterized and their photophysical properties were investigated.

Results and discussion

Synthesis

As mentioned above, the methylene bridged dpa derivatives are usually obtained by nucleophilic attack of the amino nitrogen atom of dpa on benzyl halides in presence of a base (Scheme 2a). However, several side processes can diminish the reaction yield; for example, the reported yields of benzyldi(2-pyridyl)amine vary from as high as 82% [28] to as low as 16%.[22]

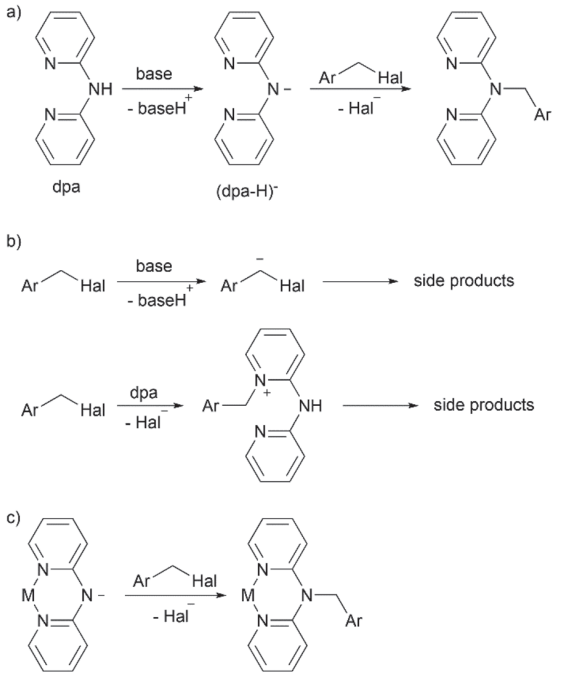

Scheme 2 Reaction between dpa and benzyl halides: (a) target reaction, (b) undesired side reactions, (c) proposed reaction with $(dpa\text{-}H)^-$ complexes.

As we demonstrated in this work, the reaction becomes particularly problematic, when an electron withdrawing group is introduced in the phenyl ring (the same trend can also be found in another recent publication[29]). In such case, the methylene group can be easier deprotonated by the base due to stabilization of the resulting anion, leading to undesired side reactions. Additionally, benzylation of the pyridine nitrogen atoms instead of the amino nitrogen atom may take place (Scheme 2b).

Inspired by reports of various transition metal complexes containing deprotonated di(2-pyridyl)amide $(dpa\text{-}H)^-$ ligands,[30–33] we suggested that use of such complexes in the benzylation reaction (Scheme 2c) could suppress the aforementioned undesired side processes. Thus, use of a base would be unnecessary in the reaction since the amino nitrogen atom of dpa is already deprotonated. Therefore, deprotonation of the methylene group of the benzyl halide would be avoided. The pyridine nitrogen atoms would be protected from benzylation by metal center. Moreover, such approach would allow more efficient synthesis of complexes of a particular metal with various non-conjugated dpa-derived ligands, which is a common research practice (for examples, see ref. 22, 23, 25, 27 and 29). Using the proposed method, such series of complexes could be easily obtained in one step from the $(dpa\text{-}H)^-$ containing complex and corresponding halides. The approach of derivatization of coordinated ligands has been applied, for example, to synthesis of various bipyridine and terpyridine complexes of ruthenium(II) and named as "Organic chemistry of coordination compounds"[34] or "Chemistry on the complex".[35]

We decided to test the proposed approach on synthesis of substituted benzyldi(2-pyridyl)amines **1–3** with substituents R = H, I, and NO_2 in *ortho*-position of the phenyl ring as representatives of methylene bridged dpa derivatives with various electronic properties of the substituents. Metal center was chosen to be platinum(II), which is often used in development of phosphorescent materials due to its strong spin–orbit coupling;[36] complexes of platinum(II) with dpa-based ligands are also considered as potential anticancer agents.[12–15] In addition, synthesis of $[Pt(dpa\text{-}H)_2]$[33] and methylation of a structurally related bis(imidoylamidinate)platinum(II) complex $[Pt\{NH{=}C(Ph){-}NC(Ph){=}NPh\}_2]$,[37] which can be seen as prototype for the dpa benzylation reaction, have been published previously (Scheme 3).

The target benzyldi(2-pyridyl)amines **1–3** and platinum(II) complexes **4–10** were synthesized using both conventional (benzylation prior to coordination) and alternative (benzylation after coordination) approaches (Scheme 4). Below particular details of syntheses are discussed in detail and comparison between the two approaches is presented.

Conventional synthetic route. Benzyldi(2-pyridyl)amines **1** and **2** were synthesized by adapting published procedure[22] *via* nucleophilic attack of dpa on corresponding benzyl bromides in presence of sodium hydroxide. However, synthesis of **3** using the same technique failed due to enhanced methylene group reactivity (for discussion and identification of side pro-

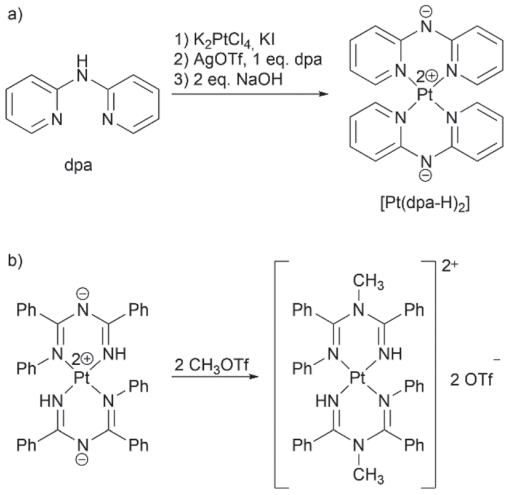

Scheme 3 Known reactions of platinum(II) complexes, which inspired this work: (a) synthesis of [Pt(dpa-H)$_2$],[23] (b) methylation of [Pt{NH=C(Ph)–NC(Ph)=NPh}$_2$].[26]

ducts, see section S1 in the ESI†), and consequently two step synthesis[38] implying water-free conditions and sodium hydride as a base was performed.

The obtained compounds were then coordinated on platinum(II) by adapting known procedures[33] in two steps. First, diiodide complexes **4–6** were obtained by reacting K_2PtCl_4 with one equivalent of **1–3** and excess of KI in water. The homoleptic complexes **[7–9]·(OTf)$_2$** were then obtained by reacting the diiodide complexes with another equivalent of the corresponding ligand **1–3** in acetonitrile in presence of silver(I) triflate (Scheme 4 top).

Alternative synthetic route. Neutral complex [Pt(dpa-H)$_2$] was synthesized using published procedure.[33] Reaction of this complex with corresponding benzyl bromides afforded target homoleptic complexes **[7–9]·Br$_2$**. Additionally, complex **[10]·Br$_2$** containing 2-cyanobenzyldi(2-pyridyl)amine ligands was synthesized with ease using this method (Scheme 4 bottom).

Yields of the two syntheses are compared in Table 1. Clearly, the alternative synthetic route provides higher overall yields of the homoleptic complexes **7–10** due to lower number and higher yields of the individual steps. In addition, introduction of the electron withdrawing groups in the benzyl moiety does not drastically affect the yields, in contrast with the conventional synthesis. Lesser reaction steps are also important for a practical synthesis. The conventional method required 9 steps to synthesize complexes **[7–9]·(OTf)$_2$** (3 reaction steps per complex), and many of them required individual approach due to variable properties (such as solubility and crystallizability) of the derivatives. On the other hand, starting from [Pt(dpa-H)$_2$], the alternative method took only 3 steps to synthesize these complexes as bromides using very similar

Table 1 Yields of complexes **7–10** in the two synthetic approaches

	Overall yield (yields of individual stages), %	
Complex	Conventional synthesis[a]	Alternative synthesis[b]
7	3 (26 × 82 × 14)	37 (38 × 97)
8	13 (44 × 48 × 61)	24 (38 × 64)
9	0.3 (9 × 20 × 15)	32 (38 × 85)
10	—	30 (38 × 79)

[a] Overall yields were obtained by multiplication of the individual yields of the corresponding stages in the following order: dpa → ligands (**1–3**), ligands (**1–3**) → diiodide complexes (**4–6**), and diiodide complexes (**4–6**) → homoleptic complexes (**[7–9]·(OTf)$_2$**). [b] Overall yields were obtained by multiplication of the yields of the corresponding individual stages in the following order: dpa → [Pt(dpa-H)$_2$], [Pt(dpa-H)$_2$] → homoleptic complexes (**[7–10]·Br$_2$**).

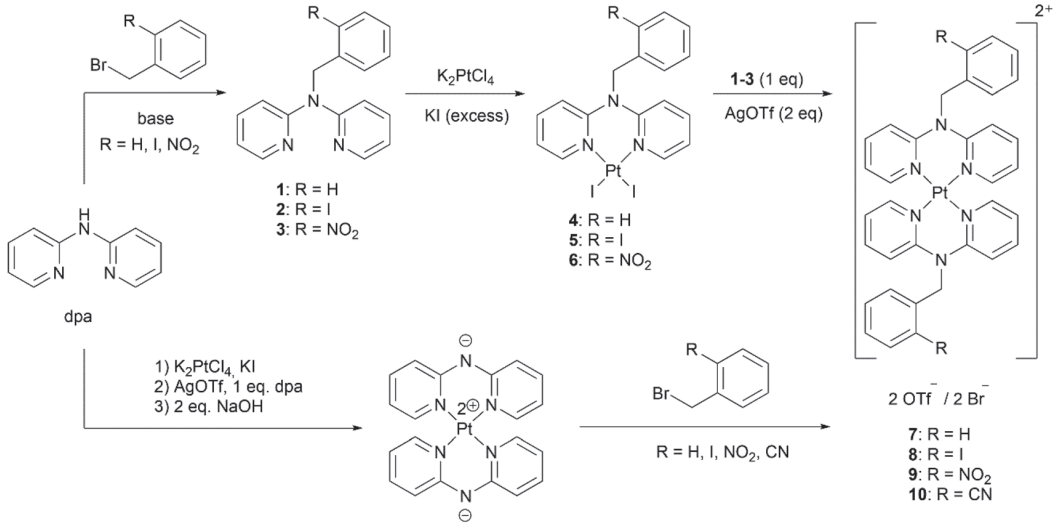

Scheme 4 Synthesis of benzyldi(2-pyridyl)amines **1–3** and their platinum(II) complexes **4–10**: the conventional (top) and alternative (bottom) approaches.

reaction conditions and workup. Moreover, any other derivative could be obtained just in one simple step using this method, as demonstrated by synthesis of **[10]·Br$_2$**.

These results demonstrate, that the alternative approach can be very convenient in synthesis of platinum(II) complexes with various methylene bridged dpa ligands. Moreover, even though separate tests were not performed, we believe that this approach can also be utilized for synthesis of platinum(II) complexes with only one methylene bridged dpa ligand. This suggestion is supported by the obtained side product dibromo(2-cyanobenzyldi(2-pyridyl)amine)platinum(II) (**S4**) in synthesis of **[10]·Br$_2$** (see section S2 in the ESI† for details).

Characterization of the products

In this section, crystal structures and general ^{1}H NMR spectral features of all the obtained benzyldi(2-pyridyl)amines **1–3** and platinum(II) complexes **4–10** are discussed.

Benzyldi(2-pyridyl)amines 1 and **2** crystallize in monoclinic space group $P2_1/n$, and **3** crystallizes in triclinic $P\bar{1}$ space group. In crystal structure of **1** pyridyl rings are in *cis–trans* conformation, whereas substituted derivatives **2** and **3** possess *cis–cis* conformation (using notation from ref. 1), and orientation of the phenyl ring in **2** and **3** is such that the substituents are turned outward from the pyridyl rings (Fig. 1). Halogen bond $N_{py}\cdots I$ ($d(N_{py}\cdots I)$ = 3.29 Å, $\angle(N_{py}\cdots I–C)$ = 166°) in crystal structure of **2** accounts for formation of the halogen bonded dimers (Fig. 2).

^{1}H NMR spectra of **1–3** possess a number of multiplet signals in aromatic area (8.3–6.8 ppm) corresponding to the hydrogen atoms of pyridyl and phenyl rings, and one singlet signal at 5.8–5.4 ppm corresponding to the methylene hydrogen atoms.

Diiodide complexes 4 and **6** crystallize in triclinic $P\bar{1}$ space group, whereas **5** crystallizes in monoclinic space group $P2_1/n$. In all complexes, the metal center is coordinated by the dpa derived ligands *via* pyridine nitrogen atoms (d(Pt–N) = 2.03–2.06 Å, $\angle$(N–Pt–N) = 84.9–85.3°), forming six-membered chelate rings in boat conformation, with 50.6–53.5° dihedral angles between the pyridine planes. Such coordination is common for platinum(II) complexes with methylene bridged dpa derivatives.[12,13] Two iodide ligands complete slightly distorted square planar configuration of the platinum metal centers with Pt–I bond lengths 2.58–2.60 Å and I–Pt–I angles 91.0–91.9°. In crystal structure of **5**, the phenyl iodine atom I3 is oriented towards platinum center, with Pt···I distance of 3.94 Å. In **6**, however, the nitro group is oriented away from platinum center (Fig. 3).

^{1}H NMR spectra of **4–6** show downfielded (9.4–9.5 ppm) aromatic signal possessing characteristic broadened satellites due to splitting from ^{195}Pt nucleus ($^3J_{H–Pt}$ = 48–64 Hz), which can therefore be assigned to pyridine hydrogen atoms in 6th position. The other aromatic and methylene proton signals of the complexes resemble those of the corresponding ligands.

Homoleptic complexes 7–10 form crystals of different morphologies depending on counter ion. In order to obtain high quality crystals, **7**, **8**, **10** were crystallized as triflates, whereas **9** was crystallized as a bromide. **[7,8]·(OTf)$_2$** and **[9]·Br$_2$** crystallize in monoclinic space group $C2/c$ (**[9]·Br$_2$** was crystallized as tetrahydrate), and **[10]·(OTf)$_2$** crystallizes in triclinic $P\bar{1}$ space group as dihydrate. Complexes **7–10** are centrosymmetric in solid state with platinum atoms at the inversion centers. Thus, asymmetric units in **7–10** contain platinum center with one

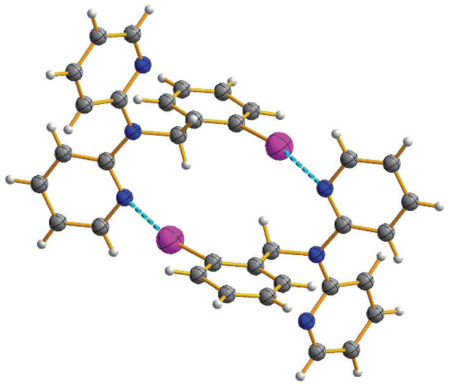

Fig. 2 Halogen bonded dimers of **2**.

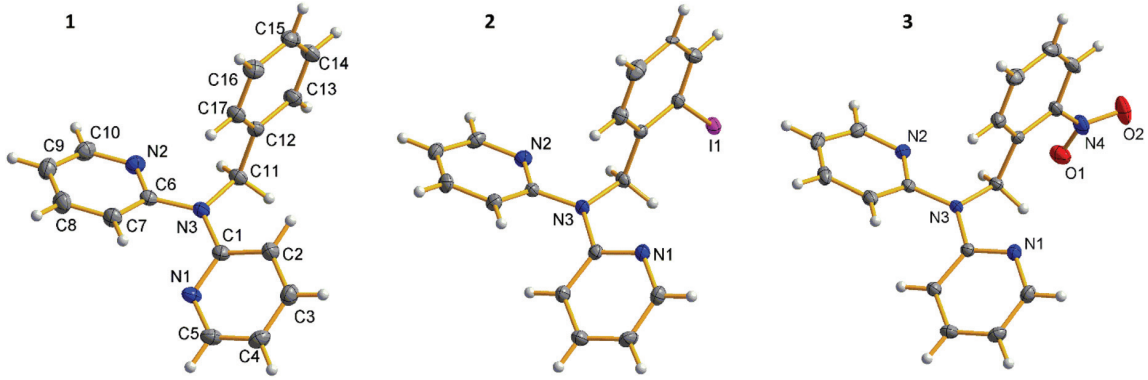

Fig. 1 Crystal structures of **1–3**.

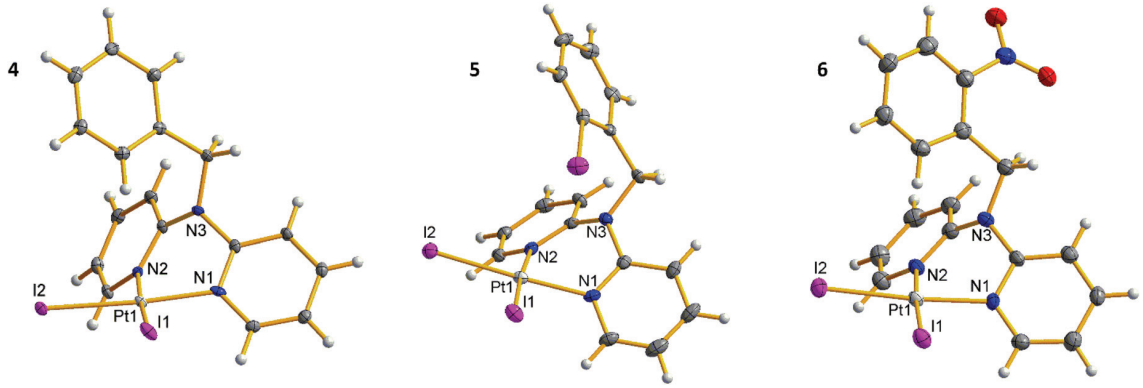

Fig. 3 Crystal structures of **4–6**.

ligand and one counter ion (and two and one water molecule in **[9]·Br$_2$** and **[10]·(OTf)$_2$** accordingly). Platinum centers possess square planar configuration with Pt–N bond lengths 2.01–2.02 Å and chelate N1–Pt–N2 angles 85.4–86.4°, and the six-membered chelate rings adopt boat conformation (dihedral angles between the pyridine planes 46.0–55.7°). Orientation of the phenyl ring in **[8]·(OTf)$_2$** is disordered between two positions: with iodine atom directed towards and away from platinum center. Nitro group in **[9]·Br$_2$** and cyano group in **[10]·(OTf)$_2$** are oriented towards platinum center with d(O2···Pt) = 3.27 Å in the former and d(N4···Pt) = 3.39 Å in the latter (Fig. 4).

^{1}H NMR spectra of **7–10** show that hydrogen atoms of the two ligands are pairwise magnetically equivalent in all complexes. Signals of the pyridine hydrogen atoms in 6th position are shifted upfield compared with the precursor diiodide complexes, and the satellites due to splitting from ^{195}Pt can barely be observed among the other aromatic signals.

Optical spectroscopy

Absorption spectra of **1–3** in methanol are presented in Fig. 5, and their features are summarized in Table S1 in the ESI.† The lowest energy absorption bands of the ligands can be assigned to the π–π* transitions within dpa moiety.[27] Studies of photophysical properties of benzyldi(2-pyridyl)amines **1–3** are complicated due to their ability to undergo photocyclization in solution.[39,40] While this process is slow enough to allow the measurement of absorption spectra, strong luminescence of the products and intermediates of the photocyclization interferes with the emission spectra of **1–3** in solution (for details, see section S3 in the ESI†). For this reason, studies of luminescent properties of the ligands were not included in this work. We have previously studied luminescent behavior of dpa hydrochloride, in which protonation of the pyridine nitrogen atoms suppresses the reaction of photocyclization in solution.[41] Analogous studies on luminescence of ligands **1–3** and other methylene bridged dpa derivatives are underway in our research group.

Absorption and photoluminescence emission spectra of **[7–10]·Br$_2$** are presented in Fig. 6 and summarized in Table 2. The lowest energy absorption bands of the complexes and the ligands possess similar wavelengths (λ_{max} ≈ 310 nm and 305 nm accordingly) and extinction coefficients ($\varepsilon \approx (13–16) \times 10^3$ l mol^{-1} cm^{-1}). The latter observation may indicate change in the nature of the lowest electronic transition upon coordination of the ligands to the platinum center. Complexes **[7–10]·Br$_2$** contain two ligands per molecule, and in the case of pure intraligand π–π* transitions approximately twice higher absorptivity would be expected for the complexes compared to the ligands.[42] In addition, previously published computational studies on platinum(II) complexes with dpa derived ligands revealed a significant contribution of the metal center in the frontier molecular orbitals.[15] Therefore, the low energy absorptions in **[7–10]·Br$_2$** are assigned to π–π* transitions within dpa moiety with an additional metal-to ligand charge transfer contribution.‡

Solutions of **[7–10]·Br$_2$** are not luminescent in methanol at room temperature. Quenching of luminescence of platinum(II) complexes is usually attributed to thermal population of relatively low lying metal centred excited states, leading to distortion of coordination geometry and consequent non-radiative relaxation.[43] In order to observe the emission, solutions of the complexes in methanol/ethanol mixture (1 : 4, v/v)[44] were cooled down to 80 K to form semi-rigid transparent glasses.

Emission properties of complexes **[7–10]·Br$_2$** share some common features. Thus, all complexes display emission bands with λ_{max} = 407–425 nm, and a good match was observed between the absorption (Fig. 6) and excitation (Fig. S6 in the ESI†) spectra. Analysis of the time-resolved spectra (see section S4 in the ESI†) reveals biexponential decays of these emission bands. In all cases, the initial fast decay is followed by the slower one, characterized by lifetimes τ_1 and τ_2 accordingly in Table 2. The obtained values allow assignment of the observed emission to phosphorescence.

However, significant differences are apparent from the emission spectra of **[8]·Br$_2$**, possessing additional shoulder at

‡This assignment is also supported by the preliminary computational DFT studies on **[8]·Br$_2$** (to be presented in the follow-up publication).

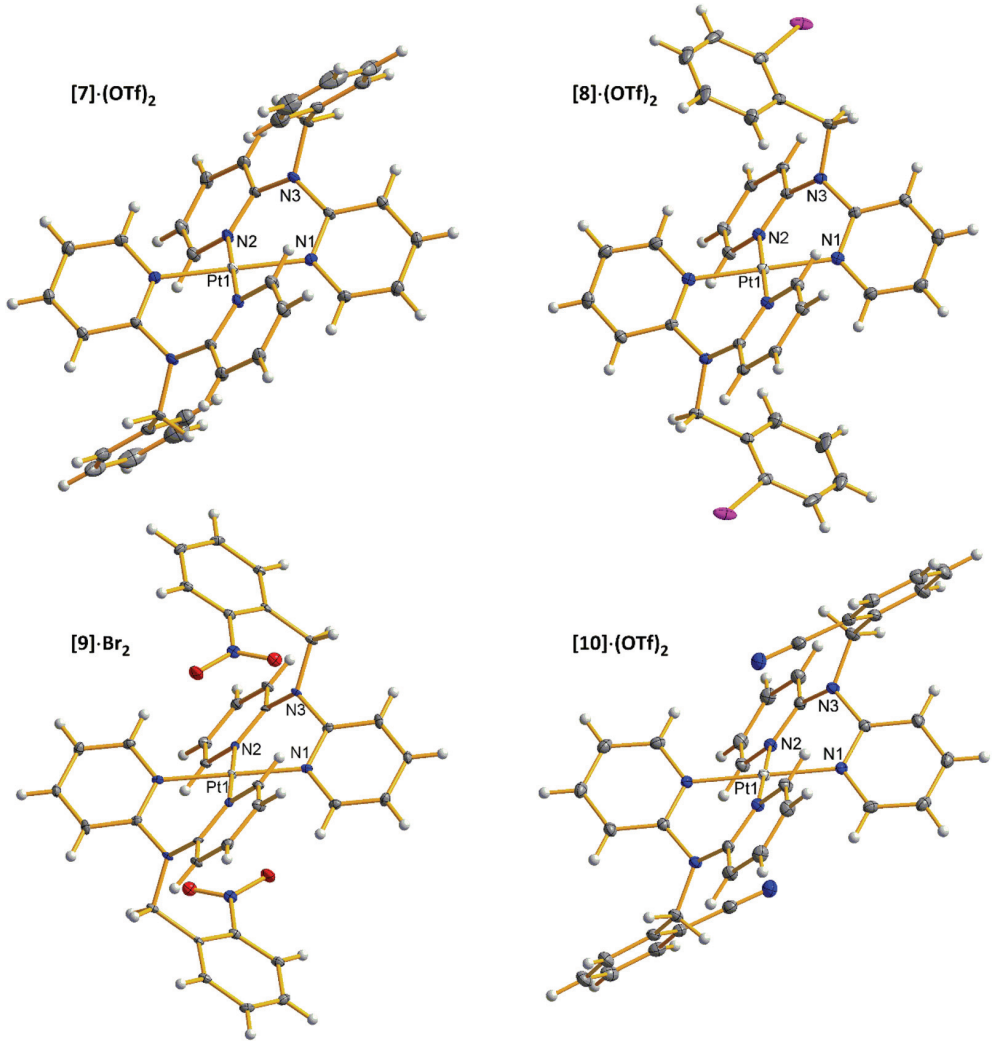

Fig. 4 Crystal structures of **7–10**. Anions and solvent molecules are omitted for clarity.

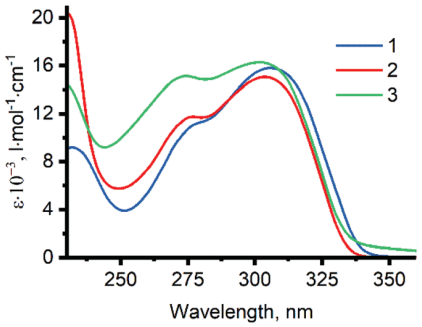

Fig. 5 Absorption spectra of ligands **1–3** (C = 50 μM) in methanol.

λ_{max} ≈ 475 nm, and **[10]·Br$_2$**, possessing additional peaks at λ_{max} = 448 and 480 nm. While in the latter case the emission spectrum only slightly changes with time at 80 K (Fig. S7 in the ESI†), the two emission bands of **[8]·Br$_2$** at λ_{max} = 417 and 470/500 nm possess strikingly different lifetimes of 39 μs and 3.7 ms accordingly. Time dependence of emission spectrum of **[8]·Br$_2$** is illustrated on Fig. 7 and Fig. S8 in the ESI.†

At higher temperatures small red shift of all of the emission peaks is accompanied by decrease of lifetimes and emission intensity until complete disappearance at 140–150 K. Temperature dependencies of the observed rate constants reveal plateaus in most of cases at temperatures close to 80 K, indicating that the temperature-dependent non-radiative processes are suppressed at this point.[45]

In addition, **[7,9]·Br$_2$** display an additional longer wavelength emission band (λ_{max} ≈ 500 nm) at temperatures of 120 K and higher, which strengthens upon continuous irradiation of the samples (Fig. S23 in the ESI†). Similar spectral changes may also take place for **[8,10]·Br$_2$**, being less apparent due to the broad emission bands of these complexes. The appearance of the new emission bands can be tentatively attributed to the

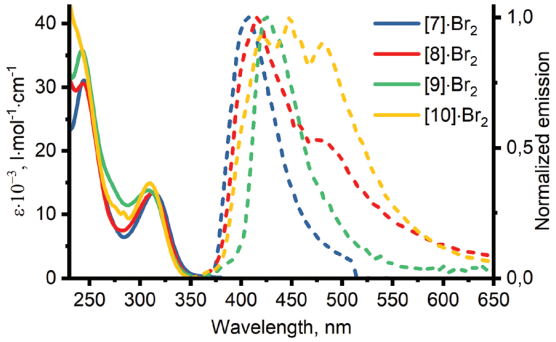

Fig. 6 Absorption (methanol solution, RT, solid lines) and phosphorescence emission (methanol/ethanol matrix, 80 K, dashed lines) spectra of **[7–10]·Br$_2$** (C = 20 μM). Emission spectra were measured under excitation at λ_{ex} = 320 nm, delay 20 ns, gate 10 μs (30 μs for **[8]·Br$_2$**).

Table 2 Absorption (methanol solution, RT) and phosphorescence emission (methanol/ethanol matrix, 80 K, λ_{ex} = 320 nm) properties of **[7–10]·Br$_2$**

Complex	λ_{abs}, nm	ε 10^{-3}, l mol^{-1} cm^{-1}	λ_{em}, nm	τ_1, μs	τ_2, μs
[7]·Br$_2$	244	31.0	407	78 ± 4	200 ± 3
	313	13.4			
[8]·Br$_2$	244	30.6	417	≤6[b]	39 ± 1
	312	13.3	470/500[a]	≤90[b]	3700 ± 60[c]
[9]·Br$_2$	243	35.8	425	≤5[b]	45 ± 1
	308	13.8			
[10]·Br$_2$	240	37.6	422/448/480[a]	21 ± 1	160 ± 20
	310	14.9			

[a] Bands with multiple local maxima. [b] Lifetimes too short for reliable determination using the applied gate times. [c] Measured at an equilibrium state, since the sample was excited by the laser at 100 Hz pulse repetition rate. Therefore, the real value may be slightly lower.

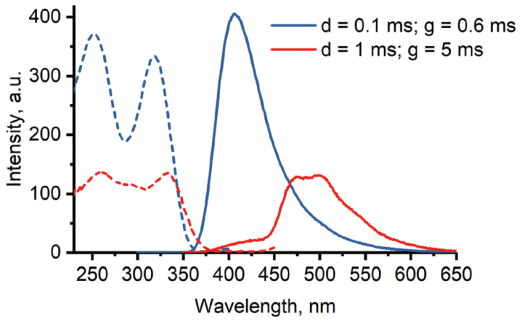

Fig. 7 Phosphorescence excitation (dashed lines, monitored at emission maximum) and emission (solid lines, monitored at excitation maximum) spectra of **[8]·Br$_2$** in methanol/ethanol glass under two sets of timing parameters (77 K, C = 20 μM, d = delay, g = gate).

formation of excimers in viscous methanol/ethanol solution at higher temperatures, which is a common feature of platinum(II) complexes.[43]

Summarizing, the obtained complexes **[7–10]·Br$_2$** demonstrate generally similar absorption and phosphorescence spectra with excited state lifetimes of microsecond order, typical for platinum(II) complexes.[43] On the other hand, the exceptionally long lifetime of the second emission band of **[8]·Br$_2$** – a unique feature of among the obtained complexes – is quite intriguing. This emission does not seem to originate either from excimer formation or from aggregation, since it is present in frozen matrix at 77 K, and does not depend on concentration (Fig. S11–18 in the ESI†). Thus, the additional green emission of **[8]·Br$_2$** can be supposedly associated with a specific conformation of the complex in the excited state, stabilized by an intramolecular interaction involving iodine atoms. Further studies of conformational flexibility and its impact on photophysical properties of **8** are currently being conducted in our research group.

Conclusions

Reaction between substituted benzyl bromides and [Pt(dpa-H)$_2$] is demonstrated to be an efficient synthetic route towards benzyldi(2-pyridyl)amine complexes of platinum(II), which can serve as an example of the proposed non-conventional approach towards synthesis of metal complexes with methylene bridged dpa derivatives. This approach involves derivatization as the last step, when the dpa moiety is already coordinated on metal center, therefore allowing efficient one-step synthesis of multiple complexes and at the same time preventing undesired side reactions. The compounds obtained in this work possess conformational flexibility due to the methylene bridge, which results in various orientations of the substituents in solid state. The complexes are not emissive in solution at room temperature, but display blue and green phosphorescence in frozen methanol/ethanol matrix at 77 K with the lifetimes of μs order. The iodine substituted complex **8** possesses additional green emission with the lifetime of about 3.7 ms. Further studies on complex **8** and origin of its dual emission are underway.

Experimental

All reagents and solvents for syntheses were purchased from Sigma-Aldrich, except for K_2PtCl_4 (Strem Chemicals and Alfa Aesar), and used as received without further purification. ^{1}H NMR spectra were recorded using Bruker Avance III HD 300 MHz and Bruker Avance 400 MHz spectrometers. Chemical shifts are expressed in ppm using residual solvent peak as internal standard. All the obtained ^{1}H NMR spectra are presented in section S5 in the ESI.† Elemental analyses (C, H, N) were preformed using Elementar Vario EL III elemental analyzer. Electrospray ionization mass spectra (ESI MS) were obtained with a Bruker micrOTOF or Agilent 6560 LC-IMMS TOF spectrometers equipped with an ESI source using methanol or acetonitrile as solvents.

Crystallography

The crystals of **1–10** and **S2–4** were immersed in cryo-oil, mounted in a MiTeGen loop and measured at 120 K on a Rigaku Oxford Diffraction Supernova diffractometer or at 170 K on a Bruker Axs KappaApexII diffractometer using Mo Kα (λ = 0.71073) radiation. The CrysAlisPro[46] or Denzo-Scalepack[47] program packages were used for cell refinements and data reductions. Multi-scan/Gaussian/Analytical absorption correction (CrysAlisPro,[46] SADABS[48]) was applied to the intensities before structure solution. The structures were solved by intrinsic phasing method using the SHELXT[49] software. Structural refinements were carried out using Olex2 [50] graphical user interface. Intrinsic disorder was modelled over two positions for one of the nitro groups in **3** and for 2-iodobenzyl moiety in **5** and **[8]·(OTf)$_2$**. C–H and O–H hydrogen atoms were positioned geometrically and constrained to ride on their parent atoms, with C–H = 0.95–1.00 Å, O–H = 0.85 Å, and U_{iso} = 1.2–1.5U_{eq} (parent atom), except for **[10]·(OTf)$_2$**, in which the H_2O hydrogen atoms were located from the difference Fourier and refined isotropically. The crystallographic details are summarized in section S6 in the ESI.†

Optical spectroscopy

HPLC grade methanol (J.T. Baker) and Uvasolv grade ethanol (Sigma-Aldrich) were used as solvents for optical measurements. Absorption spectra of **1–3** and **[7–10]·Br$_2$** were measured at ambient temperature in MeOH solution on Varian Cary 100 UV-visible spectrophotometer using quartz cuvettes with 1 cm path length in range of 220–700 nm. Steady state phosphorescence excitation and emission spectra of **[7–10]·Br$_2$** at 77 K in MeOH/EtOH (1 : 4, v/v) solution (presented in Fig. 7 and S6†) were measured on Varian Cary Eclipse Fluorescence spectrophotometer equipped with Oxford Optistat cryostat using cryogenic 1 cm quartz luminescence cuvette (FireflySci). Delay and gate times were adjusted in ranges of 0.1–1 ms and 0.6–5 ms accordingly using functions implemented in the spectrophotometer.

Phosphorescence emission decays were measured using the stroboscopic time resolution technique.[51] Samples were excited at λ_{ex} = 320 nm with 5 ns pulses (100 Hz repetition rate) using the diode pumped Q-switched Nd:YAG laser Ekspla NL230-100 with integrated optical parametric oscillator. The phosphorescence emission was detected at 90° angle using Oriel InstaSpec V ICCD detector with Acton SpectraPro sp-150i Spectrograph equipped with 300 grooves per mm grating blazed at 500 nm. Stanford Research Systems digital delay generator DG535 was used for controlling delay and gate timing parameters. Temperature of the samples was controlled within 80–150 K range using Oxford Optistat cryostat with nitrogen as static heat exchange gas. Sample solutions were placed in cryogenic 1 cm quartz luminescence cuvette (FireflySci) and deaerated by bubbling nitrogen gas for 10 minutes prior to measurements. A mechanical shutter was used to block the excitation beam between measurements to avoid photoinduced changes in the samples. The obtained spectra were processed using OriginPro software. The lifetime values were determined from the slopes of the fitted linear ln(I) *vs.* delay functions (see section S4 in the ESI†).

Synthetic procedures

Synthesis of benzyldi(2-pyridyl)amine (1). The product was synthesized according to published procedure.[22] Solution of benzyl bromide (190 mg, 1.1 mmol) in DMF (3 ml) was added to suspension of dpa (171 mg, 1 mmol) and sodium hydroxide (160 mg, 4 mmol) in DMF (5 ml) at room temperature. The mixture was stirred at 75 °C for 24 h to change color from yellowish to brown-orange. The solvent was evaporated on rotary evaporator and the residue was dissolved in mixture of water (15 ml) and chloroform (15 ml). Water phase was separated and extracted with chloroform (2 × 15 ml). The combined organic extract was dried over Na_2SO_4, filtered and evaporated. The residue was subjected to column chromatography purification on silica gel using chloroform/methanol (5 : 1, v/v) mixture as eluent. Product containing fractions were combined and evaporated to give yellow powder, which was recrystallized from acetone to obtain colorless crystals of the product (68 mg, 26%). Elemental analysis (%): C, 77.6; H, 5.4; N, 16.1. Calc. for $C_{17}H_{15}N_3$: C, 78.1; H, 5.8; N, 16.1. ^{1}H NMR (acetone-*d*6, 400 MHz): δ 8.29–8.25 (m, 2H), 7.63–7.57 (m, 2H), 7.38–7.34 (m, 2H), 7.27–7.20 (m, 4H), 7.16–7.12 (m, 1H), 6.92–6.87 (m, 2H), 5.53 (s, 2H, CH_2). ESI MS (*m*/*z*): 262.14 (calcd for $[M + H]^+$ 262.13), 545.26 (calcd for $[2M + Na]^+$ 545.24). Crystals suitable for X-ray diffraction analysis were obtained by slow evaporation of solution in acetone.

Synthesis of 2-iodobenzyldi(2-pyridyl)amine (2). Solution of 2-iodobenzyl bromide (600 mg, 2 mmol) in DMF (3 ml) was added to suspension of dpa (342 mg, 2 mmol) and sodium hydroxide (240 mg, 6 mmol) in DMF (5 ml). The resulted mixture was stirred at room temperature for 24 h to change color from yellowish to dark-yellow. Remaining solids of sodium hydroxide were filtered and solvent was evaporated on rotary evaporator. Brown residue was dissolved in mixture of water (20 ml) and chloroform (20 ml). Water phase was separated and extracted with chloroform (3 × 20 ml). Combined organic extracts were dried over Na_2SO_4, filtered and evaporated to volume of 20 ml. Acetone (20 ml) was added and the solution was left overnight at 5 °C for crystallization. Obtained yellowish crystals were filtered, washed with acetone (2 × 2 ml), and recrystallized from acetone/chloroform (1 : 1, v/v) solution to obtain the product as colorless crystals (345 mg, 44%). Elemental analysis (%): C, 52.6; H, 3.4; N, 10.9. Calcd for $C_{17}H_{14}N_3I$: C, 52.7; H, 3.6; N, 10.9. ^{1}H NMR ($CDCl_3$, 300 MHz): δ 8.31–8.29 (m, 2H), 7.83 (dd, 1H, J = 1.0, 7.9 Hz), 7.58–7.50 (m, 2H), 7.25–7.15 (m, 4H), 6.93–6.83 (m, 3H), 5.41 (s, 2H, CH_2). ESI MS (*m*/*z*): 387.99 (calcd for $[M + H]^+$ 388.03). Crystals suitable for X-ray diffraction analysis were obtained by slow evaporation of solution in chloroform.

Synthesis of 2-nitrobenzyldi(2-pyridyl)amine (3). Synthesis was conducted under nitrogen atmosphere using standard Schlenk techniques similarly to published procedure.[38] Sodium hydride (290 mg, 60% in mineral oil, 7.25 mmol) was

mixed with pentane (20 ml) and resulted suspension stirred for 3 min. When solids settled down most of the solvent was decanted to remove the oil. The procedure was repeated once more and remaining pentane was dried out under vacuum. Toluene (5 ml) was added with stirring at −78 °C followed by solution of dpa (860 mg, 5.03 mmol) in toluene (20 ml). The reaction mixture was allowed to heat up to room temperature. During this time formation of gas bubbles and cream colored precipitate was observed. The mixture was stirred for 1 h at room temperature (stirring was hampered due to formation of precipitate) and 18 h at 100 °C. After cooling to room temperature, solution of 2-nitrobenzyl bromide (1.3 g, 6.02 mmol) in toluene (20 ml) was added to the resulted gray suspension. The mixture was stirred at room temperature for 30 min and then at 100 °C overnight. After cooling to room temperature formed light brown precipitate was filtered; brown filtrate was concentrated on rotary evaporator. The obtained brown oil was dissolved in chloroform, filtered from formed white precipitate (side product **S3**, see section S1 in the ESI†), and solution subjected to column chromatography purification using chloroform/diethyl ether (1 : 1, v/v) mixture as eluent. Product containing fractions were combined and subjected to second column chromatography purification using ethyl acetate/hexane (1 : 5 → 3 : 5, v/v) mixture as eluent. Product containing fractions were combined and slowly evaporated at room temperature to produce yellow crystals, which were recrystallized from ethyl acetate/pentane/diethyl ether (1 : 2 : 1, v/v) solution to get the product as yellowish crystals (137 mg, 9%). Elemental analysis (%): C, 66.3; H, 4.3; N, 18.05. Calcd for $C_{17}H_{14}N_4O_2$: C, 66.7; H, 4.6; N, 18.3. ^{1}H NMR ($CDCl_3$, 300 MHz): δ 8.29–8.27 (m, 2H), 8.04 (dd, 1H, J = 1.3, 8.0 Hz), 7.60–7.50 (m, 3H), 7.48–7.41 (m, 1H), 7.36–7.29 (m, 1H), 7.24–7.19 (m, 2H), 6.89–6.84 (m, 2H), 5.83 (s, 2H, CH_2). ESI MS (m/z): 307.11 (calcd for $[M + H]^+$ 307.12). Crystals suitable for X-ray diffraction analysis were obtained by slow evaporation of solution in ethyl acetate/pentane/diethyl ether (1 : 2 : 1, v/v).

Synthesis of diiodo(benzyldi(2-pyridyl)amine)platinum(II) (4). Solution of K_2PtCl_4 (62 mg, 0.15 mmol) and KI (620 mg, 3.73 mmol) in water (10 ml) was stirred for 20 min. Solid **1** (45 mg, 0.17 mmol) was added to the obtained dark-red solution and the resulting suspension was stirred for 19 h at room temperature and then 30 min at 85 °C. Yellow precipitate was filtered out and washed with chloroform (5 × 1 ml) to give the product as yellow powder (87.3 mg, 82%). Elemental analysis (%): C, 28.6; H, 2.2; N, 6.1. Calcd for $C_{17}H_{15}N_3I_2Pt$: C, 28.8; H, 2.1; N, 5.9. ^{1}H NMR (THF-$d8$, 400 MHz): δ 9.45–9.29 (m, 2H, broad sidebands due to $^3J_{Pt,H}$ = 45.0 Hz), 7.93–7.87 (m, 2H), 7.84–7.79 (m, 2H), 7.38–7.27 (m, 4H), 7.18 (m, 1H), 7.11–7.06 (m, 2H), 5.37 (s, 2H, CH_2). ESI MS (m/z): 624.00 (calcd for $[M - I + CH_3CN]^+$ 624.02), 262.12 (calcd for $[M - PtI_2 + H]^+$ 262.13). Crystals suitable for X-ray diffraction analysis were obtained by slow evaporation of solution in THF.

Synthesis of diiodo(2-iodobenzyldi(2-pyridyl)amine)platinum(II) (5). Solution of K_2PtCl_4 (124 mg, 0.30 mmol) and KI (1.25 g, 7.5 mmol) in water/THF mixture (10 ml, 1 : 1, v/v) was stirred for 20 min. Solid **2** (120 mg, 0.31 mmol) was added to the obtained dark-red solution and the resulting suspension was refluxed for 16 h at 85 °C. The solvent was partly evaporated on rotary evaporator and yellow-orange powder was filtered and washed with chloroform (5 × 3 ml) and THF (5 × 3 ml) to give the product as yellow powder (120.4 mg, 48%). Elemental analysis (%): C, 24.3; H, 1.7; N, 4.9. Calcd for $C_{17}H_{14}N_3I_3Pt$: C, 24.4; H, 1.7; N, 5.0. ^{1}H NMR (THF-$d8$, 300 MHz): δ 9.49–9.29 (m, 2H, broad sidebands due to $^3J_{Pt,H}$ = 46.3 Hz), 8.40 (d, 1H, J = 7.9 Hz), 7.99–7.92 (m, 2H), 7.84 (dd, 1H, J = 1.4, 7.9 Hz), 7.70–7.30 (m, 3H), 7.16–7.08 (m, 2H), 6.99–6.91 (m, 1H), 5.43 (s, 2H, CH_2). ESI MS (m/z): 749.89 (calcd for $[M - I + CH_3CN]^+$ 749.91). Crystals suitable for X-ray diffraction analysis were obtained by slow evaporation of solution in THF.

Synthesis of diiodo(2-nitrobenzyldi(2-pyridyl)amine)platinum(II) (6). Solution of K_2PtCl_4 (61 mg, 0.15 mmol) and KI (610 mg, 3.67 mmol) in water (10 ml) was stirred for 20 min. Solution of **3** (45 mg, 0.15 mmol) in THF (4 ml) was added to the obtained dark-red solution and the resulting suspension was stirred for 20 h at 70 °C. The solvent was partly evaporated on rotary evaporator and brown precipitate was filtered and washed with water (3 ml). Resulting solids were suspended in boiling chloroform (7 ml) and yellow solution was decanted. The procedure was repeated 5 times, the obtained solutions were combined and evaporated. The residue was washed with chloroform (2 × 2 ml) and suspended in THF (3 ml). Dark solution was decanted and brown-yellow solids were washed with THF (3 × 1 ml) and chloroform (2 × 1 ml) to give the product as yellow powder (23 mg, 20%). Elemental analysis (%): C, 26.8; H, 1.8; N, 7.4. Calcd for $C_{17}H_{14}N_4O_2I_2Pt$: C, 27.0; H, 1.8; N, 7.4. ^{1}H NMR (THF-$d8$, 300 MHz): δ 9.48–9.29 (m, 2H, broad sidebands due to $^3J_{Pt,H}$ = 44.4 Hz), 9.02 (d, 1H, J = 7.7 Hz), 8.04 (dd, 1H, J = 1.1, 8.1 Hz), 8.00–7.90 (m, 2H), 7.71–7.62 (m, 1H), 7.56–7.40 (m, 2H), 7.19–7.10 (m, 1H), 5.81 (s, 2H, CH_2). ESI MS (m/z): 668.78 (calcd for $[M - I + CH_3CN]^+$ 669.00). Crystals suitable for X-ray diffraction analysis were obtained by slow evaporation of solution in THF.

General procedure for conventional synthesis of bis(benzyldi(2-pyridyl)amine)platinum(II) triflate complexes [7–9]·$(OTf)_2$

Suspension of precursor complex **4–6** (0.1 mmol) and corresponding ligand **1–3** (0.1 mmol) in acetonitrile (10 ml) was stirred at 60 °C for 10 min. Solution of silver triflate (55 mg, 0.21 mmol) in acetonitrile (5 ml) was added dropwise at this temperature within 5–7 min. Resulted mixture was stirred in darkness at 75 °C for 16 h. Yellow precipitate of silver iodide was filtered off and the filtrate was partially evaporated on rotary evaporator to volume of 2 ml and allowed to evaporate slowly at room temperature overnight. Resulted crystals were washed with THF (2 × 2 ml), recrystallized from methanol/acetonitrile mixture (1 : 1, v/v), and washed again with THF (3 × 2 ml) to give product as colorless crystals. Crystals of **[7,8]·$(OTf)_2$** suitable for X-ray diffraction analysis were obtained by slow evaporation of solution in methanol. No high quality crystals could be obtained for **[9]·$(OTf)_2$**, and crystals of **[9]·Br_2** were measured instead.

Bis(benzyldi(2-pyridyl)amine)platinum(II) triflate ([7]·(OTf)$_2$). Yield: 14 mg, 14%. Elemental analysis (%): C, 42.0; H, 2.7; N, 8.0. Calcd for $C_{36}H_{30}N_6O_6F_6S_2Pt$: C, 42.6; H, 3.0; N, 8.3. ^{1}H NMR (CD_3CN, 400 MHz): δ 8.14–8.08 (m, 4H), 7.85 (d, 4H, J = 7.1 Hz), 7.78–7.68 (m, 8H), 7.44–7.37 (m, 4H), 7.36–7.30 (m, 2H), 7.22–7.17 (m, 4H), 5.51 (s, 4H, CH_2). ESI MS (m/z): 866.13 (calcd for $[M - OTf]^+$ 866.17).

Bis(2-iodobenzyldi(2-pyridyl)amine)platinum(II) triflate ([8]·(OTf)$_2$). Yield: 83 mg, 61%. Elemental analysis (%): C, 34.1; H, 2.1; N, 6.75. Calcd for $C_{36}H_{28}N_6O_6F_6S_2I_2Pt$: C, 34.1; H, 2.2; N, 6.6. ^{1}H NMR (CD_3OD, 300 MHz): δ 8.28–8.20 (m, 4H), 7.98–7.88 (m, 8H), 7.77 (m, 4H), 7.50–7.42 (m, 2H), 7.32–7.25 (m, 4H), 7.15–7.08 (m, 2H), 5.57 (s, 4H, CH_2). ESI MS (m/z): 1117.92 (calcd for $[M - OTf]^+$ 1117.96).

Bis(2-nitrobenzyldi(2-pyridyl)amine)platinum(II) triflate ([9]·(OTf)$_2$). Yield: 17 mg, 15%. Elemental analysis (%): C, 39.1; H, 2.6; N, 9.7. Calcd for $C_{36}H_{28}N_8O_{10}F_6S_2Pt$: C, 39.1; H, 2.55; N, 10.1. ^{1}H NMR (CD_3OD, 300 MHz): δ 8.30–8.22 (m, 4H), 8.04–7.92 (m, 8H), 7.84–7.72 (m, 6H), 7.68–7.61 (m, 2H), 7.38–7.31 (m, 4H), 5.91 (s, 4H, CH_2). ESI MS (m/z): 403.59 (calcd for $[M - 2OTf]^{2+}$ 403.59).

General procedure for alternative synthesis of bis(benzyldi(2-pyridyl)amine)platinum(II) bromide complexes [7–10]·Br$_2$

[Pt(dpa-H)$_2$] (53 mg, 0.1 mmol, prepared according to previously published procedure[33] with 38% yield) and corresponding benzyl bromide (0.2 mmol) were suspended in acetonitrile (20 ml) and stirred at 75 °C for 24 h and refluxed for 2 h. Solvent was evaporated on rotary evaporator, and yellow residue was washed with chloroform (2 × 2 ml) and diethyl ether (2 × 2 ml). Resulting colorless solids were recrystallized from methanol to afford product as colorless crystalline material ([7]·Br$_2$, 86 mg, 97%; [8]·Br$_2$, 72 mg, 64%; [9]·Br$_2$, 82 mg, 85%). ^{1}H NMR spectra of [7–9]·Br$_2$ matched those presented above. Crystals of [9]·Br$_2$ suitable for X-ray diffraction analysis were obtained by slow evaporation of solution in methanol. In synthesis of [10]·Br$_2$, additional side product **S4** was isolated and identified (see section S2 in the ESI†).

Bis(2-cyanobenzyldi(2-pyridyl)amine)platinum(II) bromide ([10]·Br$_2$). Yield: 78 mg, 79%. Elemental analysis (%): C, 46.2; H, 3.2; N, 11.7. Calcd for $C_{36}H_{28}N_8Br_2Pt$: C, 46.6; H, 3.0; N, 12.1. ^{1}H NMR (CD_3OD, 300 MHz): δ 8.30–8.22 (m, 4H), 8.07–8.02 (m, 2H), 7.97–7.95 (m, 4H) 7.88–7.72 (m, 8H), 7.60–7.54 (m, 2H), 7.33–7.27 (m, 2H), 5.75 (s, 4H, CH_2). ESI MS (m/z): 846.12 (calcd for $[M - Br]^+$ 846.13), 383.60 (calcd for $[M - 2Br]^{2+}$ 383.60). Since only poor quality thin needle crystals could be obtained from [10]·Br$_2$, the reaction of anion exchange from bromide to triflate was performed using silver(I) triflate in methanol. Crystals of [10]·(OTf)$_2$ suitable for X-ray diffraction analysis were obtained by slow evaporation of the resulted filtered solution.

Conflicts of interest

There are no conflicts to declare.

Acknowledgements

E. B. and M. H. kindly acknowledge the financial support from the Academy of Finland (Proj. no. 295581). The authors would also like to acknowledge Elina Hautakangas for elemental analyses, Dr Elina Kalenius for mass spectrometry measurements, Dr Matti Tuikka for helping with X-ray analyses, and Dr Pasi Myllyperkiö and Dr Heikki Häkkänen for assisting with optical spectroscopy measurements.

Notes and references

1 D. W. Brogden and J. F. Berry, *Comments Inorg. Chem.*, 2016, **36**, 17–37.
2 C. J. Sumby, *Coord. Chem. Rev.*, 2011, **255**, 1937–1967.
3 B. Chen, G. Yu, X. Li, Y. Ding, C. Wang, Z. Liu and Y. Xie, *J. Mater. Chem. C*, 2013, **1**, 7409–7417.
4 R. Tan, Z.-B. Wang, Y. Li, D. J. Kozera, Z.-H. Lu and D. Song, *Inorg. Chem.*, 2012, **51**, 7039–7049.
5 W.-L. Jia, T. McCormick, Q.-D. Liu, H. Fukutani, M. Motala, R.-Y. Wang, Y. Tao and S. Wang, *J. Mater. Chem.*, 2004, **14**, 3344–3350.
6 J. Pang, Y. Tao, S. Freiberg, X.-P. Yang, M. D'Iorio and S. Wang, *J. Mater. Chem.*, 2002, **12**, 206–212.
7 J. Pang, E. J.-P. Marcotte, C. Seward, R. S. Brown and S. Wang, *Angew. Chem., Int. Ed.*, 2001, **40**, 4042–4045.
8 Y.-Q. Weng, F. Yue, Y.-R. Zhong and B.-H. Ye, *Inorg. Chem.*, 2007, **46**, 7749–7755.
9 A. K. Paul, H. Mansuri-Torshizi, T. S. Srivastava, S. J. Chavan and M. P. Chitnis, *J. Inorg. Biochem.*, 1993, **50**, 9–20.
10 A. K. Paul, T. S. Srivastava, S. J. Chavan, M. P. Chitnis, S. Desai and K. K. Rao, *J. Inorg. Biochem.*, 1996, **61**, 179–196.
11 C. Icsel, V. T. Yilmaz, Y. Kaya, H. Samli, W. T. A. Harrison and O. Buyukgungor, *Dalton Trans.*, 2015, **44**, 6880–6895.
12 M. J. Rauterkus, S. Fakih, C. Mock, I. Puscasu and B. Krebs, *Inorg. Chim. Acta*, 2003, **350**, 355–365.
13 S. Fakih, W. C. Tung, D. Eierhoff, C. Mock and B. Krebs, *Z. Anorg. Allg. Chem.*, 2005, **631**, 1397–1402.
14 I. Puscasu, C. Mock, M. Rauterkus, A. Röndigs, G. Tallen, S. Gangopadhyay, J. E. Wolff and B. Krebs, *Z. Anorg. Allg. Chem.*, 2001, **627**, 1292–1298.
15 P. W. Asman, *Inorg. Chim. Acta*, 2018, **469**, 341–352.
16 C. Seward and S. Wang, *Comments Inorg. Chem.*, 2005, **26**, 103–125.
17 Y. Kang and S. Wang, *Tetrahedron Lett.*, 2002, **43**, 3711–3713.
18 W.-L. Jia, D. Song and S. Wang, *J. Org. Chem.*, 2003, **68**, 701–705.
19 K.-J. Wei, Y.-S. Xie, J. Ni, M. Zhang and Q.-L. Liu, *Inorg. Chem. Commun.*, 2006, **9**, 926–930.
20 K.-J. Wei, Y.-S. Xie, J. Ni, M. Zhang and Q.-L. Liu, *Cryst. Growth Des.*, 2006, **6**, 1341–1350.

21 J. Ni, K.-J. Wei, Y. Min, Y. Chen, S. Zhan, D. Li and Y. Liu, *Dalton Trans.*, 2012, **41**, 5280–5293.

22 B. Antonioli, D. J. Bray, J. K. Clegg, K. Gloe, K. Gloe, O. Kataeva, L. F. Lindoy, J. C. McMurtrie, P. J. Steel, C. J. Sumby and M. Wenzel, *Dalton Trans.*, 2006, 4783–4794.

23 B. Antonioli, D. J. Bray, J. K. Clegg, K. Gloe, K. Gloe, A. Jäger, K. A. Jolliffe, O. Kataeva, L. F. Lindoy, P. J. Steel, C. J. Sumby and M. Wenzel, *Polyhedron*, 2008, **27**, 2889–2898.

24 D. J. Bray, J. K. Clegg, K. A. Jolliffe and L. F. Lindoy, *CrystEngComm*, 2014, **16**, 6476–6482.

25 P. W. Asman and D. Jaganyi, *Int. J. Chem. Kinet.*, 2017, **49**, 545–561.

26 J.-S. Yang, Y.-D. Lin, Y.-H. Chang and S.-S. Wang, *J. Org. Chem.*, 2005, **70**, 6066–6073.

27 M. A. Rohman, D. Sutradhar, S. Sangilipandi, K. Mohan Rao, A. K. Chandra and S. Mitra, *J. Photochem. Photobiol., A*, 2017, **341**, 115–126.

28 A. J. Swarts and S. F. Mapolie, *Dalton Trans.*, 2014, **43**, 9892–9900.

29 M. Vaquero, A. Ruiz-Riaguas, M. Martínez-Alonso, F. A. Jalón, B. R. Manzano, A. M. Rodríguez, G. García-Herbosa, A. Carbayo, B. García and G. Espino, *Chem. – Eur. J.*, 2018, **24**, 10662–10671.

30 J. F. Geldard and F. Lions, *J. Am. Chem. Soc.*, 1962, **84**, 2262–2263.

31 T. J. Hurley and M. A. Robinson, *Inorg. Chem.*, 1968, **7**, 33–38.

32 F. A. Cotton, L. M. Daniels, G. T. Jordan and C. A. Murillo, *Polyhedron*, 1998, **17**, 589–597.

33 Q. Wang, P. V. Gushchin, N. A. Bokach, M. Haukka and V. Yu. Kukushkin, *Russ. Chem. Bull.*, 2012, **61**, 828–835.

34 Y. Tor, *Synlett*, 2002, 1043–1054.

35 T. Mede, M. Jäger and U. S. Schubert, *Chem. Soc. Rev.*, 2018, **47**, 7577–7627.

36 B. Minaev, G. Baryshnikov and H. Agren, *Phys. Chem. Chem. Phys.*, 2014, **16**, 1719–1758.

37 G. H. Sarova, N. A. Bokach, A. A. Fedorov, M. N. Berberan-Santos, V. Yu. Kukushkin, M. Haukka, J. J. R. Frausto da Silva and A. J. L. Pombeiro, *Dalton Trans.*, 2006, 3798–3805.

38 S. Licciulli, I. Thapa, K. Albahily, I. Korobkov, S. Gambarotta, R. Duchateau, R. Chevalier and K. Schuhen, *Angew. Chem., Int. Ed.*, 2010, **49**, 9225–9228.

39 V. M. Clark, A. Cox and E. J. Herbert, *J. Chem. Soc. C*, 1968, 831–833.

40 J. D. Cocker, G. I. Gregory and G. B. Webb, *Br. Pat.*, GB 1262864, 1972.

41 E. Bulatov and M. Haukka, *ChemistrySelect*, 2018, **3**, 11535–11540.

42 K.-Y. Ho, W.-Y. Yu, K.-K. Cheung and C.-M. Che, *J. Chem. Soc., Dalton Trans.*, 1999, 1581–1586.

43 J. A. G. Williams, *Top. Curr. Chem.*, 2007, **281**, 205–268.

44 D. R. Scott and J. B. Allison, *J. Phys. Chem.*, 1962, **66**, 561–562.

45 T. O. Harju, J. E. I. Korppi-Tommola, A. H. Huizer and C. A. G. O. Varma, *J. Phys. Chem.*, 1996, **100**, 3592–3600.

46 Agilent, *CrysAlisPro*, Agilent Technologies Ltd, Yarnton, Oxfordshire, England, 2014.

47 Z. Otwinowski and E. Minor, in *Methods in Enzymology*, ed. C. W. Carter and R. M. Sweet, Academic Press, New York, 1997, vol. 276, *Macromolecular Crystallography*, Part A, pp. 307–326.

48 G. M. Sheldrick, *SADABS - Bruker AXS, scaling and absorption correction*, Bruker AXS, Inc., Madison, Wisconsin, USA, 2012.

49 G. M. Sheldrick, *Acta Cryst. A*, 2015, **71**, 3–8.

50 O. V. Dolomanov, L. J. Bourhis, R. J. Gildea, J. A. K. Howard and H. Puschmann, *J. Appl. Crystallogr.*, 2009, **42**, 339–341.

51 D. R. James, A. Siemiarczuk and W. R. Ware, *Rev. Sci. Instrum.*, 1992, **63**, 1710–1716.

II

A 2D Network in Co-Crystal (1:1) Based on *trans*-[$PtBr_2$(Acetoxime)$_2$] and 18-Crown-6

by

Evgeny Yu. Bulatov, Tatiana G. Chulkova, Matti Haukka & Vadim Yu. Kukushkin

J. Chem. Crystallogr., **2012**, *42*, 352-355

A 2D network in co-crystal (1:1) based on *trans*-[$PtBr_2$(acetoxime)$_2$] and 18-crown-6

Evgeny Yu. Bulatov • Tatiana G. Chulkova • Matti Haukka • Vadim Yu. Kukushkin

Evgeny Yu. Bulatov • Tatiana G. Chulkova (✉) • Vadim Yu. Kukushkin
Department of Chemistry, St. Petersburg State University, 198504 Stary Petergof, Russian Federation
e-mail: tgc@mail.ru

Matti Haukka
Department of Chemistry, University of Eastern Finland, P.O. Box 111, FI-80101, Joensuu, Finland

Abstract A 1:1 co-crystal of *trans*-[$PtBr_2$(acetoxime)$_2$] and 18-crown-6 has been obtained by a slow-evaporation of the equimolar mixture of *trans*-[$PtBr_2$(acetoxime)$_2$] and the crown ether. The compound crystallizes in the triclinic space group P-1, with unit cell parameters a = 7.4765(2) Å, b = 9.5044(2) Å, c = 10.1591(3) Å, α = 83.687(1)°, β = 70.847(1)°, γ = 79.773(1)°, Z = 1. *trans*-[$PtBr_2$(acetoxime)$_2$] is assembled with 18-crown-6 into a 2D network structure by interactions between the oxygen atoms of 18-crown-6 and the hydroxylic and methyl hydrogen atoms of the oxime ligands.

Keywords Acetoxime • Co-crystal • 18-Crown-6 • Platinum • Supramolecular chemistry

Introduction

Association of heteroatom containing macrocyclic compounds such as crown ethers with metal complexes provides a new approach for generation of supramolecular architecture. Intermolecular interactions between metal complexes and crown ethers leading to the formation of associates offer the possibility for design of different metal-containing supramolecular materials and selective extraction of coordination compounds into hydrophobic media [1]. A large amount of crown ether associates have been produced and studied by different methods [2-7]. Most of these species exhibit 1D array structure with the equimolar complex to crown ether stoichiometry. Supramolecular organization determined by hydrogen bonding between an oxygen atom of the crown ether and acidic hydrogen(s) of a ligand. In view of our interest in the oxime chemistry [8-11] and, in particular, in supramolecular aggregations involving metal-bound oximes [12], we studied association of an (acetoxime)Pt^{II} complex and a crown ether providing an infinite 2D network structure. In this study, a 2D supramolecular *trans*-[$PtBr_2$(acetoxime)$_2$]•(18-crown-6) associate has been produced by co-crystallization of *trans*-[$PtBr_2$(acetoxime)$_2$] and 18-crown-6.

Experimental

General

All the reagents and solvents employed were commercially available and used as received without further purification. FTIR spectrum (4000–400 cm^{-1}) was recorded on a Shimadzu FTIR-8400S spectrometer in KBr pellets. ^{1}H NMR measurements were performed on a Bruker-DPX 300 instrument at ambient temperature. HRMS spectra are recorded on a Bruker micrOTOF electrospray ionization mass spectrometer.

Preparation

trans-[$PtBr_2$(acetoxime)$_2$] was produced by the isomerization of *cis*-[$PtBr_2$(acetoxime)$_2$] [13] and co-crystallized with 18-crown-6 in a 1:1 molar ratio from an acetone:chloroform (2:3, v/v) solution at 20–25 °C.
trans-[$PtBr_2$(acetoxime)$_2$]•(18-crown-6) (**1**): greenish-yellow crystals, mp = 163–167 °C (dec.). HRMS (ESI, *m/z*) = 500.9094 (100%), 499.9121 (75%), 498.9112 (98%) (M – 18-crown-6 – H)$^-$, 265.1731 (2.4%) (M – [$PtBr_2$(acetoxime)$_2$] + H)$^+$, 282.2000 (100%) (M – [$PtBr_2$(acetoxime)$_2$] + H_2O)$^+$, 287.1549 (12%) (M – [$PtBr_2$(acetoxime)$_2$] + Na)$^+$, 303.1293 (24%) (M – [$PtBr_2$(acetoxime)$_2$] + K)$^+$. IR data, cm^{-1}: 3441 br ν(O–H), 1664 m ν(C=N), 1105 ms ν(C–O), 962 m ν(N–O). ^{1}H NMR in acetone-d_6, δ, ppm: 2.19 (s, 6H, CH_3), 2.61 (s, 6H, CH_3), 3.62 (s, 24H, CH_2).

Single-crystal X-ray analysis

Structure Determination and Refinement of 1

X-ray structure determination was carried out on a Bruker Smart Apex II diffractometer using Mo Kα radiation (λ = 0.71073 Å). The APEX2 [14] program package was used for cell refinements and data reductions. The structure was solved by direct methods using SHELXS-97 [15] with the WinGX [16] graphical user interface. An empirical absorption correction (SADABS [17]) was applied to the data. Structural refinements were carried out using SHELXL-97 [15]. The OH hydrogen atom was located from the difference Fourier map but idealized with O–H 0.84 Å, and U_{iso} = 1.5 U_{eq}(parent atom). Other hydrogen atoms were positioned geometrically and were also constrained to ride on their parent atoms, with C–H = 0.98–0.99 Å, and U_{iso} = 1.2–1.5 U_{eq}(parent atom). The displacement ellipsoid diagram and the packing diagram were drawn with DIAMOND [18]. The largest difference electron density peak of 3.157 eA^{-3} is located. Crystallographic data is shown in Table 1.

Table 1 Crystallographic data for **1**.

Formula	$C_{18}H_{38}Br_2N_2O_8Pt$
Formula weight	765.41
Crystal system	Triclinic
Space group	$P\ \bar{1}$
Color	Yellow
a (Å)	7.4765(2)
b (Å)	9.5044(2)
c (Å)	10.1591(3)
□□(°)	83.687(1)
□□(°)	70.847(1)
□□(°)	79.773(1)
V/(Å^3)	670.07(3)
Z	1
D_{calc}/ Mg m^{-3}	1.897
μ (mm^{-1})	8.257
F(000)	372
Crystal size	0.41 × 0.22 × 0.13 mm^3
Theta range for data collection	2.13 to 33.17°
Range of *h*, *k*, *l*	$-11\le h\le 11$, $-14\le k\le 14$, $-15\le l\le 15$
Reflections collected	14008
Independent reflections	5061 [R(int) = 0.0303]
Completeness to theta = 33.17°	98.7%
Absorption correction	Semi-empirical from equivalents
Max. and min. transmission	0.4132 and 0.1324
Refinement method	Full-matrix least-squares on F^2
Data / restraints / parameters	5061 / 0 / 144
GOF	1.096
R1 [$I>2\sigma(I)$]	0.0284
*wR*2 (all data)	0.0732
Largest diff. peak and hole (e•Å^{-3})	3.157 and –2.745

Results and Discussion

The associate *trans*-[$PtBr_2$(acetoxime)$_2$]•(18-crown-6) (**1**) has been produced by a slow co-crystallization of the equimolar mixture of *trans*-[$PtBr_2$(acetoxime)$_2$] and 18-crown-6 from an acetone:chloroform (2:3, v/v) solution at 20–25 °C. A ratio of *trans*-[$PtBr_2$(acetoxime)$_2$] and the crown ether in the associate obtained is 1:1. Associate **1** crystallizes in the triclinic space group $P\ \bar{1}$. The platinum center has a square-planar geometry. The bond angle Br(1)–Pt(1)–N(1) is close to 90°. The bond lengths around Pt(1), i.e. Pt(1)–Br(1) and Pt(1)–N(1), are close to those observed for the *trans*-

[$PtBr_2$(acetoxime)$_2$] complex [13]. In **1**, the bond length N(1)–C(1) is typical for the corresponding N–C bond in platinum(II) complexes having oxime ligands [13].
An interesting feature is the conformation of the crown ether. As it was observed for the free 18-crown-6 [19], in **1**, the crown ether has two inward-turned CH_2 groups and two oxygens with the electron pairs facing outward and away from the center (see Fig. 1). The inward-turned CH_2 groups interact with two inward-turned oxygens. The H(C4)•••O(6) and H(C10)•••O(3) distances are 2.87 Å.

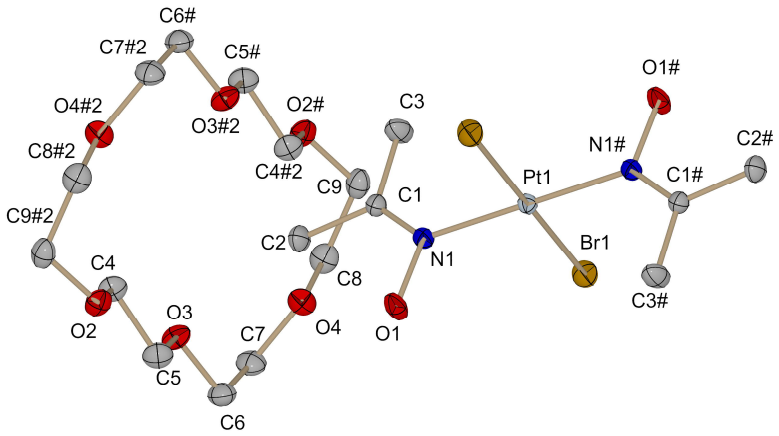

Fig. 1 Displacement ellipsoid plot of **1** at the 50% probability level.

Table 2 Selected bond lengths [Å] and angles [°] for **1**.

Pt(1)–N(1)	2.000(2)
Pt(1)–Br(1)	2.4190(3)
O(1)–N(1)	1.394(3)
N(1)–C(1)	1.284(3)
N(1)#1–Pt(1)–N(1)	180.0
N(1)–Pt(1)–Br(1)	89.98(7)
C(1)–N(1)–O(1)	113.6(2)
C(1)–N(1)–Pt(1)	129.6(2)

Symmetry transformations used to generate equivalent atoms:
#1 $-x+1, -y+1, -z+2$

Table 3 Hydrogen bonding for **1**.

D–H•••A	d(D–H)	d(H•••A)	d(D•••A)	<(DHA)
O(1)–H(1O)•••O(2)#3	0.84	1.86	2.687(3)	167

Symmetry transformations used to generate equivalent atoms:
#1 $-x+1, -y+1, -z+2$ #2 $-x+1, -y, -z+1$ #3 $-x+1, -y, -z+2$

In **1**, the *trans*-[$PtBr_2$(acetoxime)$_2$] moiety is linked to four crown ether molecules through the H(O1) and H(C2) atoms forming the infinite 2D network structure (see Fig. 2). The C(1)–N(1)–Pt(1) plane intersects 18-crown-6 ring plane at the angle of 88.5(2)°. Each of the acetoxime ligands links to two crown ethers via the conventional H(O1)•••O bonding (1.86 Å) and the non-conventional weak H(C2)•••O interaction (2.59 Å).

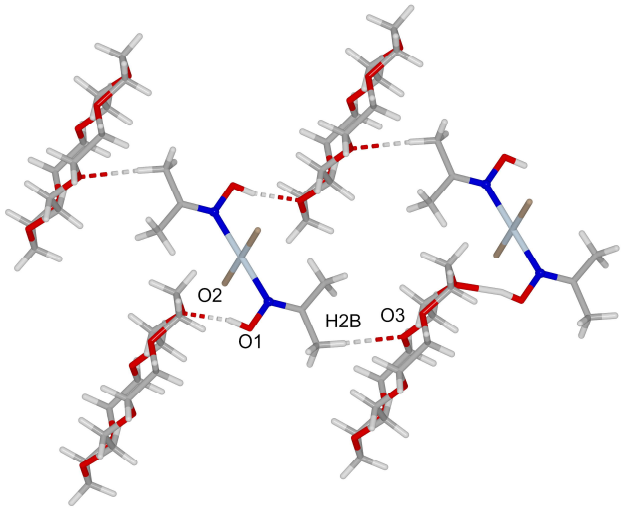

Fig. 2 View of a fragment of two-dimensional *trans*-[$PtBr_2$(acetoxime)$_2$]•(18-crown-6) network structure.

Conclusion

The complex *trans*-[$PtBr_2$(acetoxime)$_2$] co-crystallizes with 18-crown-6 forming 1:1 associate. A two-dimensional supramolecular structure based on this associate was characterized by X-ray diffraction. The crystal structure determination revealed the presence of the conventional O–H•••O and the non-conventional weak C–H•••O interactions between the hydroxylic hydrogen atom and the methyl hydrogen atom, respectively, of acetoxime and the oxygens of 18-crown-6. Owing to these interactions, the *trans*-[$PtBr_2$(acetoxime)$_2$] moiety is linked to four crown ether molecules forming a 2D network structure.

Supplementary Material

Crystallographic data reported in this paper have been deposited with the Cambridge Data Centre (CCDC deposition number 833243). The data can be obtained free of charge on application to CCDC, 12 Union Road, Cambridge, CB2 1EZ (email deposit@ccdc.cam.ac.uk).

Acknowledgements The authors are much obliged to Russian Fund for Basic Research for grant 09-03-00065-a and Saint-Petersburg State University for a research grant (2011–2013).

References

1. Batinic-Haberle I, Crumbliss AL (1995) Inorg Chem 34:928–932.
2. Colquhoun HM, Lewis DF, Stoddart JF, Williams DJ (1983) J Chem Soc Dalton Trans 607–613.
3. Colquhoun HM, Stoddart JF, Williams DJ (1981) J Chem Soc Chem Commun 851–852.
4. Colquhoun HM, Stoddart JF, Williams DJ, Wolstenholme JB, Zarzycki R (1981) Angew Chem Int Ed 20:1051–1053.
5. Cusack PA, Patel BN, Smith PJ, Allen DW, Nowell IW (1984) J Chem Soc Dalton Trans 1239–1243.
6. Ando I, Higashi M, Ujimoto K, Kurihara H (1998) Inorg Chim Acta 282:247–251.
7. Chulkova TG, Gushchin PV, Haukka M, Kukushkin VYu (2010) Inorg Chem Commun 13:580–583.
8. Kukushkin VYu, Tudela D, Pombeiro AJL (1996) Coord Chem Rev 156:333–362.
9. Kukushkin VYu, Pombeiro AJL (1999) Coord Chem Rev 181:147–175.
10. Kopylovich MN, Kukushkin VYu, Haukka M, Luzyanin KV, Pombeiro AJL (2004) J Amer Chem Soc 126:15040–15041.
11. Luzyanin KV, Kukushkin VYu, Kuznetsov ML, Garnovskii DA, Haukka M, Pombeiro AJL (2002) Inorg Chem 41:2981–2986.
12. Kukushkin VYu, Nishioka T, Tudela D, Isobe K, Kinoshita I (1997) Inorg Chem 36:6157–6165.
13. Kukushkin VYu, Tudela D, Izotova YA, Belsky VK, Stash AI (1998) Polyhedron 17:2455–2461.
14. Bruker AXS (2009) APEX2 - Software Suite for Crystallographic Programs, Bruker AXS, Inc., Madison, WI, USA.
15. Sheldrick GM (2008) Acta Crystallogr Sect A 64:112–122.
16. Farrugia LJ (1999) J Appl Crystallogr 32:837–838.
17. Sheldrick GM (2008) SADABS - Bruker AXS scaling and absorption correction, Bruker AXS, Inc., Madison, Wisconsin, USA.
18. Brandenburg K (2011) Diamond - Crystal and Molecular Structure Visualization, v. 3.2g, Crystal Impact GbR, Bonn, Germany.
19. Dunitz JD, Seiler P, Phizackerley RP (1974) Acta Crystallogr B30:2739–2741.

III

Triple Associates Based on (Oxime)Pt(II) Species, 18-Crown-6, and Water: Synthesis, Structural Characterization, and DFT Study

by

Evgeny Yu. Bulatov, Tatiana G. Chulkova, Irina A. Boyarskaya, Veniamin V. Kondratiev, Matti Haukka & Vadim Yu. Kukushkin

J. Mol. Struct., **2014**, *1068*, 176-181

Journal of Molecular Structure 1068 (2014) 176–181

Contents lists available at ScienceDirect

Journal of Molecular Structure

journal homepage: www.elsevier.com/locate/molstruc

Triple associates based on (oxime)Pt(II) species, 18-crown-6, and water: Synthesis, structural characterization, and DFT study

Evgeny Yu. Bulatov [a,b], Tatiana G. Chulkova [a,*], Irina A. Boyarskaya [a], Veniamin V. Kondratiev [a], Matti Haukka [b], Vadim Yu. Kukushkin [a]

[a] Department of Chemistry, Saint Petersburg State University, 198504 Stary Petergof, Russian Federation
[b] Department of Chemistry, University of Jyväskylä, P.O. Box 35, FI-40014 Jyväskylä, Finland

HIGHLIGHTS

- Triple associates based on (oxime)Pt(II) species, 18-crown-6, and water.
- Discrete binuclear assemblies Pt(II)–H_2O–18-crown-6–H_2O–Pt(II) and one-dimensional polymeric chain with alternating sequence.
- Electronic structures and vibrational frequencies evaluation by the DFT method.

GRAPHICAL ABSTRACT

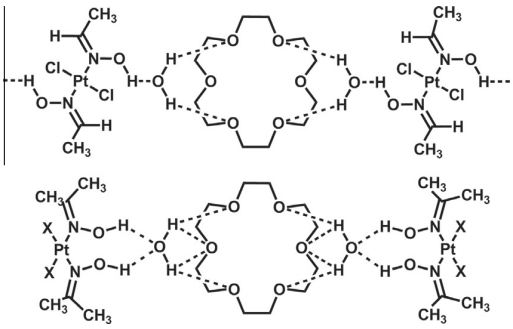

ARTICLE INFO

Article history:
Received 23 November 2013
Received in revised form 22 February 2014
Accepted 3 April 2014
Available online 13 April 2014

Keywords:
18-Crown-6
DFT studies
Hydrogen bonds
Oxime
Pt(II) complexes

ABSTRACT

The associates 2(*cis*-[$PtCl_2$(acetoxime)$_2$])·18-crown-6·$2H_2O$ (**1**), 2(*cis*-[$PtBr_2$(acetoxime)$_2$])·18-crown-6·$2H_2O$ (**2**), and *trans*-[$PtCl_2$(acetaldoxime)$_2$]·(18-crown-6)·$2H_2O$ (**3**) were synthesized by co-crystallization of free corresponding platinum species and 18-crown-6 from wet solvents and characterized by ^{1}H NMR and IR spectroscopies, high-resolution mass-spectrometry (ESI), TG/DTA, and X-ray crystallography. The (oxime)Pt(II) species are assembled with 18-crown-6 and water by hydrogen bonding between the hydroxylic hydrogen atoms of the oxime ligands and the oxygen atom of water and between the hydrogen atoms of water and the oxygen atoms of 18-crown-6. In 2(*cis*-[PtX_2(acetoxime)$_2$])·18-crown-6·$2H_2O$ (where X = Cl (**1**), Br (**2**)), the molecule of the crown ether is located between the two *cis*-[PtX_2(acetoxime)$_2$] species. The associate *trans*-[$PtCl_2$(acetaldoxime)$_2$]·(18-crown-6)·$2H_2O$ (**3**) crystallizes into a 1D array structure. Water molecules play the role of linkers between the (oxime)Pt(II) species and the crown ether molecules. The electronic structures and vibrational frequencies of the triple associates were studied by density functional theory (DFT/B3LYP).

Introduction

During the past decades, the hybrid metal complex-organic supramolecular systems have attracted significant interest owing to their promising applications in catalysis, sensors, nonlinear optics, and electronics [1–4]. A great number of such materials include crown ethers. The latter species are widely used in supramolecular chemistry insofar as the hydrophilic cavity of macrocycles can selectively recognize ions or molecules by intermolecular interactions between the guest and the host cavities. Such interactions may be formed between the acidic hydrogen of ligand and

* Corresponding author. Tel.: +7 9213480857; fax: +7 8124286939.
E-mail address: t.chulkova@spbu.ru (T.G. Chulkova).

http://dx.doi.org/10.1016/j.molstruc.2014.04.010
0022-2860/

the oxygen atoms of crown ether [5]. At the same time, the crown ether CH_2 groups can also possess significant acidity and form hydrogen bonds with basic atoms of ligands [6].

The hybrid supramolecular systems may contain two or more different building blocks, e.g. the hybrid metal complex–organic species may include the small molecules of solvents. Sometimes, the small hydrophilic molecules play the important role in the organization of supramolecular structure. It is well known, that water molecules may produce the hydrogen bonds between the hydrophilic ligands of complexes and the crown ether molecules thus forming the supramolecular structures of different kinds such as the discrete assemblies, infinite 1D arrays, 2D, or 3D architectures [1].

We believe that the self-assembly of (oxime)Pt^{II} complexes with crown ethers opens up a new route for the development of platinum-based nanomaterials with unique catalytic and physical properties. Although assembly of Pt complexes with crown ethers had a few precedents in the past [7,8], only one hybrid system based on crown ethers and (oxime)Pt species has been produced [8]. Thus, recently we reported, on the assembly of *trans*-[$PtBr_2$(acetoxime)$_2$] with 18-crown-6 [8] providing the association of these species to give a 2D net structure, which does not include water molecules (Fig. 1a). We now observed that the more polar isomeric *cis*-[PtX_2(acetoxime)$_2$] complexes (X = Cl, Br) and the one with more hydrophilic aldoximes ligand, viz. *trans*-[$PtCl_2$(acetaldoxime)$_2$], under the same conditions form triple associates with 18-crown-6 and water molecules. The latter plays the role of a linker between the assembling units (Fig. 1b and c).

Experimental

Materials and methods

All the reagents and solvents employed were commercially available and used as received without further purification. FTIR spectrum (4000–400 cm^{-1}) was recorded on a Shimadzu FTIR-8400S spectrometer in KBr pellets. ^1H NMR measurements were performed on a Bruker-DPX 300 instrument at ambient temperature. Electrospray ionization mass spectra were obtained on a Bruker micrOTOF spectrometer equipped with electrospray ionization (ESI) source and MeOH was used as the solvent. The instrument was operated both at positive and negative ion modes using a *m*/*z* range of 50–3000. The capillary voltage of the ion source was set at −4500 V (ESI^+–MS) or 3500 V (ESI^-–MS) and the capillary exit at ±(70–150) V. The nebulizer gas flow was 0.4 bar and drying gas flow 4.0 L/min. In the isotopic pattern, the most intensive peak is reported.

TG/DTA measurements were performed using NETZSCH STA 449 F1 simultaneous thermal analyzer. The heating rate was programmed at 3.7 °C min^{-1} with a protecting steam of Ar flowing at a rate of 21.9 mL min^{-1}.

*Synthesis of 2(cis-[$PtCl_2$(acetoxime)$_2$])·18-crown-6·2H_2O (**1**)*

Acetoxime (132 mg, 1.81 mmol) was added to a solution of $K_2[PtCl_4]$ (171 mg, 0.41 mmol) in water (10 mL), the mixture was heated to 90–95 °C for 1 h and cooled to room temperature. The released crystals were filtered off and dissolved in the mixture of undried acetone and chloroform (3:2, v/v). 18-Crown-6 (108 mg, 0.41 mmol) was added to the solution. The pale yellow crystals of **1** (175 mg, 76%) were produced by slow crystallization at 20–25 °C.

IR data, cm^{-1}: 3346 bm *ν*(O—H), 3248 bm *ν*(O—H), 3180 and 3104 *ν*(O—H), 1662 m *ν*(C=N), 1637–1628 bm *ν*(HOH), 1111 s *ν*(C—O), 964 sh *ν*(N—O). HRMS (ESI^+, *m*/*z*) = 282.1901 (6.9%) (M−[$PtCl_2$(acetoxime)$_2$]+NH_4)$^+$, 287.1457 (45%) (M−[$PtCl_2$(acetoxime)$_2$]+Na)$^+$, 303.1205 (100%) (M−[$PtCl_2$(acetoxime)$_2$]+K)$^+$. HRMS (ESI^-, *m*/*z*) = 410.0105 (M−18-crown-6−H)$^-$. ^1H NMR in acetone-d_6, *δ*, ppm: 2.21 (s, 12H, CH_3), 2.67 (s, 12H, CH_3), 2.90 (s, 4H, H_2O), 3.61 (s, 24H, CH_2).

*Synthesis of 2(cis-[$PtBr_2$(acetoxime)$_2$])·18-crown-6·2H_2O (**2**)*

KBr (144 mg, 1.20 mmol) was added to a solution of $K_2[PtCl_4]$ (100 mg, 0.24 mmol) in water (10 mL) and the mixture was left to stand at 20–25 °C for 2 h. After addition of acetoxime (36 mg, 0.48 mmol), the reaction mixture was left to stand at the same temperature for 3 d, and the released crystals were filtered off and dissolved in the mixture of solvents undried acetone:chloroform (3:2, v/v). The crown ether (64 mg, 0.24 mmol) was added

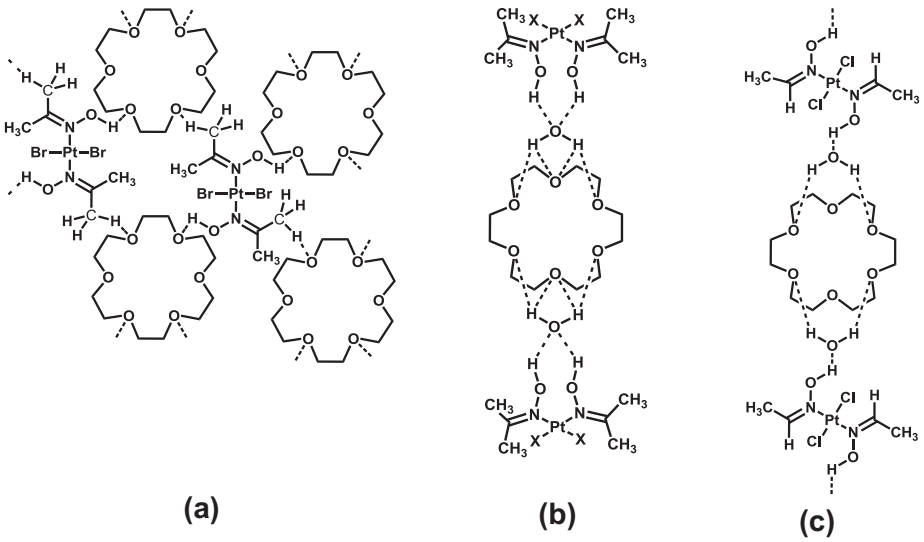

Fig. 1. View of a fragment of (a) the two-dimensional *trans*-[$PtBr_2$(acetoxime)$_2$]·(18-crown-6) network structure (8); (b) the discrete binuclear associate 2(*cis*-[PtX_2(acetoxime)$_2$])·18-crown-6·2H_2O (X = Cl, **1**; X = Br, **2**); (c) the 1D array *trans*-[$PtCl_2$(acetaldoxime)$_2$]·(18-crown-6)·2H_2O (**3**).

to the reaction mixture. The product (90 mg, 58%) crystallized from an undried acetone:chloroform (3:2, v/v) solution at 5 °C.

IR data, cm^{-1}: 3421 bm ν(O—H), 3183 bm ν(O—H), 3104 bm ν(O—H), 3068 bm ν(O—H), 1670 m ν(C=N), 1638 bm ν(HOH), 1106 vs ν(C—O), 961 m ν(N—O). HRMS (ESI^+, m/z) = 282.1898 (1.2%) (M−[$PtBr_2$(acetoxime)$_2$]+NH_4)$^+$, 287.1463 (100%) (M−[$PtBr_2$(acetoxime)$_2$]+Na)$^+$, 303.1206 (23%) (M−[$PtBr_2$(acetoxime)$_2$]+K)$^+$. HRMS (ESI^-, m/z) = 497.9110 (M−18-crown-6−H)$^-$. ^{1}H NMR in $CDCl_3$, δ, ppm: 1.96 (s, 4H, H_2O), 2.24 (s, 12H, CH_3), 2.60 (s, 12H, CH_3), 3.72 (s, 24H, CH_2).

*Synthesis of trans-[$PtCl_2$(acetaldoxime)$_2$]·(18-crown-6)·2H_2O (**3**)*

Acetaldoxime (107 mg, 1.81 mmol) was added to a solution of $K_2[PtCl_4]$ (171 mg, 0.41 mmol) in water (10 mL), the mixture was heated to 90–95 °C for 1 h and cooled to room temperature. The released crystals were filtered off and dissolved in the mixture of undried acetone and *p*-xylene (4:1, v/v). 18-Crown-6 (108 mg, 0.41 mmol) was added to the reaction mixture. The pale yellow crystals of **3** (194 mg, 69%) were produced by slow crystallization at 20–25 °C.

IR data, cm^{-1}: 3461 bm ν(O—H), 3234 bm ν(O—H), 3100 ν(=C—H), 1680 m ν(C=N), 1628 bm ν(HOH), 1109 vs ν(C—O), 963 m ν(N—O). HRMS (ESI^+, m/z) = 265.1706 (4.5%) (M−[$PtCl_2$(acetaldoxime)$_2$]+H)$^+$, 287.1571 (100%) (M−[$PtCl_2$(acetaldoxime)$_2$]+Na)$^+$, 303.1278 (51%) (M−[$PtCl_2$(acetaldoxime)$_2$]+K)$^+$. HRMS (ESI^-, m/z) = 322.9349 (100%) (M–18-crown-6–acetaldoxime–H)$^-$, 381.9718 (90%) (M–18-crown-6–H)$^-$. ^{1}H NMR in $CDCl_3$, δ, ppm: 1.63 (s, 4H, H_2O), 2.08 (d, 5.8 Hz, 6H, CH_3), 3.71 (s, 24H, CH_2), 7.71 (quart, 5.8 Hz, 2H, CH), 9.21 (s, 2H, OH).

X-ray crystallography

The single crystals of **1** and **2** were grown by a slow crystallization from an undried acetone:chloroform (3:2, v/v) solution. Complex **3** was crystallized from an undried acetone:*p*-xylene (4:1, v/v) solution. The crystals of **1**–**3** were immersed in cryo-oil, mounted in a Nylon loop, and measured at a temperature of 100 K. The X-ray diffraction data were collected on a Bruker Smart Apex II (**1**), Bruker AXS Kappa Apex II Duo (**2**) or Nonius KappaCCD (**3**) diffractometer using Mo Kα radiation (λ = 0.71073 Å). The *Apex2* [9] or *Denzo/Scalepack* [10] program packages were used for cell refinements and data reductions. The structures were solved by charge flipping or direct methods using the *Superflip* [11], *SHELXL-97* [12], or *SIR-97* [13] programs with the *WinGX* [14] graphical user interface. A semi-empirical absorption correction (*SADABS*) [15] was applied to all data. Structural refinements were carried out using *SHELXL-97* [12]. In **3**, the methyl H atoms of the CH_3 group were disordered across the mirror plane with equal occupancies. The H_2O and OH hydrogen atoms were located from the difference Fourier map but constrained to ride on their parent atom, with U_{iso} = 1.5 U_{eq}(parent atom). Other hydrogen atoms were positioned geometrically and constrained to ride on their parent atoms, with C—H = 0.95–0.99 Å and U_{iso} = 1.2–1.5 U_{eq}(parent atom). The crystallographic details are summarized in Table 5.

Computational

The full geometry optimization, Mulliken charge distribution and vibrational frequencies of **1–2** structures and model of **3** (including one *trans*-[$PtCl_2$(acetaldoxime)$_2$] complex linked by water with two 18-crown-6 molecules) has been carried out at the DFT hybrid level of theory using Becke's three-parameter hybrid exchange functional in combination with the gradient-corrected correlation functional of Lee, Yang and Parr (B3LYP) [16–19] using the Gaussian03 program packages [20]. Effective core potential model with triple-z basis sets CEP121G were used for platinum and 6-31+G(d) basis sets for other atoms.

Results and discussion

The structures of **1**–**3** were determined by X-ray diffraction. A ratio of *cis*-[PtX_2(acetoxime)$_2$] moiety and the crown ether in centrosymmetric **1** and **2** is 2:1. In **3**, the Pt complex and 18-crown-6 ether are symmetric, 2/m being their point group. In the complex, Pt is at the inversion center, while both Cl and Pt atoms are on the 2-fold axis. Furthermore, Pt and oxime atoms (except methylic hydrogens) are all on the plane of symmetry. The 18-crown-6 ether molecule is positioned perpendicular to this mirror plane in such a way that O3 oxygens lie on the plane. Complex **3** contains one crown ether molecule per one *trans*-[$PtCl_2$(acetaldoxime)$_2$] moiety. In **1**–**3**, the platinum centers exhibit square-planar geometries (Figs. 2 and 4). In isostructural **1** and **2**, the bond angles N(1)—Pt(1)—N(2) are close to 90° (Table 1). The bond distances around Pt(1) in **1**–**3**, viz. Pt(1)—X(1) and Pt(1)—N(1), are close to those observed for the *cis*-[PtX_2(acetoxime)$_2$] and *trans*-[$PtCl_2$(acetaldoxime)$_2$] complexes. The bond lengths N(1)—C(1) are typical for the corresponding N—C bond in platinum(II) complexes having oxime ligands [21].

In **1**–**3**, the crown ether molecules have the classic crown shape when all oxygen atoms are located in the inner part of the crown ether ring and all CH_2 groups are turned outside (Figs. 2 and 3). In **1**, two water molecules are involved in the hydrogen bonding between the crown ether molecule (H(1SO)···$O_{(crown\ ether)}$) and the acetoxime ligands of two *cis*-[$PtCl_2$(acetoxime)$_2$] moieties (H(O1)···O(1S) and H(O2)···O(1S)). Parameters for the hydrogen bonds are given in Table 2.

In contrast to *trans*-[$PtBr_2$(acetoxime)$_2$]·(18-crown-6), which was crystallized under the same conditions giving the 2D net structure [8], associate **2** contains water molecules. Similar to **1**, water in **2** plays the role of a linker between the *cis*-[$PtBr_2$(acetoxime)$_2$] moiety and the crown ether molecule forming the triple associate, which contains two *cis*-[$PtBr_2$(acetoxime)$_2$] moieties, one crown ether, and two water molecules. Two water molecules are situated on different sides of the crown ether and bridge the hydroxyl groups of the acetoxime ligands and the oxygen atoms of 18-crown-6. In **2**, the two acetoxime ligands of each *cis*-[$PtBr_2$(acetoxime)$_2$] moieties are linked to one water molecule via the hydrogen bonding H(O1)···O(1S) and H(O2)···O(1S) and water is linked to crown ether molecule via two bifurcated hydrogen bonds (Table 3).

In **3**, water plays the role of a linker between the *trans*-[$PtCl_2$(acetaldoxime)$_2$] moiety and the crown ether molecules forming the infinite 1D array [···H_2O·*trans*-[$PtCl_2$(acetaldoxime)$_2$]·H_2O·(18-crown-6)···]$_\infty$ (Fig. 3). The crown ether molecule is located between the two water molecules and each water molecule bridges the hydroxyl groups of the acetaldoxime ligands and the oxygen atoms of 18-crown-6. The O(1)—N(1)—Pt(1) plane intersects 18-crown-6 ring plane at the angle of 90.0(2)° (Fig. 4). Each of the acetaldoxime ligands is linked to one water molecule via the conventional H(O1)···O bonding (1.75 Å) and to one crown ether molecule via the less usual weak H(C1)···O interaction (2.31 Å). Parameters for the hydrogen bonds are represented in Table 4.

There are no significant differences between the hydrogen bond lengths in **1** and **2**. However, in **3**, the length of the hydrogen bond between the H atom of oxime ligand and the O atom of coordinated water is less than those in **1** and **2**. This can be explained by the fact that the water molecule in **3** is bound with one hydroxyl group of the oxime, whereas the coordinated water in **1** and **2** is connected with the two hydroxyls.

Table 1
Selected bond lengths [Å] and angles [°] for **1–3**.

1		2		3	
Pt(1)—N(1)	2.012(2)	Pt(1)—N(1)	2.018(4)	Pt(1)—N(1)	1.989(2)
Pt(1)—N(2)	2.014(2)	Pt(1)—N(2)	2.020(4)	Pt(1)—Cl(1)	2.3035(6)
Pt(1)—Cl(1)	2.2836(6)	Pt(1)—Br(1)	2.3974(5)	O(1)—N(1)	1.382(2)
Pt(1)—Cl(2)	2.2914(5)	Pt(1)—Br(2)	2.3952(5)	N(1)—C(1)	1.276(3)
O(1)—N(1)	1.401(2)	O(1)—N(1)	1.403(5)		
O(2)—N(2)	1.398(2)	O(2)—N(2)	1.403(4)		
N(1)—C(1)	1.284(3)	N(1)—C(1)	1.283(6)		
N(2)—C(4)	1.278(3)	N(2)—C(4)	1.274(6)		
N(1)—Pt(1)—N(2)	92.33(7)	N(1)—Pt(1)—N(2)	92.59(14)	N(1)—Pt(1)—N(1) #1	180.00
Cl(1)—Pt(1)—Cl(2)	91.74(2)	Br(1)—Pt(1)—Br(2)	91.45(2)	N(1)—Pt(1)—Cl(1)	90.00

Symmetry transformations used to generate equivalent atoms: #1 $-x+1, -y+1, -z+2$.

Table 2
Hydrogen bonding for **1**.

D—H···A	d(D—H)	d(H···A)	d(D···A)	⟨(DHA)
O(1)—H(1)···O(1S)	0.84	1.83	2.670(2)	176
O(2)—H(2)···O(1S)	0.85	1.86	2.692(2)	165
O(1S)—H(1SO)···O(5)	0.84	1.94	2.773(2)	170
O(1S)—H(1SO)···O(3)	0.86	2.09	2.865(2)	149
O(1S)—H(1SO)···O(5)#1	0.86	2.52	3.173(2)	133

Symmetry transformations used to generate equivalent atoms: #1 $-x, -y+1, -z$.

Table 3
Hydrogen bonding for **2**.

D—H···A	d(D—H)	d(H···A)	d(D···A)	⟨(DHA)
O(1)—H(1)···O(1S)	0.85	1.82	2.668(4)	175
O(2)—H(2)···O(1S)	0.85	1.85	2.693(5)	167
O(1S)—H(1SO)···O(5)	0.85	1.95	2.789(4)	171
O(1S)—H(1SO)···O(3)	0.87	2.08	2.858(4)	148
O(1S)—H(1SO)···O(5)#1	0.87	2.51	3.180(4)	134

Symmetry transformations used to generate equivalent atoms: #1 $-x, -y+1, -z$.

Table 4
Hydrogen bonding for **3**.

D—H···A	d(D—H)	d(H···A)	d(D···A)	⟨(DHA)
O(1)—H(1O)···O(4)	0.84	1.75	2.583(2)	171
O(4)—H(4O)···O(2)#2	0.84	2.03	2.8568(14)	169

Symmetry transformations used to generate equivalent atoms: #1 $-x+1, -y+1, -z+2$, #2 $x, -y+1, z$, #3 $-x+1, y, -z+1$

Table 5
Crystallographic data for **1–3**.

	1	**2**	**3**
Empirical formula	$C_{24}H_{56}Cl_4N_4O_{12}Pt_2$	$C_{24}H_{56}Br_4N_4O_{12}Pt_2$	$C_{16}H_{38}Cl_2N_2O_{10}Pt$
fw	1124.71	1302.55	684.47
Temp (K)	100(2)	100(2)	100(2)
λ (Å)	0.71073	0.71073	0.71073
Cryst syst	Triclinic	Triclinic	Monoclinic
Space group	$P\bar{1}$	$P\bar{1}$	$C2/m$
a (Å)	7.5168(2)	7.5818(3)	12.5875(3)
b (Å)	9.4347(2)	9.4835(3)	11.5718(3)
c (Å)	14.2683(3)	14.4633(5)	9.5264(2)
α (°)	78.241(1)	78.400(1)	90
β (°)	86.053(1)	85.746(2)	111.875(2)
γ (°)	89.856(1)	89.694(1)	90
V (Å^3)	988.24(4)	1015.84(6)	1287.71(6)
Z	1	1	2
ρ_{calc} (Mg/m^3)	1.890	2.129	1.765
μ (Mo Kα) (mm^{-1})	7.396	10.866	5.704
No. reflns.	25600	25128	12189
Unique reflns.	6859	4600	1964
GOOF (F^2)	1.004	1.092	1.066
R_{int}	0.0354	0.0196	0.0231
R1[a] ($I \geqslant 2\sigma$)	0.0199	0.0235	0.0135
wR2[b] (*all data*)	0.0396	0.0854	0.0324

[a] $R1 = \sum||F_o|-|F_c||/\sum|F_o|$.
[b] $wR2 = [\sum[w(F_o^2-F_c^2)^2]/\sum[w(F_o^2)^2]]^{1/2}$.

In IR spectra of **1–3**, the hydroxyl-stretching bands of the coordinated water molecules are observed in the region 3400–3050 cm^{-1}. Also the broadness and relatively low frequency of the oxime O—H stretching bands are both indicative of hydrogen bonding between the oxime ligands and water molecules.

The presence of the oxime ligands in **1** is manifested by broad IR bands of medium intensity at 3346 and 3248 cm^{-1}, assigned to symmetric and asymmetric ν(O—H)$_{oxime}$ vibrations. The medium-intensity broad bands at 3180 and 3104 cm^{-1} have been assigned to the ν(O—H)$_{coordinated\ water}$ asymmetric and symmetric modes. In **2**, the medium-intensity broad bands correspond to the symmetric and asymmetric vibrations of O—H bonds in the oxime ligands ν(O—H)$_{oxime}$ appear at 3421 and 3183 cm^{-1}, respectively. The medium-intensity broad bands at 3104 and 3068 cm^{-1} are assigned to the asymmetric and symmetric modes of the coordinated water, respectively. In the IR spectrum of **3**, the medium-intensity broad band at 3461 cm^{-1} and the weak-intensity broad band at 3234 cm^{-1} have been assigned to the ν(O—H)$_{oxime}$ symmetric and asymmetric modes, respectively. The bands associated with vibrations of the coordinated H_2O appear in the region 3600–3300 cm^{-1}. In particular, in **3**, the weak band at 3380–3370 cm^{-1} is observed as a shoulder.

TG/DTA study of **1–3** was performed using the powdered samples under argon atmosphere. The TG curve indicates that upon heating, **1** showed a weight loss of about 3 wt% between room temperature and 160 °C. The corresponding DTA curve shows a broad and weak exothermic peak centered at 83 °C and a broad and weak endothermic peak centered at 168 °C. Upon further heating, the TG curve shows a fairly large mass loss, about 40%, in the temperature range from 160 to 227 °C, which corresponds to a sharp endothermic peak centered at 227 °C on its DTA curve. Thereafter, the TG curve shows a weight loss of about 10% in the temperature range from 227 to 283 °C, which corresponds to a broad exothermic DTA peak centered at 258 °C. The first mass loss seems to be due to removal of water molecules, while the second and the third mass losses are due to decomposition of the organically modified framework.

The TG curve of **2** exhibits a mass loss of about 3% between room temperature and 152 °C. The DTA curve of **2** shows a broad and weak endothermic peak centered at 140 °C. Thereafter, the TG curve displays a mass loss of about 58% in the temperature range from 152 to 313 °C. The DTA curve shows two broad and weak exothermic peaks, centered at 159 and 264 °C, respectively,

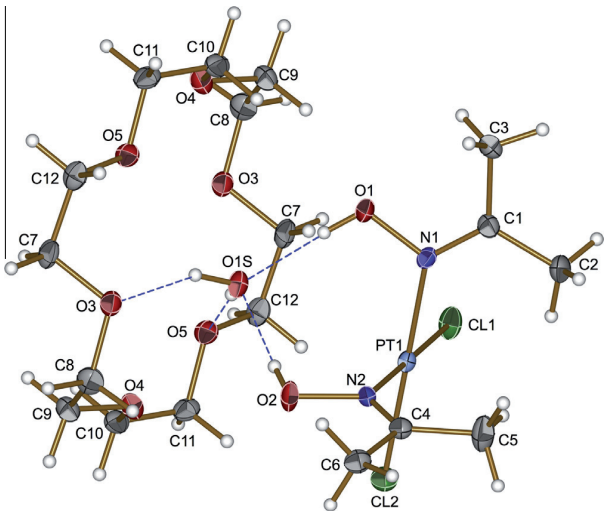

Fig. 2. Displacement ellipsoid plot of **1** at the 50% probability level. Symmetry transformations used to generate equivalent atoms: #1 $-x$, $-y+1$, $-z$.

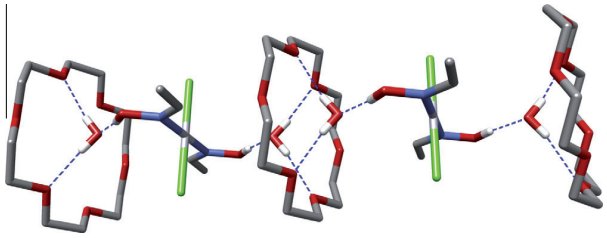

Fig. 3. 1D array structure of **3**.

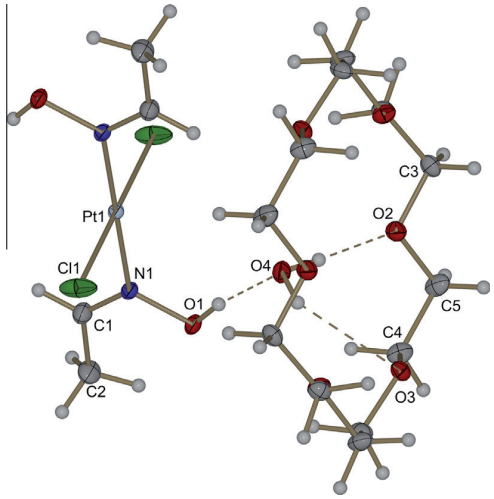

Fig. 4. Displacement ellipsoid plot of **3** at the 50% probability level.

and a sharp endothermic peak, centered at approximately 225 °C. The first mass loss is associated with elimination of the water molecules, while the other mass losses are due to decomposition of the ligands and the crown ether moiety.

The TG curve of **3** exhibits a mass loss of about 5% between the room temperature and 120 °C resulting from elimination of the water molecules. The DTA curve of **3** has two broad and weak endothermic peaks centered at 56 °C and 69 °C. A mass loss of about 56% associated with decomposition of organic ligands occurs in the temperature range from 120 to 200 °C. The DTA curve shows a sharp exothermic peak centered at 142 °C, a broad and weak exothermic peak at 158 °C, and a sharp endothermic peak centered at 196 °C. The presence of two exothermic peaks at 142 °C and 158 °C may be associated with the structure reorganization. Thus for instance, it is known, that the *trans*-(oxime)$_2$Pt(II) complexes may produce a 2D network structure with 18-crown-6 [8]. The last peak centered at 196 °C corresponds to the melting accompanied with decomposition. The analogues peaks centered at 227 °C and 225 °C are also associated with the melting with decomposition in **1** and **2**, respectively.

The water molecules in associates **1**–**3** bind with the oxime ligands and 18-crown-6 via hydrogen bonds, therefore elimination of water molecules precedes the thermal decomposition. According to the TG/DTA data, **1** is slightly more thermally stable than **2**, and **3** is less stable than **1** and **2**, because the water molecule in **3** binds with one oxime ligand via hydrogen bond, while in **1** and **2** the water molecules bind with two oxime ligands.

It is well-known that X-ray diffraction experiments cannot indicate the precise location of H-atoms. Therefore, the OH hydrogens are practically always placed at idealized positions even if a suitable electron maximum could be found from a difference Fourier map. However, the nature of the interaction can be analyzed in detail by using computational methods. In accord with this statement, we analyzed the H-bonding as well as the electronic structures and vibrational frequencies of **1**–**3** by computational methods and our results are disclosed in the section that follows.

The calculated distances d(D···A) in **1–3** correspond to the crystallographic data (Tables 2–4) within 0.05 Å. In **1–3**, all oxygen and nitrogen atoms have negative charges, while the carbon atoms and the metal center bear positive charges (Table 6). The nitrogen and oxygen atom charges of the oxime moieties in **2** are closely the same with those in **1**.

The calculated ν(O—H)$_{oxime}$ and ν(C=N)$_{oxime}$ frequencies of **1–3** are in a good agreement with the experimental data. The comparison of the calculated and experimental vibrational frequencies for **1** is given in Table 7.

Table 6
Calculated charge distribution [a] for **1**–**3**.

	1	2	3
Pt1	0.57	0.62	0.53
Cl1	−0.52		−0.65
Cl2	−0.46		
Br1		−0.47	
Br2		−0.42	
N1	−0.46	−0.45	−0.38
N2	−0.47	−0.50	
O1	−0.23	−0.24	−0.17
O2	−0.14	−0.13	
H(O1)	0.64	0.65	0.63
H(O2)	0.60	0.61	

[a] Mulliken charges are given.

Table 7
Comparison of the calculated and experimental vibrational frequencies (cm^{-1}) for **1**.

	Calculated	Experimental
ν(O—H)$_{oxime}$	3364 s	3346 s
	3360 as	
	3211 as	3248 as
	3205 as	
ν(C=N)	1737 s	1662
	1731 as	

Table 8
Calculated hydrogen bond lengths [Å], angles [°], and Wiberg bond indexes for **1–3**.

Compound	D—H···A	d(D—H)	d(H···A)	d(D···A)	⟨(DHA)	w(D—H)	w(H···A)
1	O(1)—H(1O)···O(1S)	0.99	1.69	2.73	173	0.62	0.07
	O(2)—H(2O)···O(1S)	0.99	1.77	2.69	162	0.60	0.10
	O(1S)—H(1SO)···O(5)	0.99	1.87	2.84	169	0.65	0.05
	O(1S)—H(1SO)···O(3)	0.99	1.89	2.86	169	0.65	0.05
2	O(1)—H(1)···O(1S)	1.00	1.69	2.69	174	0.62	0.07
	O(2)—H(2)···O(1S)	0.99	1.76	2.74	168	0.60	0.10
	O(1S)—H(1SO)···O(5)	0.99	1.85	2.80	161	0.65	0.05
	O(1S)—H(1SO)···O(3)	0.98	1.90	2.88	174	0.65	0.05
3	O(1)—H(1O)···O(4)	1.02	1.59	2.60	172	0.56	0.13
	O(4)—H(4O)···O(2)#2	0.98	1.95	2.89	161	0.68	0.03

The hydrogen bond between the H atom of oxime ligand and the O atom of coordinated water in **3** is stronger ($w(H_{oxime}\cdots O_{water}) = 0.13$) than those in **1** ($w(H_{oxime}\cdots O_{water}) = 0.07$ and 0.10) and **2** ($w(H_{oxime}\cdots O_{water}) = 0.07$ and 0.10). This is consistent with the larger shift of the oxime OH group vibration band in the experimental IR spectrum of **3**. Also, the hydrogen bond $H_{water}\cdots O_{crown\ ether}$ in **1** and **2** is approximately twice stronger than those in **3** (Table 8).

The energy of structure stabilization due to the hydrogen bond formation for **1–3** was calculated as the difference between the energy of associate and the sum of energies of (oxime)Pt(II) species, 18-crown-6 molecules, and water molecules. The individual species, i.e. the (oxime)Pt(II) species and the molecules of 18-crown-6, were frozen in their aggregate geometries. The determined structure stabilization energies for **1–3** are −276, −280, and −186 kJ/mol, respectively. The average hydrogen bond energy in **1** and **2** is 34–35 kJ/mol, and that in **3** is 31 kJ/mol. In accord with our estimation of hydrogen bond energies and bond orders, the hydrogen bonds in **1–3** can be attributed to relatively strong H-bonds.

Hence, theoretical calculations support the hydrogen bonding interactions responsible for the generation of the triple associates.

Conclusion

The water molecules play the role of linkers between the hydrophilic (oxime)Pt(II) moieties and the crown ether molecules in **1–3**, in contrast to the case described earlier [8], where less hydrophilic *trans*-[$PtBr_2$(acetoxime)$_2$] is directly linked with 18-crown-6. Triple associates **1** and **2** have a binuclear structure with bifurcated hydrogen bonds. Two *cis*-[PtX_2(acetoxime)$_2$] complexes link with 18-crown-6 via water molecules [*cis*-[PtX_2(acetoxime)$_2$]·H_2O·(18-crown-6)·H_2O·*cis*-[PtX_2(acetoxime)$_2$]] (where X = Cl, Br). Complex **3** crystallizes forming the infinite 1D array [···H_2O·*trans*-[$PtCl_2$(acetaldoxime)$_2$]·H_2O·(18-crown-6)···]$_\infty$, where (acetaldoxime)$_2$ Pt^{II} functionality in the *trans*-[$PtCl_2$(acetaldoxime)$_2$] complex links to the crown ether molecules indirectly, viz., through water molecules thus forming the infinite chain. Self-assembly of the building blocks, viz. (oxime)Pt(II) species, 18-crown-6, and water, proceeds by weak hydrogen bonds. According to TG/DTA data, associate **1** is thermally more stable than **2**, and **2** is more stable than **3**. Both the bond lengths and the vibrational frequencies for **1–3** produced by DFT calculations are in a good agreement with the X-ray and IR experimental data.

Acknowledgements

The authors are obliged to Russian Fund for Basic Research for Grant 13-03-12411 and Saint Petersburg State University for a research Grant (2013–2015). We also thank the Centre of Magnetic Resonance and the Center of Thermal Analysis and Calorimetry of Saint Petersburg State University, where NMR and TGA studies were performed.

Appendix A. Supplementary data

Crystallographic data reported in this paper have been deposited with the Cambridge Crystallographic Data Centre (**1**, CCDC 880416; **2**, CCDC 880417; **3**, CCDC 868793). The data can be obtained free of charge on application to CCDC, 12 Union Road, Cambridge, CB2 1EZ (email deposit@ccdc.cam.ac.uk). Supplementary data associated with this article can be found, in the online version, at http://dx.doi.org/10.1016/j.molstruc.2014.04.010.

References

[1] R.W. Saalfrank, B. Demleitner, Ligand and metal control of self-assembly in supramolecular chemistry, in: J.P. Sauvage (Ed.), Transition Metals in Supramolecular Chemistry, Vol. 5, Wiley& Sons, Chichester, 1999, p. 152. Chapter 1.
[2] S.S. Zhu, P.J. Carroll, T.M. Swanger, J. Am. Chem. Soc. 118 (1996) 8713.
[3] P. Sgarbossa, R. Bertani, V. Di Noto, M. Piga, G.A. Giffin, G. Terraneo, T. Pilati, P. Metrangolo, G. Resnati, Cryst. Growth Des. 12 (2012) 297.
[4] H. Tsukube, Coord. Chem. Rev. 148 (1996) 1.
[5] I. Ando, M. Higashi, K. Ujimoto, H. Kurihara, Inorg. Chim. Acta 282 (1998) 247.
[6] M. Calleja, J.W. Steed, J. Chem. Crystallogr. 33 (2003) 609.
[7] T.G. Chulkova, P.V. Gushchin, M. Haukka, V.Yu. Kukushkin, Inorg. Chem. Commun. 13 (2010) 580.
[8] E.Yu. Bulatov, T.G. Chulkova, M. Haukka, V.Yu. Kukushkin, J. Chem. Crystallogr. 42 (2012) 352.
[9] Bruker AXS APEX2 – Software Suite for Crystallographic Programs, Bruker AXS Inc., Madison, Wisconsin, USA, 2009.
[10] Z. Otwinowski, W. Minor, Processing of X-ray diffraction data collected in oscillation mode, in: C.W. Carter, J. Sweet (Eds.), Methods in Enzymology. Macromolecular Crystallography, Part A, Vol. 276, Academic Press, New York, USA, 1997, p. 307.
[11] L. Palatinus, G.J. Chapuis, J. Appl. Crystallogr. 40 (2009) 786.
[12] G.M. Sheldrick, Acta Crystallogr. Sect. A 64 (2008) 112.
[13] A. Altomare, M.C. Burla, M.C. Camalli, C. Giacovazzo, A. Guagliardi, A.G.G. Moliterni, G. Polidori, R.J. Spagna, Appl. Cryst. 32 (1999) 115.
[14] L.J. Farrugia, J. Appl. Crystallogr. 32 (1999) 837.
[15] G.M. Sheldrick, SADABS – Bruker AXS Scaling and Absorption Correction, Bruker AXS Inc., Madison, Wisconsin, USA, 2008.
[16] A.D. Becke, J. Chem. Phys. 98 (1993) 5648.
[17] P.J. Stephen, F.J. Devlin, C.S. Ashvar, C.F. Chabalovski, M.J. Frisch, Faraday Discuss. 99 (1994) 103.
[18] P.J. Stephen, F.J. Devlin, C.F. Chabalowski, M.J. Frisch, J. Phys. Chem. 98 (1994) 11623.
[19] C. Lee, W. Yang, R.G. Parr, Phys. Rev. B37 (1988) 785.
[20] M.J. Frish, G.W. Trucks, H.B. Schlegel, et al. Gausian03, revision D.01, Gaussian Inc.: Wallingford, CT 2004.
[21] V.Yu. Kukushkin, V.K. Belsky, E.A. Aleksandrova, V.E. Konovalov, G.A. Kirakosyan, Inorg. Chem. 31 (1992) 3836.

IV

An Efficient Method for Selective Oxidation of (Oxime)Pt(II) to (Oxime)Pt(IV) Species Using *N,N*-Dichlorotosylamide

by

Anastasiia M. Afanasenko, Evgeny Yu. Bulatov, Tatiana G. Chulkova, Matti Haukka & Fedor M. Dolgushin

Transition Met. Chem., **2016**, *41*, 387-392

An efficient method for selective oxidation of (oxime)Pt(II) to (oxime)Pt(IV) species using *N*,*N*-dichlorotosylamide

Anastasiia M. Afanasenko[1] • Evgeny Yu. Bulatov[2] • Tatiana G. Chulkova[1] • Matti Haukka[2] • Fedor M. Dolgushin[3]

✉ Tatiana G. Chulkova

t.chulkova@spbu.ru

[1] Institute of Chemistry, Saint Petersburg State University, Universitetskiy Pr., 26, 198504 Stary Petergof, Russian Federation

[2] Department of Chemistry, University of Jyväskylä, P.O. Box 35, FI-40014 Jyväskylä, Finland

[3] A.N. Nesmeyanov Institute of Organoelement Compounds, 28 Vavilov Street, 119991 Moscow, Russian Federation

Abstract

The oxidation of (oxime)Pt^{II} species using the electrophilic chlorine based oxidant *N*,*N*-dichlorotosylamide (4-$CH_3C_6H_4SO_2NCl_2$) was studied. The reactions of *trans*-[$PtCl_2$(oxime)$_2$] (where oxime = acetoxime, cyclopentanone oxime, or acetaldoxime) with this oxidant lead to *trans*-[$PtCl_4$(oxime)$_2$] products. The oxidation of *trans*-[Pt(*o*-$OC_6H_4CH=NOH)_2$] at room temperature gave *trans*-[$PtCl_2$(*o*-$OC_6H_4CH=NOH)_2$], whereas the same reaction upon heating was accompanied by electrophilic substitution of the benzene rings.

Keywords: Chlorination, Ligand reactivity, Oximes, Platinum complexes

Introduction

The oxidations of Pt^{II} species with a variety of electrophilic chlorinating reagents have been reported. The oxidative chlorination of platinum(II) species by molecular chlorine is a common method of synthesis of platinum(IV) complexes [1]. The reactions with Cl_2 proceed via oxidative addition to the metal center with formation of the appropriate Pt^{IV} complexes. In particular, the platinum(II) complexes $[PtCl_2(RR'CNOH)_2]$ are converted into $[PtCl_4(RR'CNOH)_2]$ by treatment with Cl_2. The oxime ligands usually remain intact; however, in some cases, the ligands also react with molecular chlorine, and, e.g., passage of Cl_2 through a chloroform solution of $[Pt(o\text{-}OC_6H_4CH{=}NOH)_2]$ resulted in both the oxidative addition of chlorine to the platinum(II) center and chlorination of the benzene ring (Scheme 1) [2].

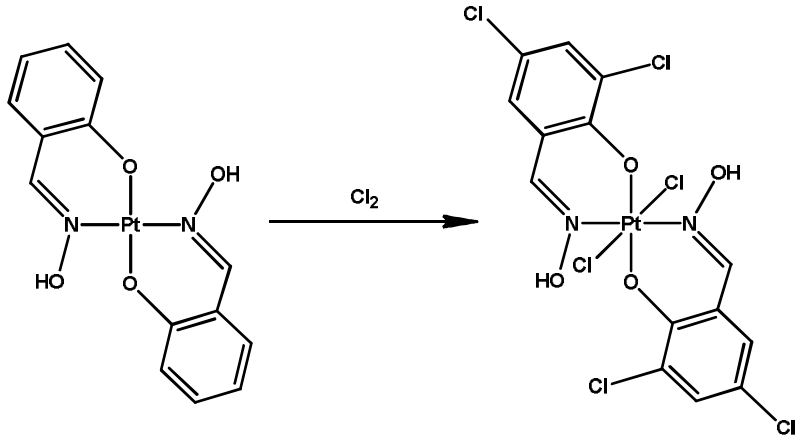

Scheme 1 Chlorination of $[Pt(o\text{-}OC_6H_4CH{=}NOH)_2]$ with Cl_2.

Overall, the platinum(IV) complex $[PtCl_2(2\text{-}O\text{-}3,5\text{-}Cl_2C_6H_2CH{=}NOH)_2]$ was isolated in 85% yield. In contrast to molecular chlorine, NOCl is a more selective chlorination agent. Oxidation of the metal center occurred selectively when nitrosyl chloride was used instead of Cl_2, giving $[PtCl_2(o\text{-}OC_6H_4CH{=}NOH)_2]$ without any chlorination of the benzene rings (Scheme 2) [2].

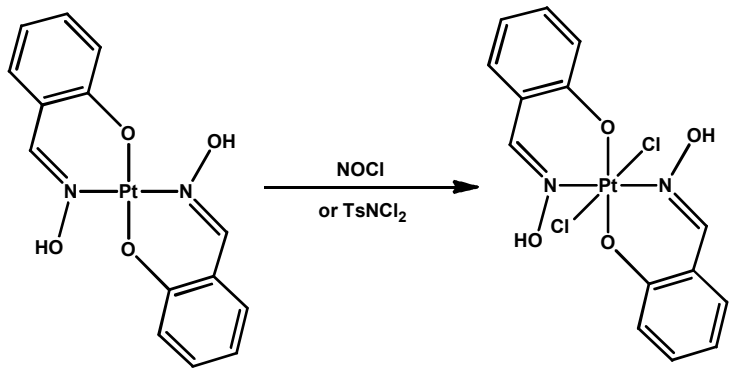

Scheme 2 Chlorination of [Pt(*o*-$OC_6H_4CH{=}NOH)_2$] with NOCl and $TsNCl_2$.

However, like chlorine, nitrosyl chloride is a highly toxic gas and this property restricts the usage of these reagents. While the reactions of (oxime)Pt^{II} species with other electrophilic chlorinating reagents have not been previously reported, related transformations of Pt^{II} to Pt^{IV} (or Pt^{III}) with various chlorinating oxidants have been documented. The oxidations of Pt^{II} complexes with iodobenzene dichloride ($PhICl_2$) [3-5], *N*-chlorosuccinimide (NCS) [5, 6], *N*,*N*-dichlorobenzenesulphonamide ($PhSO_2NCl_2$) [7], PCl_5 [8], and $SbCl_5$ [9] have been described.

In this study, we used *N*,*N*-dichlorotosylamide as a chlorinating agent for the selective chlorination of [$PtCl_2$(oxime)$_2$] complexes. *N*,*N*-Dichlorotosylamide is a relatively active solid reagent, which can be used as a stoichiometric solid chlorine equivalent providing selective oxidation of Pt(II) centers. This reagent is more convenient to use than chlorine and also more stable at room temperature than hypervalent iodine reagents.

Experimental

Materials and Instrumentation

All reagents and solvents were commercially available and used as received without further purification. *N*,*N*-Dichlorotosylamide (dichloramine T) was purchased from Sigma-Aldrich. FTIR spectra were recorded on Shimadzu FTIR-8400S (4000 – 400 cm^{-1}) and IRAffinity-1S (4000 – 300 cm^{-1}) spectrometers using KBr pellets. ^{1}H NMR measurements were performed on a Bruker-DPX 400 instrument at ambient temperature. Electrospray ionization mass spectra were obtained on a Bruker micrOTOF spectrometer equipped with electrospray ionization (ESI) source using MeOH as the solvent. The instrument was operated in both positive and negative ion modes using a *m/z* range of 50 – 3000. The capillary voltage of the ion source was set at –4500 V (ESI^+– MS) or 3500 V (ESI^-– MS) and the capillary exit at ±(70 – 150) V. The nebulizer gas flow was 0.4 bar and drying gas flow 4.0 L/min. In the isotopic patterns, the most intense peak is reported.

Syntheses

Trans-[$PtCl_2$(acetoxime)$_2$] (**1**) [10, 11], *trans*-[$PtCl_2$(acetaldoxime)$_2$] (**2**) [12], *trans*-[$PtCl_2$(cyclopentanone oxime)$_2$] (**3**) [10], and *trans*-[Pt(*o*-$OC_6H_4CH{=}NOH)_2$] (**4**) [13] were obtained according to the published methods.

Synthesis of **5**–**7**. Full details are provided for *trans*-[$PtCl_4$(acetoxime)$_2$] (**5**); *trans*-[$PtCl_4$(acetaldoxime)$_2$] (**6**) and *trans*-[$PtCl_4$(cyclopentanone oxime)$_2$] (**7**) were synthesized by analogous procedures.

Complex **5**: Complex **1** (0.019 g, 0.045 mmol) and *N*,*N*-dichlorotosylamide (0.011 g, 0.045 mmol) were suspended in chloroform (5 mL). The reaction mixture was refluxed for 2 h, after which the solvent was removed under reduced pressure and the residue was purified by column chromatography on silica gel (60 Å; Merck) with chloroform as the eluent to give pure complex **5** as a yellow solid (R_f 0.59). Yield: 78%. M. P. = 189–191 °C (dec.). ^{1}H NMR ($CDCl_3$), δ (ppm): 9.08 (s, 2H, $^3J_{HPt}$ = 4.4 Hz, OH), 2.81 (s, 6H, $^4J_{HPt}$ = 8.0 Hz, CH_3), 2.50 (s, 6H, $^4J_{HPt}$ = 7.2 Hz, CH_3). IR (cm^{-1}): 3350 w *ν*(O–H), 1635 w *ν*(C=N). Anal. Calcd. for $C_6H_{14}Cl_4N_2O_2Pt$: C, 14.9; H, 2.9; N, 5.8. Found: C, 14.9; H, 2.9; N, 5.9%.

Complex **6**: Yield: 71%. R_f 0.61. Crystals suitable for X-ray diffraction were grown from a concentrated chloroform solution. Yellow crystals. M. p. = 174–176 °C (dec.). ^{1}H NMR ($CDCl_3$), δ (ppm): 9.37 (s, 2H, OH), 8.04 (q, 2H, $^3J_{HH}$ = 5.6 Hz, CH), 2.47 (d, 6H, $^3J_{HH}$ = 6.0 Hz, CH_3). IR (cm^{-1}): 3279 s *ν*(O–H), 1654 m *ν*(C=N). Anal. Calcd. for $C_4H_{10}Cl_4N_2O_2Pt$: C, 10.6; H, 2.2; N, 6.2. Found: C, 10.5; H, 2.6; N, 6.2%.

Complex **7**: Yield: 83%. R_f 0.56. Crystals suitable for X-ray diffraction were grown from a concentrated chloroform solution. Yellow crystals. M. p. = 196–199 °C (dec.). ^{1}H NMR ($CDCl_3$), δ (ppm): 9.06 (s, 2H, $^3J_{HPt}$ = 5.1 Hz, OH), 3.52 (t, 4H, $^3J_{HH}$ = 7.1 Hz, CH_2), 3.15 (t, 4H, $^3J_{HH}$ = 7.1 Hz, CH_2), 1.83–1.95 (m, 8H, CH_2). IR (cm^{-1}): 3326 s *ν*(O–H), 1643 m *ν*(C=N). Anal. Calcd. for $C_{10}H_{18}Cl_4N_2O_2Pt$: C, 22.4; H, 3.4; N, 5.2. Found: C, 22.3; H, 3.3; N, 5.4%.

Synthesis of [$PtCl_2$(*o*-OC_6H_4CH=NOH)$_2$] (**8**). A solution of complex **4** (0.021 g, 0.045 mmol) in chloroform (5 mL) was treated with *N*,*N*-dichlorotosylamide (0.010 g, 0.045 mmol) and the mixture left overnight at ambient temperature. The solvent was removed under reduced pressure and the residue was purified by column chromatography on silica gel (60 Å; Merck) with chloroform as the eluent to give pure complex **8** as a reddish-brown solid (R_f 0.62). Yield: 60 %.

^{1}H NMR ($CDCl_3$), δ (ppm): 10.86 (s, 2H, $^3J_{PtH}$ = 15.2 Hz, OH), 8.11 (s, 2H, $^3J_{PtH}$ = 40.0 Hz,–CH=N), 7.39 (ddd, 2H, ^{3}J = 7.7 Hz, ^{4}J = 1.5 Hz), 7.25 (dd, 2H, ^{3}J = 13.9 Hz, ^{4}J = 1.40 Hz), 7.01 (d, 2H, ^{3}J = 8.44 Hz), 6.76 (dd, 2H, ^{3}J = 7.12 Hz). IR (cm^{-1}): 3275 m ν(O–H), 3015 w ν(C_{sp2}–H), 1651 s ν(C=N), 1599 s, 1549 m ν(C_{Ar}=C_{Ar}), 346 w ν(Pt–Cl). HRMS (ESI^-), m/z: 535.9760 $[M–H]^-$ (calc. 535.9744). Anal. calcd. for $C_{14}H_{12}Cl_2N_2O_4Pt$: C, 31.2; H, 2.3; N, 5.2. Found: C, 30.7; H, 1.8; N, 5.2%.

X-ray crystal structure determinations

Crystals of complexes **1**, **6**, and **7** were immersed in cryo-oil, mounted in a nylon loop, and analysed at a temperature of 100 K. The X-ray diffraction data were collected on a Bruker Axs Smart Apex II or Nonius KappaCCD diffractometer using Mo Kα radiation (λ = 0.710 73 Å). The *Apex2* [14] *or Denzo-Scalepack* [15] program packages were used for cell

refinements and data reductions. The structures were solved by direct methods using *SHELXS-97* [16] with the *WinGX* [17] graphical user interface. A semi-empirical absorption correction (*SADABS*) [18] was applied to all data. Structural refinements were carried out using *SHELXL-97 or Bruker SHELXTL* [16]. In all structures, the OH hydrogen atoms were located from the difference Fourier maps, but constrained to ride on their parent oxygen with $U_{iso} = 1.5 \cdot U_{eq}$ (parent atom). Other hydrogen atoms were positioned geometrically and constrained to ride on their parent atoms, with C–H = 0.95–0.99 Å and $U_{iso} = 1.2–1.5\ U_{eq}$(parent atom). The crystallographic details are summarized in Table 1.

Table 1 Crystal Data.

	1	**6**	**7**
empirical formula	$C_6H_{14}Cl_2N_2O_2Pt$	$C_4H_{10}Cl_4N_2O_2Pt$	$C_{10}H_{18}Cl_4N_2O_2Pt$
fw	412.18	455.03	535.15
temp (K)	100(2)	100(2)	100(2)
λ(Å)	0.71073	0.71073	0.71073
cryst syst	Monoclinic	Monoclinic	Monoclinic
space group	$P2_1/n$	$P2_1/c$	$P2_1/n$
a (Å)	4.5083(2)	12.0890(3)	6.4314(7)
b (Å)	8.5087(3)	6.61410(10)	14.2483(15)
c (Å)	14.5045(5)	13.8331(3)	8.5805(9)
β (deg)	91.856(2)	91.571(2)	101.659(2)
V (Å^3)	556.10(4)	1105.65(4)	770.06(14)
Z	2	4	2
ρ_{calc} (Mg/m^3)	2.462	2.734	2.308
μ(Mo Kα) (mm^{-1})	13.069	13.628	9.802
No. reflns.	7453	18253	7554
Unique reflns.	2118	3013	2027
GOOF (F^2)	1.068	1.176	0.972
R_{int}	0.0267	0.0443	0.0316
R1[a] ($I \geq 2\sigma$)	0.0193	0.0240	0.0222
wR2[b] ($I \geq 2\sigma$)	0.0380	0.0525	0.0558

[a] $R1 = \Sigma||F_o| - |F_c||/\Sigma|F_o|$. [b] $wR2 = [\Sigma[w(F_o^2 - F_c^2)^2]/ \Sigma[w(F_o^2)^2]]^{1/2}$.

Results and discussion

The reactions of (oxime)Pt^{II} complexes with *N*,*N*-dichlorotosylamide were studied. *N*,*N*-Dichlorotosylamide was used as a solid source of "positive chlorine". To the best of our knowledge, this is the first example of use of *N*,*N*-dichlorotosylamide for selective oxidation of platinum(II) species; the only precedent being the application of *N*,*N*-dichlorobenzenesulfonamide for the oxidative chlorination of *trans*-[$PtCl_2$(HN=C(OMe)Et)$_2$] [7]. It is known that *N*,*N*-dichlorotosylamide is relatively reactive, but can nevertheless be easily handled [19]. In order to study the reactivity of *N*,*N*-dichlorotosylamide in the oxidative chlorination of (oxime)Pt^{II} complexes, we chose a series of coordination compounds with different oxime ligands, *i.e.* aldoximes (acetaldoxime and salicylaldoxime) and ketoximes (acetoxime and cyclopentanone oxime). The (oxime)Pt^{II} complexes were synthesized by the previously published reaction between $K_2[PtCl_4]$ and oximes in a 1:2 molar ratio in water. The prepared compounds were characterized by elemental analyses, HRMS (ESI), IR and ^{1}H NMR spectroscopies; complex **1** was also characterized by X-ray single-crystal diffraction (Fig. 1).

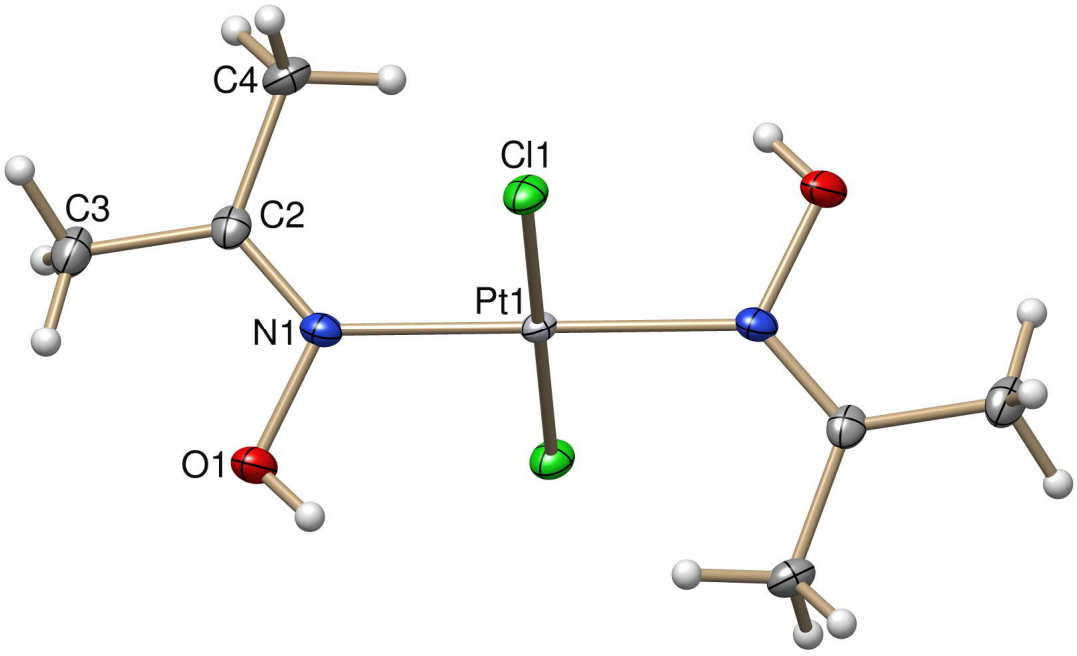

Fig. 1 Displacement ellipsoid plot of complex **1** at the 50% probability level (symmetry transformations used to generate equivalent non-labeled atoms: -x,-y+2,-z+2).

In complex **1**, each Pt atom has a centrosymmetric square-planar environment provided by two acetoxime N and two Cl atoms (Pt–N 2.008(2) Å, Pt–Cl 2.3019(6) Å, N–Pt–Cl 89.91(7)°) (Table 2). The N(1)–C(2) bond length in **1** (1.286(4) Å) is typical of N=C bonds in (oxime)Pt^{II} compounds. The O(1)–N(1)–Pt(1)–Cl(1) torsion angle is 67.38º. The structure of **1** displays column packing, which runs along the a-axis (Fig. 2). Owing to the $OH_{oxime}\cdots Cl$ hydrogen bonding (the H(1O)···Cl(1#) distance is 2.23 Å, whilst the O(1)–H(1O)···Cl(1#) angle is 164.4°), the *trans*-$[PtCl_2(acetoxime)_2]$ molecules are linked together into 1D arrays along the crystallographic a-axis.

Table 2 Selected bond lengths [Å] and angles [°] for **1**, **6**, and **7**.

	1	**6**	**7**
Pt(1)–N(1)	2.008(3)	2.030(3)	2.046(3)
Pt(1)–N(2)		2.041(3)	
Pt(1)–Cl(1)	2.3019(7)	2.3271(8)	2.3103(9)
Pt(1)–Cl(2)		2.3085(8)	2.3187(9)
Pt(1)–Cl(3)		2.3102(8)	
Pt(1)–Cl(4)		2.3240(8)	
N(1)–C(1)			1.281(5)
N(1)–C(2)	1.286(4)	1.273(5)	
N(2)–C(3)		1.266(5)	
O(1)–N(1)	1.404(3)	1.386(4)	1.401(4)
O(2)–N(2)		1.395(4)	
Cl(1)–Pt(1)–N(1)	89.91(7)	88.99(8)	92.25(9)
Cl(2)–Pt(1)–N(1)		92.30(9)	89.64(8)
Cl(3)–Pt(1)–N(1)		88.39(8)	
Cl(4)–Pt(1)–N(1)		89.46(9)	
Cl(1)–Pt(1)–Cl(3)		177.17(3)	
Cl(2)–Pt(1)–Cl(4)		177.75(3)	
N(1)–Pt(1)–N(2)		178.75(11)	

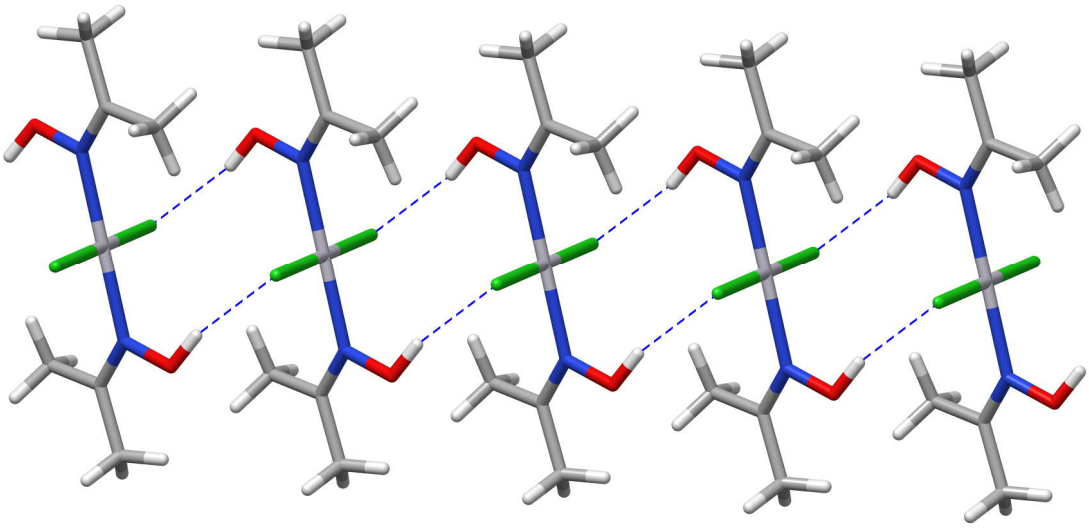

Fig. 2 Crystal packing of complex **1**.

Treatment of the *trans*-[$PtCl_2$(oxime)$_2$] complexes (where oxime = acetoxime, cyclopentanone oxime, or acetaldoxime) with *N*,*N*-dichlorotosylamide under identical conditions as used for the chlorination of [$PtCl_2$(imino ester)$_2$] [19] afforded *trans*-[$PtCl_4$(oxime)$_2$] (Scheme 3).

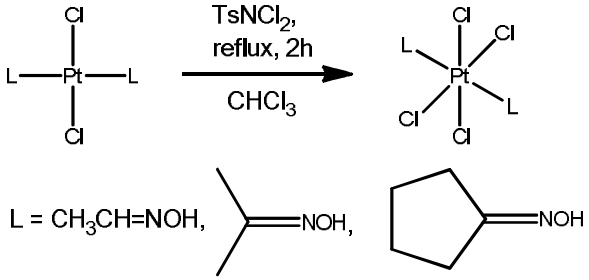

Scheme 3 Chlorination of the *trans*-[$PtCl_2$(oxime)$_2$] complexes by $TsNCl_2$.

In these reactions, a suspension of *trans*-[$PtCl_2$(oxime)$_2$] and *N*,*N*-dichlorotosylamide in a 1:1 molar ratio was refluxed for 2 h. As in the case of chlorination of *trans*-[$PtCl_2$(oxime)$_2$] (where oxime is acetoxime, cyclopentanone oxime, and acetaldoxime) by molecular chlorine, chlorination by *N*,*N*-dichlorotosylamide leads to the platinum(IV) complexes *trans*-[$PtCl_4$(oxime)$_2$]. Thus, only the oxidative chlorination of the platinum center is observed and the oxime

ligands remain unchanged. All our attempts to grow crystals of complex **5** suitable for single-crystal X-ray diffraction failed. However, crystals of good quality were obtained for complexes **6** and **7** by slow crystallization from chloroform.

In complex **6**, the platinum has a slightly distorted octahedral geometry with two axial acetaldoxime ligands and four chloride ligands (Fig. 3). The values of the Pt–Cl bond lengths agree well with those of previously characterized platinum(IV) chloride complexes, although all Pt–Cl bonds in complex **6** have different lengths due to the intramolecular interactions O(1)–H(1O)···Cl(4) (the H(1O)···Cl(4) distance is 2.29 Å, the O(1)–H(1O)···Cl(4) angle is 146.7°) and O(2)–H(2O)···Cl(1) (the H(2O)···Cl(1) distance is 2.28 Å, the O(2)–H(2O)···Cl(1) angle is 144.2°). The O(1)–N(1)–Pt(1)–Cl(4) and O(2)–N(2)–Pt(1)–Cl(1) torsion angles are 31.35 and 22.30°, respectively.

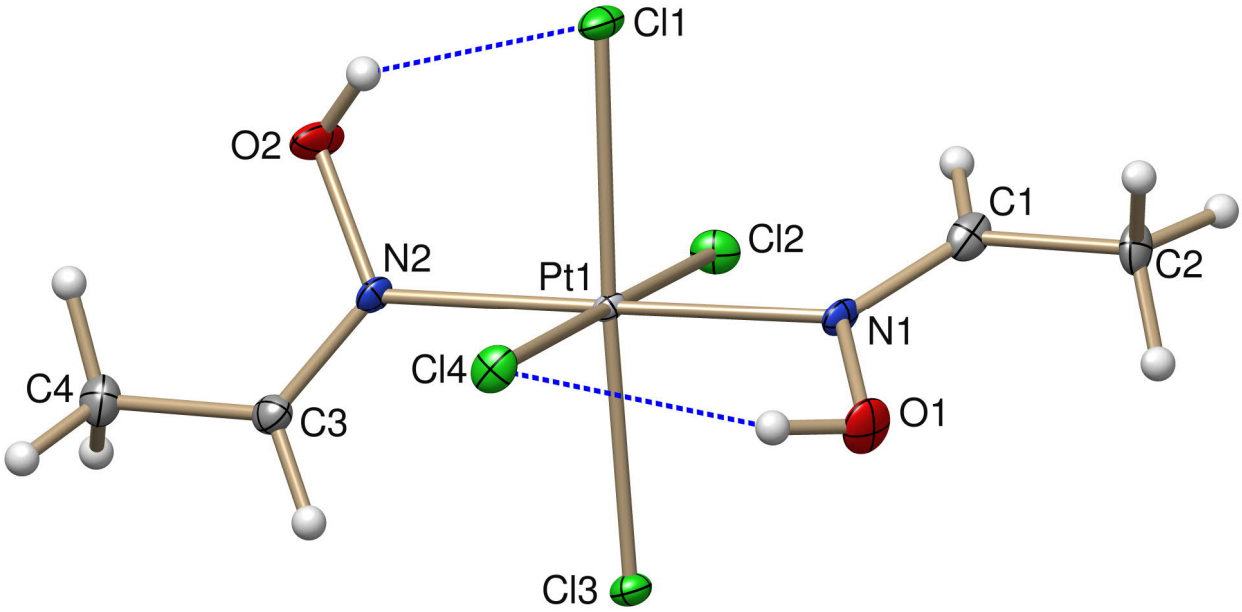

Fig. 3 Displacement ellipsoid plot of complex **6** at the 50% probability level.

In complex **7**, the coordination geometry of the platinum is octahedral (Fig. 4). The oxime ligands occupy the axial positions. The Pt–Cl(1), Pt–Cl(2), and Pt–N(1) bond lengths are 2.3103(9), 2.3187(9), and 2.046(3) Å, respectively. The crystal structure determination revealed the presence of intramolecular O(1)–H(1O)···Cl(1A) hydrogen bonds (the H(1O)···Cl(1A) distance is 2.36 Å, the O(1)–H(1O)···Cl(1A) angle is 130.1°). The O(1)–N(1)–Pt(1)–Cl(1A) torsion angle is 40.20°.

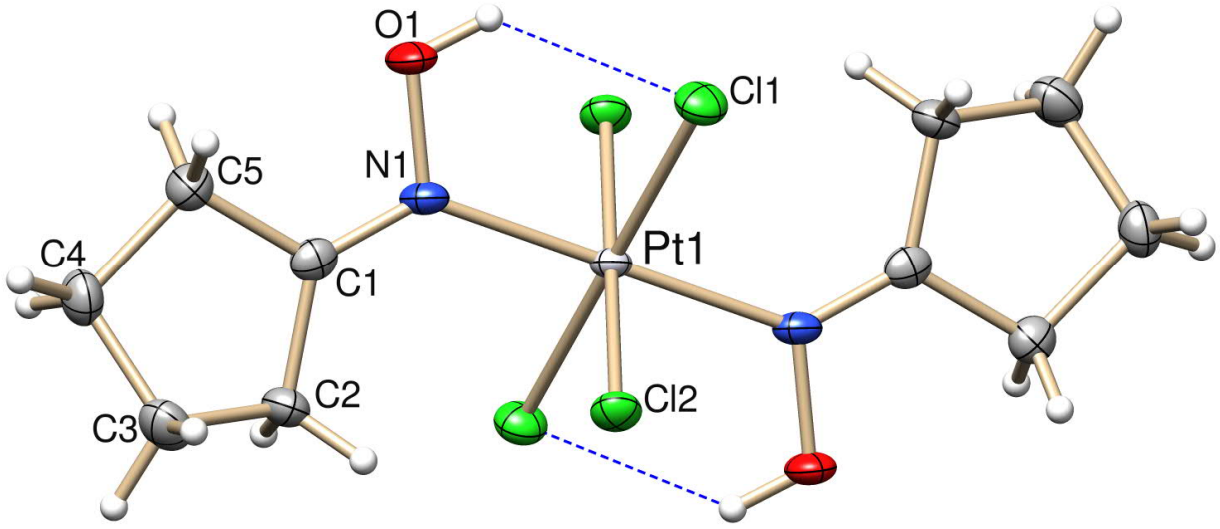

Fig. 4 Displacement ellipsoid plot of complex **7** at the 50% probability level (symmetry transformations used to generate equivalent non-labeled atoms: -x,-y,-z).

Chlorination of complex **4** under the same conditions as mentioned above leads to oxidation of the platinum center along with electrophilic substitution in the benzene rings. According to HRMS data, the reaction product has the formula $[PtCl_2(o\text{-}OC_6H_3ClCH{=}NOH)_2]$. However, when the reaction was carried out at room temperature only oxidation of Pt(II) to Pt(IV) was observed and the salicylaldoximato ligands remained intact (Scheme 2). Several attempts were made to obtain suitable crystals of complex **8** for X-ray diffraction studies. Unfortunately, crystals of sufficient quality could not be obtained. The reaction product was characterized by HRMS (ESI) and elemental analyses. Also, the infrared spectrum of this compound included a Pt–Cl band at 346 cm^{-1}. The ^1H NMR spectrum confirmed that electrophilic substitution in the benzene ring does not proceed.

Conclusions

In conclusion, the chlorination of (oxime)Pt^{II} (where oxime = aldoxime, cyclic or acyclic ketoxime) with *N*,*N*-dichlorotosylamide leads to selective oxidation of the Pt^{II} center, whereas the oxime ligands remain intact. The oxime ligands, which contain benzene rings activated to electrophilic substitution, do not react with $TsNCl_2$ under mild conditions. Furthermore, *N*,*N*-dichlorotosylamide can find a wide synthetic application in selective chlorination of the metal centers in the complexes, where the ligands may be easily subjected to electrophilic substitution processes.

Supplementary material

Crystal data have been deposited at the Cambridge Crystallographic Data Centre (CCDC) with deposition numbers CCDC 1041706, CCDC 1041705, and CCDC 1041612 for **1**, **6**, and **7**, respectively. These data can be obtained free of charge from The Cambridge Crystallographic Data Centre via www.ccdc.cam.ac.uk/data_request/cif.

Acknowledgements We are grateful to Prof. V.Yu. Kukushkin (Saint Petersburg State University) for helpful discussions and insightful comments. We also thank the Centre for Chemical Analysis and Materials Research, Educational Resource Center of Chemistry, and Centre of Magnetic Resonance of Saint Petersburg State University, where elemental analysis, HRMS (ESI), FT-IR, and NMR studies were performed.

References

1. Kukushkin VY, Belsky VK, Aleksandrova EA, Konovalov VE, Kirakosyan GA (1992) Inorg Chem 31: 3836–3840
2. Kaplan SF, Kukushkin VY, Shova S, Suwinska K, Wagner G, Pombeiro AJL (2001) Eur J Inorg Chem 4: 1031–1038
3. Mamtora J, Crosby SH, Newman CP, Clarkson GJ, Rourke JP (2008) Organometallics 27: 5559–5565
4. Meyer D, Ahrens S, Strassner T (2010) Organometallics 29: 3392–3396
5. Whitfield SR, Sanford MS (2008) Organometallics 27: 1683–1689
6. Ravera M, Gabano E, Pelos i G, Fregonese F, Tinello S, Osella D (2014) Inorg Chem 53: 9326−9335
7. Chulkova TG, Gushchin PV, Haukka M, Kukushkin VY (2010) Inorg Chem Commun 13: 580−583
8. Kukushkin VY, Kiseleva NP (1988) Koord Khim 14: 693−695
9. Kukushkin VY, Tkachuk VM (1989) Koord Khim 15: 136
10. Kukushkin VY, Tudela D, Izotova YA, Belsky VK, Stash AI (1998) Polyhedron 17: 2455–2461
11. Kukushkin VY, Izotova YA, Tudela D, Guedes da Silva MFC, Pombeiro AJL (2004) Inorg Synth 34: 81–85
12. Bulatov EY, Chulkova TG, Boyarskaya IA, Kondratiev VV, Haukka M, Kukushkin VY (2014) J Mol Struct 1068: 176–181
13. Cox EG, Pinkard FW, Wardlaw W, Webster KC (1935) J Chem Soc: 459−462
14. Bruker AXS (2009) APEX2 - Software Suite for Crystallographic Programs, Bruker AXS, Inc., Madison, WI, USA
15. Otwinowski ZM, Minor W (1997) In: Carter CWS, Sweet J (ed) Methods in Enzymology. Academic Press, New York, USA: 307−326
16. Sheldrick GM (2008) Acta Cryst A64: 112−122
17. Farrugia LJ (1999) J Appl Cryst 32: 837−838
18. Sheldrick GM (2008) SADABS - Bruker AXS scaling and absorption correction. Bruker AXS, Inc.: Madison, Wisconsin, USA
19. Dneprovskii AS, Eliseenkov EV, Chulkova TG (2002) Russ J Org Chem 38: 338−343

V

Unusual Intramolecular Pt···I Non-covalent Interactions in Bis(2-iodobenzyldi(2-pyridyl)amine)platinum(II) Complex

by

Evgeny Bulatov, Toni Eskelinen, Alexander Ivanov, Peter Tolstoy,
Pipsa Hirva & Matti Haukka

Manuscript

Request a copy from author.